Establishing determinants of oxygen delivery and neuromuscular function at the heavy-to-severe intensity exercise threshold

by

Shane Michael Hammer

B.S., Kansas State University, 2015
M.S., Kansas State University, 2017

AN ABSTRACT OF A DISSERTATION

submitted in partial fulfillment of the requirements for the degree

DOCTOR OF PHILOSOPHY

Department of Kinesiology
College of Health and Human Sciences

KANSAS STATE UNIVERSITY
Manhattan, Kansas

2020

Abstract

Critical power/force (CP/CF) demarcates the boundary between the heavy- and severe-intensity exercise domains and is established as an important threshold for skeletal muscle metabolism, oxygen delivery, neuromuscular fatigue, and therefore exercise tolerance. Despite extensive study, the underlying mechanisms which precipitate the stark differences in physiological responses to exercise at intensities surrounding CP/CF remain unclear. The overall aim of this dissertation was to determine potential contraction-intensity dependent alterations in limb blood flow and microvascular oxygen delivery and investigate the effect of oxygen delivery limitations on neuromuscular function at the heavy-to-severe intensity exercise threshold (i.e., CP/CF). In our first investigation (Chapter 2), we demonstrated that limb blood flow and microvascular oxygen delivery responses during isometric handgrip exercise reached a physiological ceiling above, but not below, CF. Additionally, we determined that CF was the highest contraction-intensity at which this level of microvascular oxygen delivery could acutely sustain maximal-effort exercise. The second investigation (Chapter 3) demonstrated that limb vascular conductance is limited above CP and we provide evidence that limb blood flow limitations during severe-intensity exercise result, at least in part, from muscular contraction-induced vascular impedance. Importantly, this study utilized a dynamic large-muscle mass exercise model (supine leg cycling) to improve generalizability of our findings to activities of daily living. Utilizing complete blood flow occlusion and vascular reperfusion, the final investigation (Chapter 4) identified fatigue-induced restriction to central motor drive during maximal-effort handgrip exercise and established that CF represents an oxygen delivery-dependent balance between motor-unit activation and peripheral fatigue development. Collectively, contraction-intensity dependent limitations in oxygen delivery appear to exist during severe-intensity exercise

such that progressive development of peripheral fatigue may result in restrictions to motor-unit activation. This dissertation presents novel findings that significantly contribute to our overall understanding of the physiological determinants of oxygen delivery, fatigue development, and exercise tolerance, which may be particularly relevant in patient populations that experience pathological limitations to oxygen delivery during exercise (e.g., heart failure and peripheral artery disease).

Establishing determinants of oxygen delivery and neuromuscular function at the heavy-to-severe intensity exercise threshold

by

Shane Michael Hammer

B.S., Kansas State University, 2015
M.S., Kansas State University, 2017

A DISSERTATION

submitted in partial fulfillment of the requirements for the degree

DOCTOR OF PHILOSOPHY

Department of Kinesiology
College of Health and Human Sciences

KANSAS STATE UNIVERSITY
Manhattan, Kansas

2020

Approved by:

Major Professor
Thomas J. Barstow

Copyright

Abstract

Critical power/force (CP/CF) demarcates the boundary between the heavy- and severe-intensity exercise domains and is established as an important threshold for skeletal muscle metabolism, oxygen delivery, neuromuscular fatigue, and therefore exercise tolerance. Despite extensive study, the underlying mechanisms which precipitate the stark differences in physiological responses to exercise at intensities surrounding CP/CF remain unclear. The overall aim of this dissertation was to determine potential contraction-intensity dependent alterations in limb blood flow and microvascular oxygen delivery and investigate the effect of oxygen delivery limitations on neuromuscular function at the heavy-to-severe intensity exercise threshold (i.e., CP/CF). In our first investigation (Chapter 2), we demonstrated that limb blood flow and microvascular oxygen delivery responses during isometric handgrip exercise reached a physiological ceiling above, but not below, CF. Additionally, we determined that CF was the highest contraction-intensity at which this level of microvascular oxygen delivery could acutely sustain maximal-effort exercise. The second investigation (Chapter 3) demonstrated that limb vascular conductance is limited above CP and we provide evidence that limb blood flow limitations during severe-intensity exercise result, at least in part, from muscular contraction-induced vascular impedance. Importantly, this study utilized a dynamic large-muscle mass exercise model (supine leg cycling) to improve generalizability of our findings to activities of daily living. Utilizing complete blood flow occlusion and vascular reperfusion, the final investigation (Chapter 4) identified fatigue-induced restriction to central motor drive during maximal-effort handgrip exercise and established that CF represents an oxygen delivery-dependent balance between motor-unit activation and peripheral fatigue development. Collectively, contraction-intensity dependent limitations in oxygen delivery appear to exist during severe-intensity exercise

such that progressive development of peripheral fatigue may result in restrictions to motor-unit activation. This dissertation presents novel findings that significantly contribute to our overall understanding of the physiological determinants of oxygen delivery, fatigue development, and exercise tolerance, which may be particularly relevant in patient populations that experience pathological limitations to oxygen delivery during exercise (e.g., heart failure and peripheral artery disease).

Table of Contents

List of Figures

List of Tables

Dedication

To my wife, Sarah:

The completion of this dissertation marks the end of an exciting chapter in our lives and the beginning of a new journey. I wouldn't have wanted to share these moments with anyone else and I'm so excited to continue dreaming with you. I love you so much.

To my grandpa, Glen:

You always told me to find something I love to do and someone who would pay me to do it. I'm halfway there. I miss your smile every day.

Preface

Chapter 2 of this dissertation represents an original research article that has been published following the peer-review process (citation below) and is reproduced here with the permission of the publisher. Chapters 3 & 4 of this dissertation represent original research articles that are currently in the peer-review process.

Hammer SM, Alexander AM, Didier KD, Huckaby LM & Barstow TJ. Limb blood flow and muscle oxygenation responses during handgrip exercise above vs. below critical force. *Microvascular Research (In Press)*. https://doi.org/10.1016/j.mvr.2020.104002, 2020.

Chapter 1 - Introduction

It has been demonstrated repeatedly that maximal exercise performance is delimited by the physiological parameters of critical power (CP) and the finite work capacity that exists above it (W') (Jones *et al.*, 2010; Poole *et al.*, 2016). CP demarcates the boundary between heavy- and severe-intensity exercise domains (Poole *et al.*, 1988). Above CP (severe-intensity) exercise tolerance is described, and the time to task failure (T_{lim}) can be accurately predicted, by the hyperbolic power-duration relationship defined by the equation (Whipp *et al.*, 1982):

$$T_{lim} = \frac{W'}{P - CP}$$

Following on A.V. Hill's observations of elite athletic performances (Hill, 1925), Monod and Scherrer originally described the CP threshold as a local phenomenon confined to intramuscular factors (Monod & Scherrer, 1965). However, a contraction-time dependency for local circulation was observed and it was speculated that any work performed under arrested blood flow conditions is above CP (Monod & Scherrer, 1965). These observations alluded to the currently accepted conclusion that oxygen delivery plays a significant role in the determination of CP (Jones *et al.*, 2010; Vanhatalo *et al.*, 2010; Broxterman *et al.*, 2014; Broxterman *et al.*, 2015a; Poole *et al.*, 2016).

CP is a well-established physiological threshold (Poole *et al.*, 2016) that differentiates between steady-state and progressive metabolic (Poole *et al.*, 1988; Jones *et al.*, 2008) and neuromuscular (Burnley *et al.*, 2012) responses to exercise. However, it remains unknown if any differences exist in the limb blood flow (LBF) response to heavy- versus severe-intensity exercise in humans. During rhythmic exercise, LBF is highest during the relaxation phase of the contraction-relaxation cycle when intramuscular pressure is low (Barcroft & Dornhorst, 1949;

Walloe & Wesche, 1988; Robergs *et al.*, 1997; Radegran & Saltin, 1998; Lutjemeier *et al.*, 2005). Thus, altering relaxation time between contractions (i.e., duty-cycle or contraction-frequency) has a profound effect on both LBF and CP (Hoelting *et al.*, 2001; Broxterman *et al.*, 2014; Bentley *et al.*, 2017; Caldwell *et al.*, 2018). Additionally, muscular contractions have been shown to impede LBF at high intensities (Lutjemeier *et al.*, 2005). These findings are consistent with reports of submaximal plateaus in microvascular blood flow during incremental exercise (Boushel *et al.*, 2002; Habazettl *et al.*, 2010; Hammer *et al.*, 2018) suggesting high-intensity contractions may exert an impeding effect. While the oxygen delivery dependency of CP is well documented (Moritani *et al.*, 1981; Vanhatalo *et al.*, 2010; Dekerle *et al.*, 2012), the influence of muscular contraction on limb vascular conductance (LVC) (i.e., evidence for LBF impedance) during exercise at intensities surrounding CP remains unknown. LBF limitations can have profound effects on metabolite-induced fatigue development (Broxterman *et al.*, 2015b). Thus, identifying CP as a threshold for LBF impedance would have large implications regarding our understanding of exercise tolerance.

Interestingly, a critical level of metabolite-induced fatigue development appears to define severe-intensity exercise tolerance (Amann *et al.*, 2006; Amann & Dempsey, 2008; Hureau *et al.*, 2014; Hureau *et al.*, 2016). Accordingly, it has been postulated that ensemble sensory input from skeletal muscle group III/IV afferents contributes toward volitional termination of exhaustive exercise (Gandevia, 2001; Hureau *et al.*, 2018). Specifically, a centrally-originating critical tolerance level to sensory feedback is thought to exist that, once attained, reduces skeletal muscle activation to prevent detrimental levels of metabolic perturbation within skeletal muscle (Amann *et al.*, 2009; Blain *et al.*, 2016). Interestingly, peripheral fatigue development at task failure during constant work rate exercise is nearly identical to levels reached, and sustained, during continuous maximal-effort exercise (Burnley, 2009). Progressive deactivation of motor-units during both whole-body (Vanhatalo *et al.*, 2011) and single-joint exercise (Burnley, 2009) has been demonstrated during continuous maximal effort exercise, during which T_{lim} is not defined by the inability to meet force- or power-output requirements, but rather exercise continues until a nadir in maximal-effort force- (i.e., critical force; CF) (Burnley, 2009; Broxterman *et al.*, 2017) or power-output (i.e., CP) (Vanhatalo *et al.*, 2007) is reached. Considering the effects of LBF occlusion on metabolite accumulation and group III/IV sensory afferent nerve firing rates (Rowell & O'Leary, 1990; Adreani & Kaufman, 1998), manipulations in blood flow may elucidate if a relationship exists between restriction to motor-unit activation via a 'sensory tolerance limit' (Gandevia, 2001; Hureau *et al.*, 2018) and CP/CF determination during maximal-effort exercise.

The overall aim of this dissertation was to determine potential contraction-intensity dependent alterations in LBF and microvascular oxygen delivery and investigate the effect of oxygen delivery limitations on neuromuscular function at the heavy-to-severe intensity exercise threshold (i.e., CP/CF). Specifically, we aimed to determine if any differences exist in the LBF and microvascular oxygen delivery responses between heavy- and severe-intensity exercise. Further, utilizing a dynamic large-muscle mass exercise model to improve generalizability, we sought to determine if limitations in LBF above CP were, at least in part, the result of muscular contraction-induced vascular impedance. Finally, this dissertation aimed to identify relationships between fatigue development and restriction to CMD during maximal-effort handgrip exercise and determine if the heavy-to-severe intensity threshold represents an oxygen delivery-dependent balance between motor-unit activation and peripheral fatigue development.

References

Adreani CM & Kaufman MP. (1998). Effect of arterial occlusion on responses of group III and IV afferents to dynamic exercise. *J Appl Physiol (1985)* 84, 1827-1833.

Amann M & Dempsey JA. (2008). Locomotor muscle fatigue modifies central motor drive in healthy humans and imposes a limitation to exercise performance. *J Physiol* 586, 161-173.

Amann M, Eldridge MW, Lovering AT, Stickland MK, Pegelow DF & Dempsey JA. (2006). Arterial oxygenation influences central motor output and exercise performance via effects on peripheral locomotor muscle fatigue in humans. *J Physiol* 575, 937-952.

Amann M, Proctor LT, Sebranek JJ, Pegelow DF & Dempsey JA. (2009). Opioid-mediated muscle afferents inhibit central motor drive and limit peripheral muscle fatigue development in humans. *J Physiol* 587, 271-283.

Barcroft H & Dornhorst AC. (1949). The Blood Flow through the Human Calf during Rhythmic Exercise. *J Physiol-London* 109, 402-&.

Bentley RF, Poitras VJ, Hong T & Tschakovsky ME. (2017). Characteristics and effectiveness of vasodilatory and pressor compensation for reduced relaxation time during rhythmic forearm contractions. *Experimental Physiology* 102, 621-634.

Blain GM, Mangum TS, Sidhu SK, Weavil JC, Hureau TJ, Jessop JE, Bledsoe AD, Richardson RS & Amann M. (2016). Group III/IV muscle afferents limit the intramuscular metabolic perturbation during whole body exercise in humans. *J Physiol* 594, 5303-5315.

Boushel R, Langberg H, Gemmer C, Olesen J, Crameri R, Scheede C, Sander M & Kjaer M. (2002). Combined inhibition of nitric oxide and prostaglandins reduces human skeletal muscle blood flow during exercise. *J Physiol* 543, 691-698.

Broxterman RM, Ade CJ, Craig JC, Wilcox SL, Schlup SJ & Barstow TJ. (2015a). Influence of blood flow occlusion on muscle oxygenation characteristics and the parameters of the power-duration relationship. *Journal of applied physiology (Bethesda, Md : 1985)* 118, 880-889.

Broxterman RM, Ade CJ, Wilcox SL, Schlup SJ, Craig JC & Barstow TJ. (2014). Influence of duty cycle on the power-duration relationship: observations and potential mechanisms. *Respir Physiol Neurobiol* 192, 102-111.

Broxterman RM, Craig JC, Smith JR, Wilcox SL, Jia C, Warren S & Barstow TJ. (2015b). Influence of blood flow occlusion on the development of peripheral and central fatigue during small muscle mass handgrip exercise. *J Physiol* 593, 4043-4054.

Broxterman RM, Layec G, Hureau TJ, Amann M & Richardson RS. (2017). Skeletal muscle bioenergetics during all-out exercise: mechanistic insight into the oxygen uptake slow component and neuromuscular fatigue. *J Appl Physiol* 122, 1208-1217.

Burnley M. (2009). Estimation of critical torque using intermittent isometric maximal voluntary contractions of the quadriceps in humans. *J Appl Physiol* 106, 975-983.

Burnley M, Vanhatalo A & Jones AM. (2012). Distinct profiles of neuromuscular fatigue during muscle contractions below and above the critical torque in humans. *J Appl Physiol* 113, 215-223.

Caldwell JT, Sutterfield SL, Post HK, Lovoy GM, Banister HR, Hammer SM & Ade CJ. (2018). Vasoconstrictor responsiveness through alterations in relaxation time and metabolic rate during rhythmic handgrip contractions. *Physiol Rep* 6, e13933.

Dekerle J, Mucci P & Carter H. (2012). Influence of moderate hypoxia on tolerance to high-intensity exercise. *Eur J Appl Physiol* 112, 327-335.

Gandevia SC. (2001). Spinal and supraspinal factors in human muscle fatigue. *Physiol Rev* 81, 1725-1789.

Habazettl H, Athanasopoulos D, Kuebler WM, Wagner H, Roussos C, Wagner PD, Ungruhe J, Zakynthinos S & Vogiatzis I. (2010). Near-infrared spectroscopy and indocyanine green derived blood flow index for noninvasive measurement of muscle perfusion during exercise. *Journal of applied physiology (Bethesda, Md : 1985)* 108, 962-967.

Hammer SM, Alexander AM, Didier KD, Smith JR, Caldwell JT, Sutterfield SL, Ade CJ & Barstow TJ. (2018). The noninvasive simultaneous measurement of tissue oxygenation and microvascular hemodynamics during incremental handgrip exercise. *J Appl Physiol* 124, 604-614.

Hill AV. (1925). The physiological basis of athletic records. *Nature* 116, 544-548.

Hoelting BD, Scheuermann BW & Barstow TJ. (2001). Effect of contraction frequency on leg blood flow during knee extension exercise in humans. *J Appl Physiol (1985)* 91, 671-679.

Hureau TJ, Ducrocq GP & Blain GM. (2016). Peripheral and Central Fatigue Development during All-Out Repeated Cycling Sprints. *Med Sci Sports Exerc* 48, 391-401.

Hureau TJ, Olivier N, Millet GY, Meste O & Blain GM. (2014). Exercise performance is regulated during repeated sprints to limit the development of peripheral fatigue beyond a critical threshold. *Exp Physiol* 99, 951-963.

Hureau TJ, Romer LM & Amann M. (2018). The 'sensory tolerance limit': A hypothetical construct determining exercise performance? *Eur J Sport Sci* 18, 13-24.

Jones AM, Vanhatalo A, Burnley M, Morton RH & Poole DC. (2010). Critical power: implications for determination of V O2max and exercise tolerance. *Med Sci Sports Exerc* 42, 1876-1890.

Jones AM, Wilkerson DP, DiMenna F, Fulford J & Poole DC. (2008). Muscle metabolic responses to exercise above and below the "critical power" assessed using 31P-MRS. *American journal of physiology Regulatory, integrative and comparative physiology* 294, R585-593.

Lutjemeier BJ, Miura A, Scheuermann BW, Koga S, Townsend DK & Barstow TJ. (2005). Muscle contraction-blood flow interactions during upright knee extension exercise in humans. *Journal of applied physiology (Bethesda, Md : 1985)* 98, 1575-1583.

Monod H & Scherrer J. (1965). The Work Capacity of a Synergic Muscular Group. *Ergonomics* 8, 329-338.

Moritani T, Nagata A, Devries HA & Muro M. (1981). Critical Power as a Measure of Physical Work Capacity and Anaerobic Threshold. *Ergonomics* 24, 339-350.

Poole DC, Burnley M, Vanhatalo A, Rossiter HB & Jones AM. (2016). Critical Power: An Important Fatigue Threshold in Exercise Physiology. *Med Sci Sports Exerc* 48, 2320-2334.

Poole DC, Ward SA, Gardner GW & Whipp BJ. (1988). Metabolic and respiratory profile of the upper limit for prolonged exercise in man. *Ergonomics* 31, 1265-1279.

Radegran G & Saltin B. (1998). Muscle blood flow at onset of dynamic exercise in humans. *Am J Physiol-Heart C* 274, H314-H322.

Robergs RA, Icenogle MV, Hudson TL & Greene ER. (1997). Temporal inhomogeneity in brachial artery blood flow during forearm exercise. *Med Sci Sport Exer* 29, 1021-1027.

Rowell LB & O'Leary DS. (1990). Reflex control of the circulation during exercise: chemoreflexes and mechanoreflexes. *J Appl Physiol (1985)* 69, 407-418.

Vanhatalo A, Doust JH & Burnley M. (2007). Determination of critical power using a 3-min all-out cycling test. *Med Sci Sport Exer* 39, 548-555.

Vanhatalo A, Fulford J, DiMenna FJ & Jones AM. (2010). Influence of hyperoxia on muscle metabolic responses and the power-duration relationship during severe-intensity exercise in humans: a 31P magnetic resonance spectroscopy study. *Experimental Physiology* 95, 528-540.

Vanhatalo A, Poole DC, DiMenna FJ, Bailey SJ & Jones AM. (2011). Muscle fiber recruitment and the slow component of O-2 uptake: constant work rate vs. all-out sprint exercise. *Am J Physiol-Reg I* 300, R700-R707.

Walloe L & Wesche J. (1988). Time Course and Magnitude of Blood-Flow Changes in the Human Quadriceps Muscles during and Following Rhythmic Exercise. *J Physiol-London* 405, 257-273.

Whipp BJ, Huntsman DJ, Storer TW, Lamarra N & Wasserman K. (1982). A Constant Which Determines the Duration of Tolerance to High-Intensity Work. *Fed Proc* 41, 1591-1591.

Chapter 2 - Limb blood flow and muscle oxygenation responses during handgrip exercise above vs. below critical force

Summary

This study compared the brachial artery blood flow ($\dot{Q}_{BA}$) and microvascular oxygen delivery responses during handgrip exercise above vs. below critical force (CF; the isometric analog of critical power). $\dot{Q}_{BA}$ and microvascular oxygen delivery are important determinants of oxygen utilization and metabolite accumulation during exercise, both of which increase progressively during exercise above CF. However, the $\dot{Q}_{BA}$ and microvascular oxygen delivery responses above vs. below CF remain unknown. We hypothesized that $\dot{Q}_{BA}$, deoxygenated-heme (deoxy-[heme]; an estimate of microvascular fractional oxygen extraction), and total-heme concentrations (total-[heme]; an estimate of changes in microvascular hematocrit) would demonstrate physiological maximums above CF despite increases in exercise intensity. Seven men and six women performed 1) a 5-min rhythmic isometric-handgrip maximal-effort test (MET) to determine CF and 2) two constant target-force tests above (severe-intensity; S1 and S2) and two constant target-force tests below (heavy-intensity; H1 and H2) CF. CF was 189.3±16.7 N (29.7±1.6 %MVC). At end-exercise, $\dot{Q}_{BA}$ was greater for tests above CF (S1: 418±147 mL/min; S2: 403±137 mL/min) compared to tests below CF (H1: 287±97 mL/min; H2: 340±116 mL/min; all $p<0.05$) but was not different between S1 and S2. Further, end-test $\dot{Q}_{BA}$ during both tests above CF was not different from $\dot{Q}_{BA}$ estimated at CF (392±37 mL/min). At end-exercise, deoxy-[heme] was not different between tests above CF (S1: 150±50 µM; S2: 155±57 µM), but was greater during tests above CF compared to tests below CF (H1: 101±24 µM; H2: 111±21 µM; all $p<0.05$).

At end-exercise, total-[heme] was not different between tests above CF (S1: 404±58 μM; S2: 397±73 μM), but was greater during tests above CF compared to H1 (352±58 μM; $p<0.01$) but not H2 (371±57 μM). These data suggest limb blood flow limitations exist and maximal levels of muscle microvascular oxygen delivery and extraction occur during exercise above, but not below, CF.

Introduction

It has been demonstrated repeatedly that maximal exercise performance is delimited by the physiological parameters of critical power (CP) and the finite work capacity that exists above it (W') (Jones *et al.*, 2010; Poole *et al.*, 2016). CP demarcates the boundary between heavy- and severe-intensity exercise domains (Poole *et al.*, 1988). Severe-intensity exercise is characterized by metabolic profiles distinct from those of exercise performed at lower work rates. During exercise performed above CP, decreases in intramuscular pH and phosphocreatine concentration and escalations in concentrations of blood lactate and intramuscular inorganic phosphate, and oxygen uptake ($\dot{V}O_2$) continue until task failure (Poole *et al.*, 1988; Poole *et al.*, 1991; Jones *et al.*, 2008). The continuous rise in $\dot{V}O_2$ (i.e., the $\dot{V}O_2$ slow component) despite a fixed work rate is evidence of an increasingly inefficient muscular metabolic system during exercise at higher intensities (Poole *et al.*, 1991; Barstow *et al.*, 1996; Rossiter *et al.*, 2002).

Contributing factors to the continuous rise in $\dot{V}O_2$ observed during severe-intensity exercise include the progressive recruitment of less efficient motor units subsequent to fatigue development in muscle fibers that were initially recruited (Krustrup *et al.*, 2004; Endo *et al.*, 2007) and progressive metabolic inefficiency in already contracting muscle fibers (Zoladz *et al.*, 2008; Hepple *et al.*, 2010). Many studies have determined that differences exist in gas exchange (Poole *et al.*, 1988), metabolic (Jones *et al.*, 2008), and neuromuscular responses (Burnley *et al.*, 2012) to exercise at intensities surrounding this critical threshold. However, it remains unknown if any differences exist in the blood flow response to heavy- vs. severe-intensity exercise in humans.

In the rat hindlimb, Copp et al. (Copp *et al.*, 2010b) measured blood flow responses of active skeletal muscles during exercise performed above and below critical speed (CS; the running analog of CP). It was established that, while muscle blood flow was greater in all muscles irrespective of fiber-type composition, blood flow was distributed proportionately more so to muscles and muscle regions comprised of less efficient fast glycolytic fibers (Type-IIb/d/x) compared to regions made-up of primarily oxidative fibers (Type I and IIa) during exercise above, relative to below, CS (Copp *et al.*, 2010b). Importantly, type-II fibers demonstrate a lower oxygen delivery-to-oxygen utilization ($\dot{Q}O_2/\dot{V}O_2$) ratio (Behnke *et al.*, 2003; McDonough *et al.*, 2005; Koga *et al.*, 2014) and, therefore, require a greater level of oxygen extraction during exercise. Unlike whole limb blood flow responses during incremental exercise (Andersen & Saltin, 1985; Richardson *et al.*, 1993), blood flows of individual muscles demonstrate sub-maximal plateaus (Boushel *et al.*, 2002; Habazettl *et al.*, 2010; Vogiatzis *et al.*, 2015; Hammer *et al.*, 2018). Recent work during small muscle mass (Hammer *et al.*, 2018) and whole-body exercise (Chin *et al.*, 2011) has demonstrated an association between submaximal plateaus in muscle microvascular oxygen delivery and recruitment of previously inactive muscles . Taken together, these findings suggest that less metabolically efficient motor units (i.e., having greater oxygen cost associated with force production) are recruited in order to meet the increased force requirements of severe-intensity exercise and that further increases in limb blood flow are distributed to these newly recruited muscle regions.

To date, we are unaware of any experimental evidence that compares the integrative responses of blood flow and muscle oxygen extraction during exercise at intensities surrounding CP. During exercise, increases in muscle $\dot{V}O_2$ must be supported by increases in convective oxygen delivery ($\dot{Q}O_2$) and/or diffusive oxygen extraction (i.e., the arterial-venous oxygen content difference; CaO_2-CvO_2). Interestingly, when combined with measurements from other studies (Armstrong & Laughlin, 1985; Copp *et al.*, 2010a; Copp *et al.*, 2010c), the total hindlimb blood flow responses measured by Copp et al. revealed a possible maximum for whole limb blood flow during severe-intensity exercise (Copp *et al.*, 2010b). According to the Fick principle ($\dot{V}O_2 = \dot{Q} \times (CaO_2\text{-}CvO_2)$), a maximal blood flow response, and therefore no further increase in $\dot{Q}O_2$, combined with attainment of maximal $\dot{V}O_2$ ($\dot{V}O_{2max}$; (Poole *et al.*, 1988)) suggests a physiological upper limit in muscle oxygen extraction within the severe-intensity exercise domain.

The aim of this study was to compare the brachial artery blood flow ($\dot{Q}_{BA}$) and microvascular oxygen delivery responses to rhythmic handgrip exercise in humans at intensities above vs. below critical force (CF; the isometric analog of CP). We hypothesized that $\dot{Q}_{BA}$, deoxygenated-heme concentration (deoxy-[heme]; an index of microvascular convective oxygen conductance and estimation of fractional oxygen extraction (DeLorey *et al.*, 2003; Grassi *et al.*, 2003; Ferreira *et al.*, 2007; Broxterman *et al.*, 2014; Broxterman *et al.*, 2015; Hammer *et al.*, 2018)), and total-heme concentration (total-[heme]; an index of microvascular diffusive oxygen conductance via changes in microvascular hematocrit (Davis & Barstow, 2013; Okushima *et al.*, 2016; Hammer *et al.*, 2018)) would demonstrate physiological maximums within the severe-intensity exercise domain (above CF).

Methods

Ethical approval

All experimental procedures were approved by the Institutional Review Board for Research Involving Human Subjects at Kansas State University and conformed to the standards set forth by the Declaration of Helsinki with the exception of database registration. Subjects were informed of all testing procedures and potential risks of participation before providing written, informed consent.

Subjects

Seven men and six women (mean ± SD; 22 ± 2 yr, 171 ± 7 cm, 70.2 ± 8.8 kg) volunteered to participate in this study. While overall sex differences may exist, it has been demonstrated that muscle blood flow during exercise is not modulated by phases of the menstrual cycle (Limberg *et al.*, 2010; Smith *et al.*, 2017). Therefore, no attempt was made to control for menstrual cycle phase in the women. Each subject completed a medical health history evaluation to confirm the absence of any known cardiovascular, pulmonary, or metabolic disease. Subjects were instructed to abstain from vigorous activity 12 hrs. prior and caffeine and food consumption 2 hrs. prior to the scheduled testing times.

Experimental Design

All subjects were familiarized with the testing protocols prior to data collection. All exercise tests were performed on a custom-built single-arm isometric handgrip system. A handle was fixed 5.5 cm from a palmar support rail via a cable system instrumented with an in-line tension load cell. Force-output from the load cell was digitized and displayed on a nearby monitor. The system was calibrated prior to the study. All tests were performed in the supine position with the arm outstretched 90 degrees at heart level. Handgrip exercise was performed at 20 contractions per min with a 50% duty-cycle (i.e., 1.5 s contraction and 1.5 s relaxation). Contraction and relaxation cues were provided to each subject via a prerecorded audio file. On separate days subjects performed a 5-min rhythmic isometric-handgrip maximal-effort test (MET) to determine CF followed by two heavy-intensity constant target-force tests (below CF) and two severe-intensity constant target-force tests (above CF). The 5-min MET was followed by a 24 hour recovery period before any additional tests were performed.

Maximal-effort tests. The rhythmic isometric MET used to determine CF has been previously validated in the forearm (Kellawan & Tschakovsky, 2014) and during knee extension exercise (Burnley, 2009). In short, subjects performed a maximal voluntary contraction (MVC) for 1.5 s followed by 1.5 s of relaxation before performing another MVC. This cycle was repeated for the duration of the test (5-min). The mechanistic basis of the MET is a gradual utilization of W' during the early phase of the test followed by a plateau in force production (or power output during cycling) at CF (Vanhatalo *et al.*, 2007, 2008). Pilot testing determined a 5-min exercise protocol was sufficient to elicit an approximate 60 s plateau in maximal force production at the contraction frequency and duty-cycle used in this study (20 contractions per min; 50% duty-cycle). Unlike the familiarization trial, subjects were blinded to force production during the MET to avoid voluntary force targeting and instill confidence in the end-test force plateau. Additionally, subjects remained unaware of the time or number of contractions remaining in the test. Subjects were strongly encouraged to produce maximal voluntary force during each contraction and to relax fully between contractions.

Constant target-force tests. Target forces of the severe-intensity exercise tests (above CF) were selected to elicit a time to task failure (T_{lim}) of 8-12 min (S1) and 3-6 min (S2). A target force equal to CF + 20% was used during the first constant target-force test for each subject and labeled S1 or S2 depending on T_{lim}. Remaining target-forces were selected such that heavy-intensity tests (below CF; H1 and H2) were in proportion to S1 and S2 relative to CF. All remaining constant target-force tests were performed in random order. A line was generated on the force-output display to indicate the target-force for each test. Subjects were instructed to produce force rapidly and continuously at the required target-force throughout the contraction audio cue. T_{lim} was determined when the subject failed to reach and maintain target-force during three consecutive contractions despite strong verbal encouragement. All tests were terminated after 15-min of exercise if task failure had yet to occur.

Measurements

Force production. Average force production was calculated from 0.25 s to 1.25 s of each 1.5 s contraction to minimize the effect of delayed force commencement or premature relaxation. MVC of each subject was determined as the highest average contraction force among the first three contractions during the MET. CF of each subject was determined as the average force production during the final 10 contractions (30 s) of the MET.

Doppler ultrasound. Brachial artery mean blood velocity (V_{mean}) and vessel diameter were measured simultaneously using a two-dimensional Doppler ultrasound system (LOGIQ e; GE Healthcare; Milwaukee, WI). The ultrasound system was operated in duplex mode with a phased linear array transducer probe operated at an imaging frequency of 10.0 MHz. To avoid the bifurcation of the brachial artery, all measurements were made 2–5 cm proximal to the antecubital fossa (Ade *et al.*, 2012; Limberg *et al.*, 2020). Doppler velocity measurements were executed at a Doppler frequency of 4.0 MHz and corrected for an angle of insonation < 60° (Limberg *et al.*, 2020). Data from the LOGIQ e system were stored on a local hard drive for post hoc analysis via software provided by GE Healthcare. V_{mean} was defined as the time-averaged mean velocity across each complete cardiac cycle at rest and contraction-relaxation cycle during exercise. Brachial artery vessel diameter was analyzed at a perpendicular angle along the central axis of the vessel during the R-wave of the cardiac cycle. Cross-sectional area (CSA) of the vessel was calculated as $CSA = \pi r^2$. $\dot{Q}_{BA}$ was calculated as the product of CSA and V_{mean}. $\dot{Q}_{BA}$ was determined at rest during a minimum of 5 consecutive cardiac cycles. During the exercise tests, average $\dot{Q}_{BA}$ was calculated from 3 consecutive contraction-relaxation cycles (9 s) during the final 30 s of each min.

Frequency-domain near-infrared spectroscopy. A multi-distance frequency-domain near-infrared spectroscopy (FD-NIRS) system (OxiplexTS; ISS; Champaign, IL) was used to measure absolute oxygenated- and deoxygenated-heme concentrations (oxy-[heme] and deoxy-[heme], respectively) of the flexor digitorum superficialis (FDS) of the right forearm at rest and during each exercise test. The belly of the FDS was located using electromyography and tissue palpations as previously described (Broxterman *et al.*, 2014). The principles and algorithms of the FD-NIRS technology have been reviewed by Gratton et al. (Gratton *et al.*, 1997) and have been previously described (Ferreira *et al.*, 2006; Hammer *et al.*, 2019). The applications of NIRS to skeletal muscle research have been reviewed in depth (Barstow, 2019). The OxiplexTS consists of one detector fiber bundle and eight light-emitting diodes (LED) operating at wavelengths of 690 and 830 nm (four LEDs per wavelength). The LED-detector fiber bundle separation distances are 2.5, 3.0, 3.5, and 4.0 cm. This system was originally designed for cerebral oxygenation applications where hemoglobin is the predominant chromophore. To provide units equivalent to hemoglobin concentrations, the raw FD-NIRS signals were divided by a factor of 4 in the system's software. However, in skeletal muscle intracellular myoglobin becomes a significant source of the FD-NIRS oxygenation signals (Davis & Barstow, 2008). Therefore, the output variable signals from this study were multiplied by a factor of 4 to return the data into raw units of [heme] (Craig *et al.*, 2014; Hammer *et al.*, 2018). FD-NIRS data were collected continuously at 50 Hz. Total-[heme] was calculated as deoxy-[heme] + oxy-[heme]. Tissue oxygen saturation (S_tO_2) was calculated as (oxy-[heme]/total-[heme]) × 100. All FD-NIRS signals were analyzed using 20 s time-binned averages.

Statistical Analysis

SigmaStat (Systat Software; Point Richmond, CA) was used to perform statistical analysis. Data are expressed as means ± standard deviation unless otherwise noted. Linear regression was used to describe changes in average contraction force at the end of the MET and predict $\dot{Q}_{BA}$ of severe-intensity exercise tests. One-way ANOVAs with repeated measures were used to test for changes in FD-NIRS measurements during the MET and differences between actual and predicted end-exercise $\dot{Q}_{BA}$ during S1 and S2. Two-way ANOVAs with repeated measures were used to test for differences in Doppler ultrasound and FD-NIRS measurements at rest and end-exercise among tests. When a significant overall effect was detected, a Tukey's post hoc analysis was performed to determine where significant differences existed. Results were considered statistically significant when $p < 0.05$.

Results

Maximal-effort tests (METs). Average contraction force decreased progressively during the MET until the final ~ 60 s. The raw force profile of a representative subject is displayed in Figure 1. Linear regression of the average contraction force during the CF-determination interval of each individual test (final 10 contractions) revealed a slope of 0.2 N/contraction (range: -1.9 - 1.6 N/contraction) which was not statistically different from zero ($p = 0.42$). Additionally, the CV of average contraction force among the final 10 contractions was < 8% of CF for each subject. These findings indicate a plateau in force production and low inter-contraction variability during the CF-determination timeframe. CF was 189.3 ± 16.7 N (29.7 ± 1.6 % MVC). The temporal profiles of FD-NIRS measurements during the MET are displayed in Figure 2. FD-NIRS variables reached values not different from end-exercise within 60-80 s. Oxy-[heme] and S_tO_2 decreased significantly from rest (281 ± 75 μM; 77.7 ± 3.3 %) to end-exercise (253 ± 57 μM; 62.3 ± 6.7 %; both $p < 0.001$). Deoxy-[heme] and total-[heme] increased significantly from rest (77.3 ± 13.5 μM; 358 ± 84 μM) to end-exercise (153 ± 48 μM; 406.5 ± 86.5 μM; both $p < 0.001$). Unfortunately, the maximal-effort nature of contractions during the MET precluded Doppler ultrasound measurements of sufficient quality for data analysis.

Constant target-force tests. Characteristics of the constant target-force tests are listed in Table 1.

Doppler ultrasound. The temporal profiles of $\dot{Q}_{BA}$ during the constant target-force tests are displayed in Figure 3. No differences in resting $\dot{Q}_{BA}$ were detected among tests. $\dot{Q}_{BA}$ increased significantly from rest to end-exercise during all intensities (all $p < 0.01$). $\dot{Q}_{BA}$ at end-exercise was greater during H2 (340 ± 116 mL/min) than during H1 (287 ± 97 mL/min; $p = 0.019$), greater during tests above CF (S1: 418 ± 147 mL/min; S2: 403 ± 137 mL/min) than during H2 ($p = 0.004$), and was not different between S1 and S2 ($p = 0.83$) suggesting a maximum in limb blood flow during exercise above CF. Additionally, there were no significant differences in end-exercise $\dot{Q}_{BA}$ among tests above CF and estimated $\dot{Q}_{BA}$ at CF (392 ± 37 mL/min) predicted by linear regression of H1 and H2 end-exercise values (Figure 4).

FD-NIRS. The temporal profiles of FD-NIRS measurements during the constant target-force tests are displayed in Figure 5. No differences in resting FD-NIRS measurements were detected among tests. Oxy-[heme] did not significantly change during exercise at any intensity and was not statistically different at end-exercise (H1: 251 ± 45 μM; H2: 260 ± 43 μM; S1: 254 ± 29 μM; S2: 244 ± 47 μM) from oxy-[heme] at the end of the MET. Deoxy-[heme] increased significantly from rest to end-exercise (H1: 101 ± 24 μM; H2: 111 ± 21 μM; S1: 150 ± 50 μM; S2: 155 ± 57 μM) at all intensities (all $p < 0.01$). Total-[heme] increased significantly from rest to end-exercise (H1: 352 ± 58 μM; H2: 371 ± 57 μM; S1: 404 ± 58 μM; S2: 397 ± 73 μM) at all intensities (all $p < 0.01$). S_tO_2 decreased significantly from rest to end-exercise (H1: 70.2 ± 4.6 %; H2: 69.7 ± 3.2 %; S1: 63.4 ± 7.5 %; S2: 61.9 ± 8.1 %) at all intensities (all $p < 0.01$). At end-exercise, there were no differences between H1 and H2, or between S1 and S2 in deoxy-[heme], total-[heme], or S_tO_2. At end-exercise, deoxy-[heme] was greater during tests above CF compared to tests below CF (all $p < 0.05$) but was not statistically different from deoxy-[heme] at the end of the MET. Total-[heme] was greater during tests above CF compared to H1 (both $p < 0.01$) but not H2 and was not statistically different from total-[heme] at the end of the MET. Finally, S_tO_2 was lower during tests above CF compared to tests below CF (all $p < 0.05$) and was not statistically different from S_tO_2 at the end of the MET.

Discussion

Major Findings

The principal novel finding of this study was that CF is an important threshold for limb blood flow and muscle microvascular oxygen delivery responses during small muscle mass exercise in humans. Consistent with our hypothesis, there were no differences in end-exercise $\dot{Q}_{BA}$, deoxy-[heme], or total-[heme] among handgrip intensities above CF, suggesting respective task-specific physiological maximums within the severe-intensity domain (Figures 3 and 5). Additionally, end-exercise $\dot{Q}_{BA}$ in the severe-intensity domain demonstrated a physiological plateau that was not different than the $\dot{Q}_{BA}$ estimated for CF (Figure 4). Thus, $\dot{Q}_{BA}$ at end-exercise above CF was disproportionately lower than predicted from tests below CF in the majority of subjects. Combined, these findings suggest that CF represents a threshold in relative muscular force that limits skeletal muscle perfusion and oxygen extraction during exercise.

Limb blood flow responses surrounding CF. $\dot{Q}_{BA}$ responses to severe-intensity exercise (above CF) were distinct from those during heavy-intensity exercise (below CF; Figure 3). Increasing force production below CF resulted in concurrent increases in end-exercise $\dot{Q}_{BA}$. However, severe-intensity exercise (above CF) elicited an end-exercise $\dot{Q}_{BA}$ which was not different from $\dot{Q}_{BA}$ predicted for CF regardless of force requirements (Figure 4). These findings suggest that $\dot{Q}_{BA}$ reaches a task-specific (i.e., exercise modality, duty cycle, etc.) physiological maximal above CF. Simply stated, exercise hyperemia is determined by the ratio of vascular driving pressure (i.e., blood pressure) to downstream vascular resistance. During exercise, a cohort of vasoactive intermediaries (e.g., nitric oxide, adenosine, and other metabolites) reduce vascular resistance and facilitate flow despite opposition from limiting factors such as sympathetically mediated vasoconstriction and mechanical vascular compression (Tschakovsky *et al.*, 2002; Caldwell *et al.*, 2018). Rhythmic exercise is defined by oscillations in muscular force generation and therefore intramuscular pressures that, when substantially high, lead to mechanical vascular compression (Sadamoto *et al.*, 1983; Robergs *et al.*, 1997; Lutjemeier *et al.*, 2005). End-exercise $\dot{Q}_{BA}$ values from the present study are similar to previous measurements during severe-intensity dynamic handgrip exercise at the same duty-cycle and contraction frequency (50%; 20 contraction per min) (Broxterman *et al.*, 2014). When relaxation-time was increased through duty-cycle alterations at the same power output, ~25% greater time-matched $\dot{Q}_{BA}$ values were observed and exercise was significantly more tolerable (Broxterman *et al.*, 2014). These observations lend credence to a significant contribution of intramuscular pressure-induced impedance to muscle blood flow in the severe-intensity-domain. Indeed, immediate increases in $\dot{Q}_{BA}$ during early recovery suggest that $\dot{Q}_{BA}$ was limited during handgrip exercise utilizing a 50%, but not 20%, duty-cycle (Broxterman *et al.*, 2014). Likewise, immediate increases in limb vascular conductance following knee-extension exercise suggest muscular contraction-induced impedance to muscle perfusion at higher exercise intensities (Lutjemeier *et al.*, 2005).Limitations in muscle perfusion must be compensated for by increases in fractional oxygen extraction in order to sustain a given metabolic rate (i.e., $\dot{V}O_2$).

Data from this study support a task-specific (i.e., exercise modality, duty cycle, etc.) physiological maximum during severe-intensity exercise not only in limb blood flow (i.e., $\dot{Q}_{BA}$; Figures 3 and 4) but also fractional oxygen extraction (i.e., deoxy-[heme]; Figure 5B) and microvascular hematocrit (i.e., total-[heme]; Figure 5C). Combined with decreased RBC transit time (i.e., increased flow), the ~50 % greater fractional oxygen extraction during exercise above CF, compared to below, suggests enhanced longitudinal capillary recruitment (Poole *et al.*, 2011).

Indeed, increases in limb blood flow can augment microvascular oxygen extraction (Richardson *et al.*, 1993). Although in the present study $\dot{Q}_{BA}$ and deoxy-[heme] were greater during severe- compared to heavy-intensity exercise, the tendency for disproportionately lower $\dot{Q}_{BA}$ than predicted from heavy-intensity exercise tests among subjects (Figure 4) suggests a muscular perfusion limitation. Increasing relaxation time is likely to increase maximal $\dot{Q}_{BA}$ (Broxterman *et al.*, 2014; Bentley *et al.*, 2017) and potentially augment the extraction of oxygen through additional longitudinal recruitment (Richardson *et al.*, 1993; Poole *et al.*, 2011). Additionally, the propensity for microvascular hematocrit, and therefore surface area for diffusion, to be elevated above CF, compared to below, corroborates an increased diffusive capacity (DO_2) of the exercising muscles (Kindig *et al.*, 2002; Poole *et al.*, 2011) (Figure 5C).

Muscle microvascular oxygen delivery. Interestingly, FD-NIRS indices of microvascular oxygen delivery within the FDS muscle reached end-exercise values within ~ 60-80 s of MET exercise onset (Figure 2). These responses are similar to $\dot{V}O_2$ (Burnley *et al.*, 2006; Vanhatalo *et al.*, 2011) and oxidative ATP synthesis rate (Broxterman *et al.*, 2017) responses during all-out cycling and knee-extension exercise, respectively. During maximal-effort exercise, reduced maximal force production is likely consequential to progressive decruitment of motor units as a result of skeletal muscle fatigue development despite conservation of $\dot{V}O_{2max}$ (Zoladz *et al.*, 2008; Vanhatalo *et al.*, 2011; Vanhatalo *et al.*, 2016). Indeed, Vanhatalo et al. demonstrated a progressive decline in absolute integrated electromyography signal of the vastus lateralis muscle during maximal-effort cycling exercise indicating decruitment of initially active motor units (Vanhatalo *et al.*, 2011). These no longer activated muscle fibers, although perhaps not contributing appreciably to force generation, have been speculated to maintain an oxygen requirement associated with recovery processes (Pringle *et al.*, 2003). Burnley et al. demonstrated that metabolic perturbations during maximal-effort exercise are not unique to those that, at least in part, determine exercise tolerance during exhaustive constant-force tests (Burnley *et al.*, 2010). Additionally, a common tolerance level for intramuscular metabolic instability among severe-exercise intensities has been linked with determinate peripheral fatigue development within individual muscles (Jones *et al.*, 2008; Vanhatalo *et al.*, 2010; Burnley *et al.*, 2012). These findings support a strong mechanistic link between the force generating capability of skeletal muscle and the intramuscular metabolic milieu (Broxterman *et al.*, 2017). The deoxy-[heme] signal is a reflection of the microvascular-to-myocyte oxygen driving pressure (i.e., microvascular PO_2) (Grassi *et al.*, 2003). Matching $\dot{Q}O_2$-to-$\dot{V}O_2$, thereby maintaining a substantially high microvascular PO_2, is critical to minimize intramuscular metabolic disturbances and subsequent functional consequences (Wilson *et al.*, 1977; McDonough *et al.*, 2005). Therefore, the evident ceiling for microvascular oxygen delivery during the MET in this study (Figure 2) is likely concomitant with progressive intramuscular metabolic perturbations.

Consistent with previous data (Broxterman *et al.*, 2015), measurements of muscle microvascular oxygen delivery reached a common end-exercise value during severe-intensity exercise tests (Figure 5). Importantly, these values were not different from the end-test values of the MET. Under conditions where $\dot{V}O_2$ remains constant, such as at $\dot{V}O_{2max}$ during maximal-effort exercise (Burnley *et al.*, 2006; Vanhatalo *et al.*, 2011), deoxy-[heme] indicates the level of microvascular fractional oxygen extraction (i.e., $\dot{Q}O_2$-to-$\dot{V}O_2$ matching) (DeLorey *et al.*, 2003; Grassi *et al.*, 2003; Ferreira *et al.*, 2006). Figure 2 shows that deoxy-[heme] reached peak values rapidly and that these values were maintained while force production continued to fall until reaching a sustainable level (i.e., CF; Figure 1). Remarkably, during severe-intensity exercise, when force requirements are above CF, exercise was tolerable until the same level of fractional oxygen extraction was reached (Figure 5). Task failure was subsequently manifest by reductions in maximal force production below the respective target-forces. These data suggest that CF, and exercise tolerance in the severe-intensity domain, are determined, at least in part, by factors governing $\dot{Q}O_2$-to-$\dot{V}O_2$ matching within exercising muscles. Consistent with this notion, Okushima et al. described the temporal and spatial heterogeneity of oxygen extraction among and within muscle of the leg (Okushima *et al.*, 2015). It was concluded that, while whole limb oxygen extraction may not be limiting (Mortensen *et al.*, 2005), regional limitations in oxygen extraction may exist (Okushima *et al.*, 2015). Combined, these data suggest that discrete limitations in regional oxygen extraction capacities within skeletal muscles may precipitate exercise intolerance above CF.

Experimental Considerations

This study utilized a forearm model of exercise to maximize Doppler ultrasound measurement quality and increase the relative proportion of muscle volume for FD-NIRS measurements. It is important to consider the implications of these findings during whole-body exercise when cardiovascular and pulmonary limits become more important and intramuscular limitations may play a lesser role in determining exercise tolerance compared to small muscle mass exercise. Additionally, similar to heterogeneity within and among muscles of the thigh (Chin *et al.*, 2011; Okushima *et al.*, 2015; Vogiatzis *et al.*, 2015), variability in recruitment patterns (Hammer *et al.*, 2018) and tissue oxygenation in muscles of the forearm must be considered. During incremental exercise, it becomes apparent that limitations to performance are indeed, at a minimum, muscle-region specific (Chin *et al.*, 2011; Okushima *et al.*, 2015; Hammer *et al.*, 2018). A recent shift in the whole-limb oxygen delivery paradigm is supported by evidence of additional muscle recruitment secondary to microvascular oxygen delivery plateaus in individual muscle regions during incremental exercise (Chin *et al.*, 2011; Hammer *et al.*, 2018). Unfortunately, measurements of muscle recruitment (i.e., electromyography) were not logistically able to be made in this study. Future studies should aim to characterize muscle recruitment heterogeneity during maximal-effort and constant-force tests to elucidate physiological consequences to muscle-specific oxygen extraction limitations.

Lutjemeier et al. provided evidence supporting muscular contraction-induced impedance to muscle blood flow through increases in limb vascular conductance during the early recovery phase of upright knee-extension exercise (Lutjemeier *et al.*, 2005). Specifically, during higher exercise intensities, blood flow remained unchanged during early recovery while mean arterial pressure (MAP) decreased, suggesting the muscle vasculature was more compliant when the influence of muscular contraction was removed. Due to the physical strain of subjects during the severe-intensity exercise bouts, oscillometric blood pressure measurements were not reliably obtained during this study. It is possible that during exercise above CF, the plateau in end-exercise $\dot{Q}_{BA}$ was a result of inadequate increases in MAP, as opposed to muscular-contraction induced impedance *per se*. While the data from this study cannot substantiate or refute this interpretation, limb vascular conductance measurements during severe-intensity exercise in future studies might elucidate indications of muscular contraction-induced blood flow impedance as a determinant of CF.

Conclusions

This study determined that CF is an important determinant of limb blood flow responses to exercise. Specifically, $\dot{Q}_{BA}$ reached a task-specific (i.e., exercise modality, duty cycle, etc.) physiological maximum during severe-intensity exercise (above CF) that was not significantly different from $\dot{Q}_{BA}$ predicted at CF. Consequently, end-exercise $\dot{Q}_{BA}$ above CF was disproportionately lower than predicted from tests below CF in the majority of subjects and muscle fractional oxygen extraction reached a critical limit wherein exercise was no longer tolerable. Maximal-effort exercise revealed that this level of extraction was only sufficient to sustain force generation at CF. Collectively, these findings accentuate the physiological significance of the heavy-to-severe intensity exercise threshold with regard to exercise tolerance and suggest limitations in muscle perfusion through increased muscular force generation may play a major role in its determination.

References

Ade CJ, Broxterman RM, Wong BJ & Barstow TJ. (2012). Anterograde and retrograde blood velocity profiles in the intact human cardiovascular system. *Experimental physiology* 97, 849-860.

Andersen P & Saltin B. (1985). Maximal perfusion of skeletal muscle in man. *J Physiol* 366, 233-249.

Armstrong RB & Laughlin MH. (1985). Rat muscle blood flows during high-speed locomotion. *Journal of applied physiology (Bethesda, Md : 1985)* 59, 1322-1328.

Barstow TJ. (2019). Understanding near infrared spectroscopy and its application to skeletal muscle research. *J Appl Physiol* 126, 1360-1376.

Barstow TJ, Jones AM, Nguyen PH & Casaburi R. (1996). Influence of muscle fiber type and pedal frequency on oxygen uptake kinetics of heavy exercise. *J Appl Physiol* 81, 1642-1650.

Behnke BJ, McDonough P, Padilla DJ, Musch TI & Poole DC. (2003). Oxygen exchange profile in rat muscles of contrasting fibre types. *J Physiol* 549, 597-605.

Bentley RF, Poitras VJ, Hong T & Tschakovsky ME. (2017). Characteristics and effectiveness of vasodilatory and pressor compensation for reduced relaxation time during rhythmic forearm contractions. *Experimental Physiology* 102, 621-634.

Boushel R, Langberg H, Gemmer C, Olesen J, Crameri R, Scheede C, Sander M & Kjaer M. (2002). Combined inhibition of nitric oxide and prostaglandins reduces human skeletal muscle blood flow during exercise. *J Physiol* 543, 691-698.

Broxterman RM, Ade CJ, Craig JC, Wilcox SL, Schlup SJ & Barstow TJ. (2015). Influence of blood flow occlusion on muscle oxygenation characteristics and the parameters of the power-duration relationship. *Journal of applied physiology (Bethesda, Md : 1985)* 118, 880-889.

Broxterman RM, Ade CJ, Wilcox SL, Schlup SJ, Craig JC & Barstow TJ. (2014). Influence of duty cycle on the power-duration relationship: observations and potential mechanisms. *Respir Physiol Neurobiol* 192, 102-111.

Broxterman RM, Layec G, Hureau TJ, Amann M & Richardson RS. (2017). Skeletal muscle bioenergetics during all-out exercise: mechanistic insight into the oxygen uptake slow component and neuromuscular fatigue. *J Appl Physiol* 122, 1208-1217.

Burnley M. (2009). Estimation of critical torque using intermittent isometric maximal voluntary contractions of the quadriceps in humans. *J Appl Physiol* 106, 975-983.

Burnley M, Doust JH & Vanhatalo A. (2006). A 3-min all-out test to determine peak oxygen uptake and the maximal steady state. *Med Sci Sport Exer* 38, 1995-2003.

Burnley M, Vanhatalo A, Fulford J & Jones AM. (2010). Similar metabolic perturbations during all-out and constant force exhaustive exercise in humans: a 31P magnetic resonance spectroscopy study. *Experimental Physiology* 95, 798-807.

Burnley M, Vanhatalo A & Jones AM. (2012). Distinct profiles of neuromuscular fatigue during muscle contractions below and above the critical torque in humans. *J Appl Physiol* 113, 215-223.

Caldwell JT, Sutterfield SL, Post HK, Lovoy GM, Banister HR, Hammer SM & Ade CJ. (2018). Vasoconstrictor responsiveness through alterations in relaxation time and metabolic rate during rhythmic handgrip contractions. *Physiol Rep* 6, e13933.

Chin LM, Kowalchuk JM, Barstow TJ, Kondo N, Amano T, Shiojiri T & Koga S. (2011). The relationship between muscle deoxygenation and activation in different muscles of the quadriceps during cycle ramp exercise. *Journal of applied physiology (Bethesda, Md : 1985)* 111, 1259-1265.

Copp SW, Hirai DM, Hageman KS, Poole DC & Musch TI. (2010a). Nitric oxide synthase inhibition during treadmill exercise reveals fiber-type specific vascular control in the rat hindlimb (vol 298, pg R478, 2010). *Am J Physiol-Reg I* 298, R849-R849.

Copp SW, Hirai DM, Musch TI & Poole DC. (2010b). Critical speed in the rat: implications for hindlimb muscle blood flow distribution and fibre recruitment. *J Physiol-London* 588, 5077-5087.

Copp SW, Hirai DM, Schwagerl PJ, Musch TI & Poole DC. (2010c). Effects of neuronal nitric oxide synthase inhibition on resting and exercising hindlimb muscle blood flow in the rat. *J Physiol-London* 588, 1321-1331.

Craig JC, Broxterman RM & Barstow TJ. (2014). Influence Of Adipose Tissue Thickness (ATT) On NIRS-derived Total [Hb plus Mb] At Four Sites. *Med Sci Sport Exer* 46, 356-356.

Davis ML & Barstow TJ. (2008). Estimated Influence of Myoglobin on NIRS Signals at Rest and During Exercise. *Med Sci Sport Exer* 40, S267-S267.

Davis ML & Barstow TJ. (2013). Estimated contribution of hemoglobin and myoglobin to near infrared spectroscopy. *Respir Physiol Neurobiol* 186, 180-187.

DeLorey DS, Kowalchuk JM & Paterson DH. (2003). Relationship between pulmonary O2 uptake kinetics and muscle deoxygenation during moderate-intensity exercise. *Journal of applied physiology (Bethesda, Md : 1985)* 95, 113-120.

Endo MY, Kobayakawa M, Kinugasa R, Kuno S, Akima H, Rossiter HB, Miura A & Fukuba Y. (2007). Thigh muscle activation distribution and pulmonary VO2 kinetics during moderate, heavy, and very heavy intensity cycling exercise in humans. *Am J Physiol-Reg I* 293, R812-R820.

Ferreira LF, Koga S & Barstow TJ. (2007). Dynamics of noninvasively estimated microvascular O2 extraction during ramp exercise. *J Appl Physiol (1985)* 103, 1999-2004.

Ferreira LF, Lutjemeier BJ, Townsend DK & Barstow TJ. (2006). Effects of pedal frequency on estimated muscle microvascular O-2 extraction. *Eur J Appl Physiol* 96, 558-563.

Grassi B, Pogliaghi S, Rampichini S, Quaresima V, Ferrari M, Marconi C & Cerretelli P. (2003). Muscle oxygenation and pulmonary gas exchange kinetics during cycling exercise on-transitions in humans. *Journal of applied physiology (Bethesda, Md : 1985)* 95, 149-158.

Gratton E, Fantini S, Franceschini MA, Gratton G & Fabiani M. (1997). Measurements of scattering and absorption changes in muscle and brain. *Philos Trans R Soc Lond B Biol Sci* 352, 727-735.

Habazettl H, Athanasopoulos D, Kuebler WM, Wagner H, Roussos C, Wagner PD, Ungruhe J, Zakynthinos S & Vogiatzis I. (2010). Near-infrared spectroscopy and indocyanine green derived blood flow index for noninvasive measurement of muscle perfusion during exercise. *Journal of applied physiology (Bethesda, Md : 1985)* 108, 962-967.

Hammer SM, Alexander AM, Didier KD, Smith JR, Caldwell JT, Sutterfield SL, Ade CJ & Barstow TJ. (2018). The noninvasive simultaneous measurement of tissue oxygenation and microvascular hemodynamics during incremental handgrip exercise. *J Appl Physiol* 124, 604-614.

Hammer SM, Hueber DM, Townsend DK, Huckaby LM, Alexander AM, Didier KD & Barstow TJ. (2019). Effect of assuming constant tissue scattering on measured tissue oxygenation values during tissue ischemia and vascular reperfusion. *J Appl Physiol* 127, 22-30.

Hepple RT, Howlett RA, Kindig CA, Stary CM & Hogan MC. (2010). The O-2 cost of the tension-time integral in isolated single myocytes during fatigue. *Am J Physiol-Reg I* 298, R983-R988.

Jones AM, Vanhatalo A, Burnley M, Morton RH & Poole DC. (2010). Critical power: implications for determination of V O2max and exercise tolerance. *Med Sci Sports Exerc* 42, 1876-1890.

Jones AM, Wilkerson DP, DiMenna F, Fulford J & Poole DC. (2008). Muscle metabolic responses to exercise above and below the "critical power" assessed using 31P-MRS. *American journal of physiology Regulatory, integrative and comparative physiology* 294, R585-593.

Kellawan JM & Tschakovsky ME. (2014). The single-bout forearm critical force test: a new method to establish forearm aerobic metabolic exercise intensity and capacity. *PLoS One* 9, e93481.

Kindig CA, Richardson TE & Poole DC. (2002). Skeletal muscle capillary hemodynamics from rest to contractions: implications for oxygen transfer. *Journal of applied physiology (Bethesda, Md : 1985)* 92, 2513-2520.

Koga S, Rossiter HB, Heinonen I, Musch TI & Poole DC. (2014). Dynamic heterogeneity of exercising muscle blood flow and O2 utilization. *Medicine and science in sports and exercise* 46, 860-876.

Krustrup P, Soderlund K, Mohr M & Bangsbo J. (2004). The slow component of oxygen uptake during intense, sub-maximal exercise in man is associated with additional fibre recruitment. *Pflug Arch Eur J Phy* 447, 855-866.

Limberg JK, Casey DP, Trinity JD, Nicholson WT, Wray DW, Tschakovsky ME, Green DJ, Hellsten Y, Fadel PJ, Joyner MJ & Padilla J. (2020). Assessment of resistance vessel function in human skeletal muscle: guidelines for experimental design, Doppler ultrasound, and pharmacology. *Am J Physiol-Heart C* 318, H301-H325.

Limberg JK, Eldridge MW, Proctor LT, Sebranek JJ & Schrage WG. (2010). Alpha-adrenergic control of blood flow during exercise: effect of sex and menstrual phase. *Journal of applied physiology (Bethesda, Md : 1985)* 109, 1360-1368.

Lutjemeier BJ, Miura A, Scheuermann BW, Koga S, Townsend DK & Barstow TJ. (2005). Muscle contraction-blood flow interactions during upright knee extension exercise in humans. *Journal of applied physiology (Bethesda, Md : 1985)* 98, 1575-1583.

McDonough P, Behnke BJ, Padilla DJ, Musch TI & Poole DC. (2005). Control of microvascular oxygen pressures in rat muscles comprised of different fibre types. *J Physiol-London* 563, 903-913.

Mortensen SP, Dawson EA, Yoshiga CC, Dalsgaard MK, Damsgaard R, Secher NH & Gonzalez-Alonso J. (2005). Limitations to systemic and locomotor limb muscle oxygen delivery and uptake during maximal exercise in humans. *J Physiol* 566, 273-285.

Okushima D, Poole DC, Barstow TJ, Rossiter HB, Kondo N, Bowen TS, Amano T & Koga S. (2016). Greater (V)over dotO(2peak) is correlated with greater skeletal muscle deoxygenation amplitude and hemoglobin concentration within individual muscles during ramp-incremental cycle exercise. *Physiological Reports* 4.

Okushima D, Poole DC, Rossiter HB, Barstow TJ, Kondo N, Ohmae E & Koga S. (2015). Muscle deoxygenation in the quadriceps during ramp incremental cycling: Deep vs. superficial heterogeneity. *Journal of applied physiology (Bethesda, Md : 1985)* 119, 1313-1319.

Poole DC, Burnley M, Vanhatalo A, Rossiter HB & Jones AM. (2016). Critical Power: An Important Fatigue Threshold in Exercise Physiology. *Med Sci Sports Exerc* 48, 2320-2334.

Poole DC, Copp SW, Hirai DM & Musch TI. (2011). Dynamics of muscle microcirculatory and blood-myocyte O-2 flux during contractions. *Acta Physiol* 202, 293-310.

Poole DC, Schaffartzik W, Knight DR, Derion T, Kennedy B, Guy HJ, Prediletto R & Wagner PD. (1991). Contribution of Exercising Legs to the Slow Component of Oxygen-Uptake Kinetics in Humans. *J Appl Physiol* 71, 1245-1253.

Poole DC, Ward SA, Gardner GW & Whipp BJ. (1988). Metabolic and respiratory profile of the upper limit for prolonged exercise in man. *Ergonomics* 31, 1265-1279.

Pringle JSM, Doust JH, Carter H, Tolfrey K & Jones AM. (2003). Effect of pedal rate on primary and slow-component oxygen uptake responses during heavy-cycle exercise. *J Appl Physiol* 94, 1501-1507.

Richardson RS, Poole DC, Knight DR, Kurdak SS, Hogan MC, Grassi B, Johnson EC, Kendrick KF, Erickson BK & Wagner PD. (1993). High muscle blood flow in man: is maximal O2 extraction compromised? *Journal of applied physiology (Bethesda, Md : 1985)* 75, 1911-1916.

Robergs RA, Icenogle MV, Hudson TL & Greene ER. (1997). Temporal inhomogeneity in brachial artery blood flow during forearm exercise. *Med Sci Sport Exer* 29, 1021-1027.

Rossiter HB, Ward SA, Kowalchuk JM, Howe FA, Griffiths JR & Whipp BJ. (2002). Dynamic asymmetry of phosphocreatine concentration and O-2 uptake between the on- and off-transients of moderate- and high-intensity exercise in humans. *J Physiol-London* 541, 991-1002.

Sadamoto T, Bondepetersen F & Suzuki Y. (1983). Skeletal-Muscle Tension, Flow, Pressure, and Emg during Sustained Isometric Contractions in Humans. *Eur J Appl Physiol O* 51, 395-408.

Smith JR, Hageman KS, Harms CA, Poole DC & Musch TI. (2017). Respiratory muscle blood flow during exercise: Effects of sex and ovarian cycle. *Journal of applied physiology (Bethesda, Md : 1985)* 122, 918-924.

Tschakovsky ME, Sujirattanawimol K, Ruble SB, Valic Z & Joyner MJ. (2002). Is sympathetic neural vasoconstriction blunted in the vascular bed of exercising human muscle? *J Physiol-London* 541, 623-635.

Vanhatalo A, Black MI, DiMenna FJ, Blackwell JR, Schmidt JF, Thompson C, Wylie LJ, Mohr M, Bangsbo J, Krustrup P & Jones AM. (2016). The mechanistic bases of the power-time relationship: muscle metabolic responses and relationships to muscle fibre type. *J Physiol-London* 594, 4407-4423.

Vanhatalo A, Doust JH & Burnley M. (2007). Determination of critical power using a 3-min all-out cycling test. *Med Sci Sport Exer* 39, 548-555.

Vanhatalo A, Doust JH & Burnley M. (2008). A 3-min all-out cycling test is sensitive to a change in critical power. *Med Sci Sport Exer* 40, 1693-1699.

Vanhatalo A, Fulford J, DiMenna FJ & Jones AM. (2010). Influence of hyperoxia on muscle metabolic responses and the power-duration relationship during severe-intensity exercise in humans: a 31P magnetic resonance spectroscopy study. *Experimental Physiology* 95, 528-540.

Vanhatalo A, Poole DC, DiMenna FJ, Bailey SJ & Jones AM. (2011). Muscle fiber recruitment and the slow component of O-2 uptake: constant work rate vs. all-out sprint exercise. *Am J Physiol-Reg I* 300, R700-R707.

Vogiatzis I, Habazettl H, Louvaris Z, Andrianopoulos V, Wagner H, Zakynthinos S & Wagner PD. (2015). A method for assessing heterogeneity of blood flow and metabolism in exercising normal human muscle by near-infrared spectroscopy. *Journal of applied physiology (Bethesda, Md : 1985)* 118, 783-793.

Wilson DF, Erecinska M, Drown C & Silver IA. (1977). Effect of oxygen tension on cellular energetics. *Am J Physiol* 233, C135-140.

Zoladz JA, Gladden LB, Hogan MC, Nieckarz Z & Grassi B. (2008). Progressive recruitment of muscle fibers is not necessary for the slow component of (V)over-dot(O2) kinetics. *J Appl Physiol* 105, 575-580.

Table 2.1 Constant target-force exercise tests

	Target Force (N)	% MVC	T_{lim} (s)
H1	132.4 ± 51.0	20.7 ± 5.5	–
H2	160.9 ± 54.9	25.2 ± 5.4	–
CF	189.3 ± 16.7 *	29.7 ± 1.6	–
S1	218.8 ± 68.7	34.2 ± 6.5	598 ± 208
S2	247.2 ± 77.5	38.7 ± 7.5	346 ± 113

Values are means ± SD. CF, critical force; H1 and H2, exercise tests below CF (heavy-intensity); S1 and S2, exercise tests above CF (severe-intensity); target force, force requirement during each test; % MVC, % of peak force during the first 3 contractions of the maximal-effort test; T_{lim}, time to task failure. All subjects reached the 15-min cutoff for H1 and H2. *Average contraction force during the final 10 contractions of the maximal-effort test.

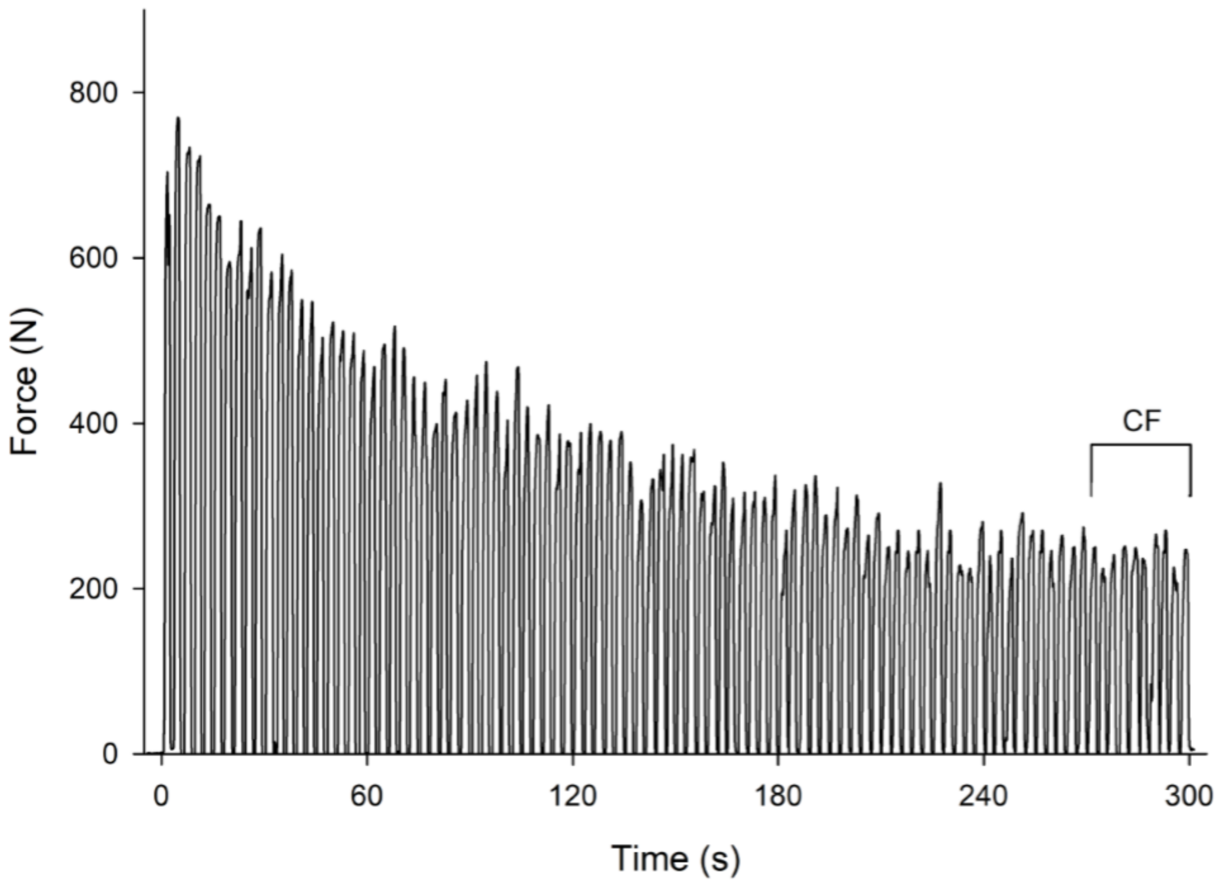

Figure 2.1 Raw force signal during a representative maximal-effort exercise test (MET).

Note the progressive decline in force generation until the final ~ 60 s. The timeframe for critical force (CF) determination is denoted by brackets surrounding the final 10 contractions (30 s) of the test. CF determined from this test was 233.6 N (30.7 % maximal voluntary contraction).

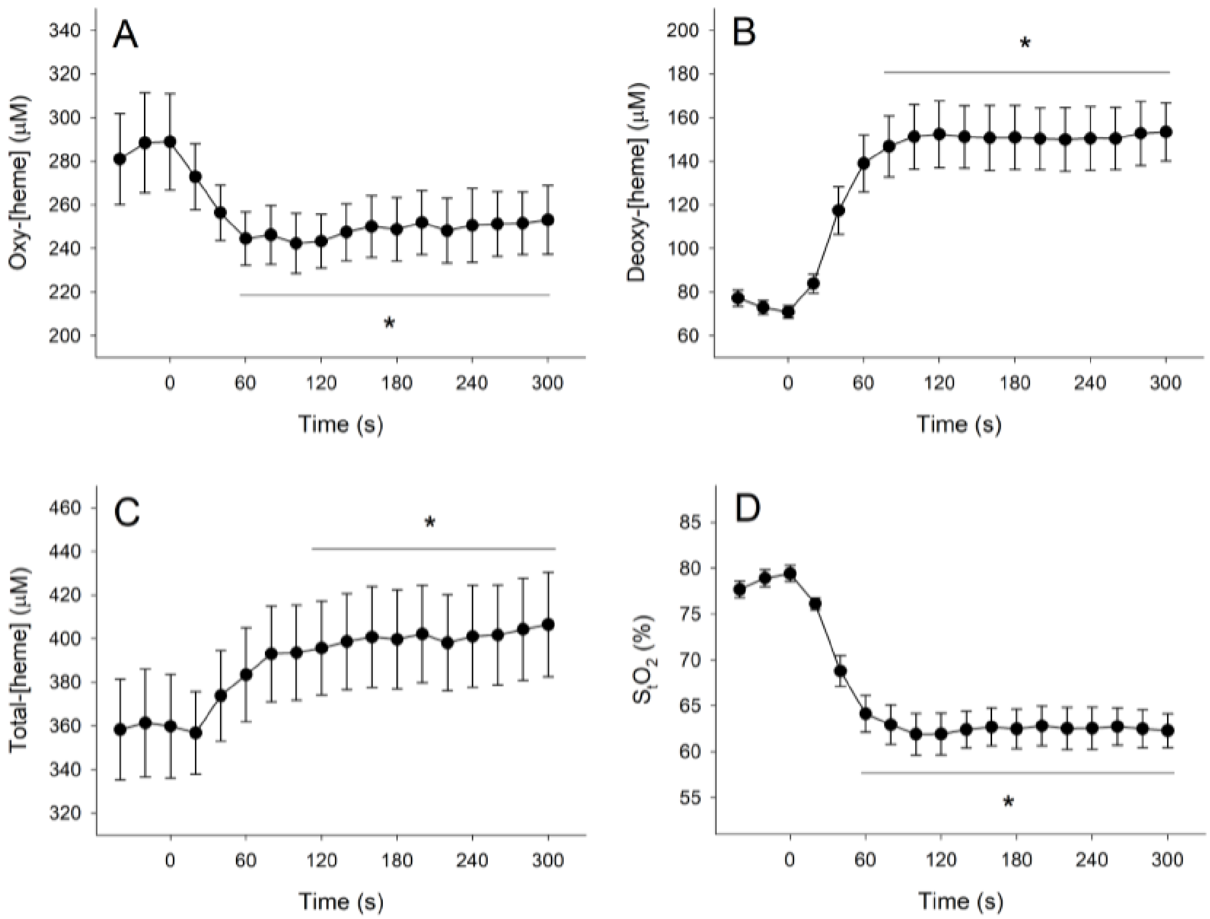

Figure 2.2 Mean frequency-domain near-infrared spectroscopy (FD-NIRS) data during the maximal-effort exercise tests (METs).

Shown are temporal responses of oxygenated- (oxy-[heme]; A), deoxygenated- (deoxy-[heme]; B), and total- (total-[heme]; C) heme concentrations with percent tissue saturation (S_tO_2; D) during the 5-min exercise test. Values are means ± standard error. * Significantly different from rest ($p < 0.001$) and not statistically different from end-exercise. Note the FD-NIRS signals reach end-exercise-like values within ~ 60-80 s.

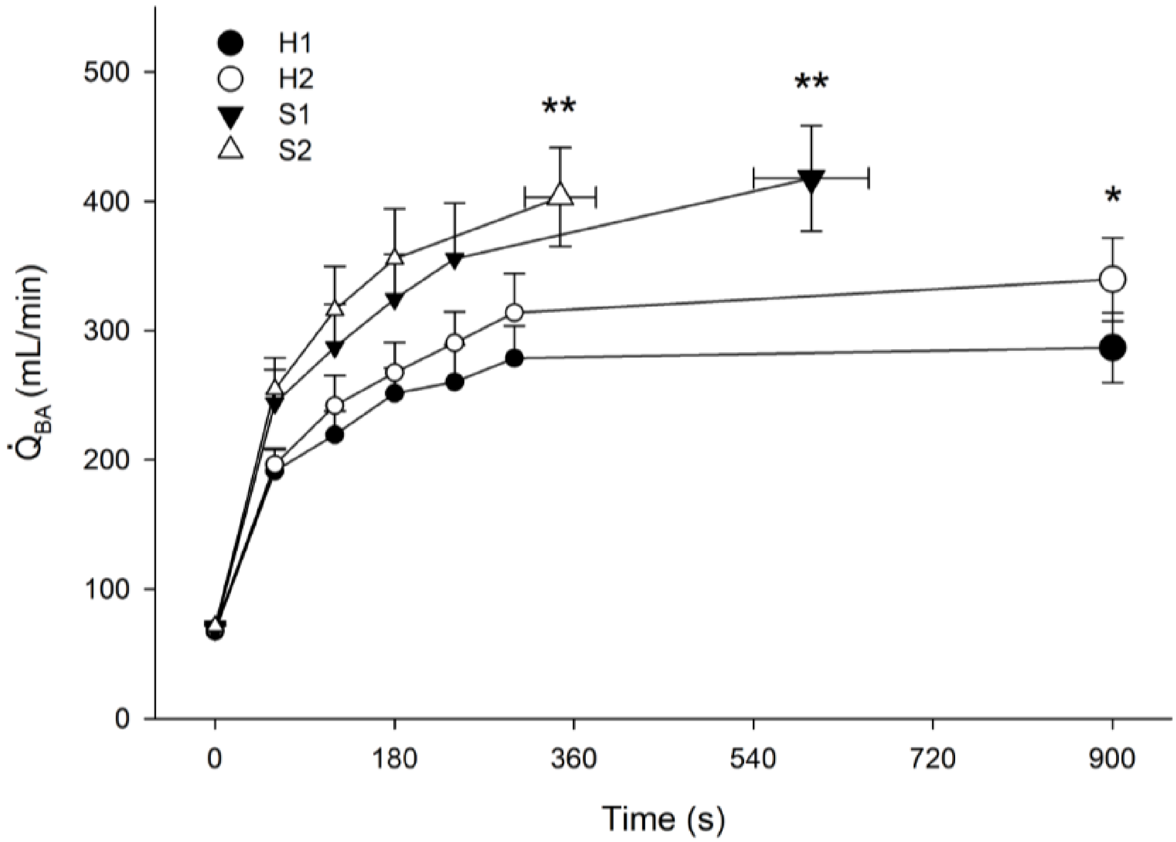

Figure 2.3 Brachial artery blood flow ($\dot{Q}_{BA}$) responses during the constant target-force tests.

Temporal $\dot{Q}_{BA}$ data from exercise below (● H1 and ○ H2) and above (▼ S1 and Δ S2) critical force (CF). * Significantly greater than $\dot{Q}_{BA}$ at end-exercise during H1 ($p < 0.05$). ** Significantly greater than $\dot{Q}_{BA}$ at end-exercise during H2 ($p < 0.05$).

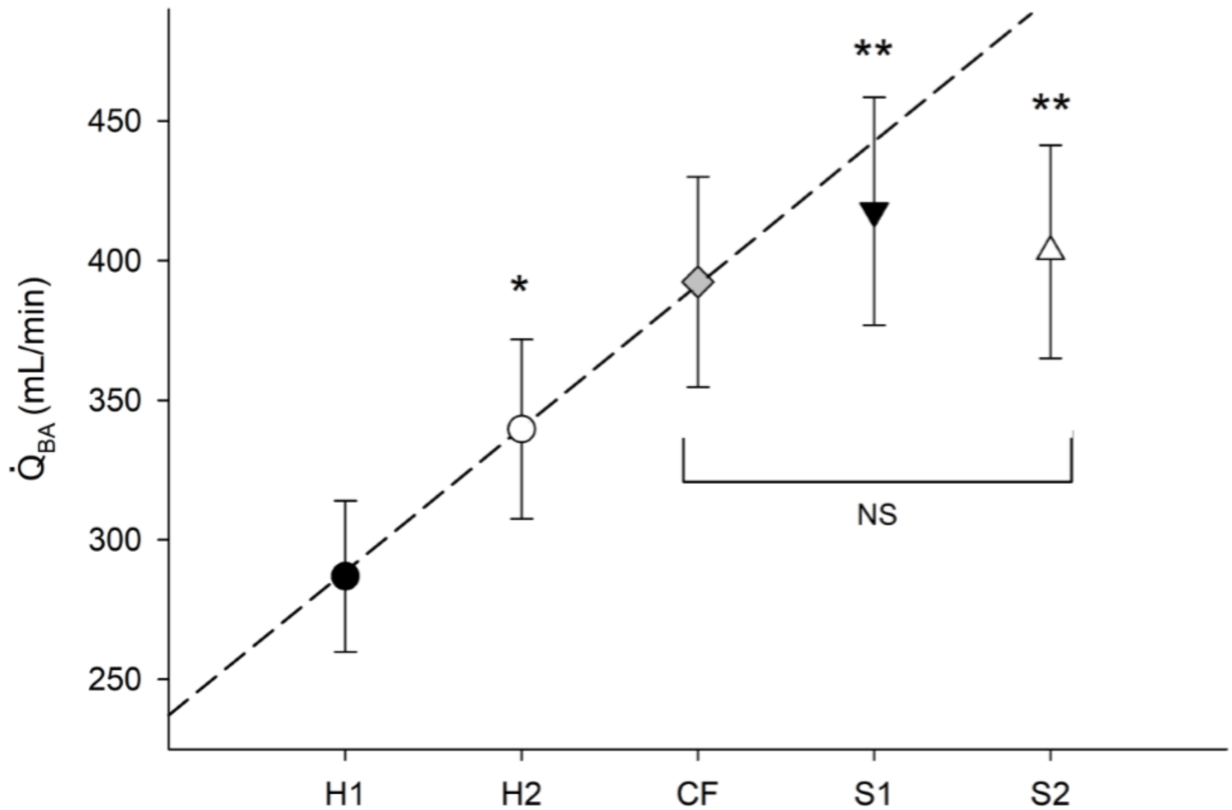

Figure 2.4 End-exercise brachial artery blood flow ($\dot{Q}_{BA}$) values from the constant target-force tests.

$\dot{Q}_{BA}$ at end-exercise below (● H1 and ○ H2) and above (▼ S1 and ∆ S2) critical force (CF, and $\dot{Q}_{BA}$ predicted at CF by linear regression of H1 and H2 end-exercise $\dot{Q}_{BA}$ measurements (♦). * Significantly greater than $\dot{Q}_{BA}$ at end-exercise during H1 ($p < 0.05$). ** Significantly greater than $\dot{Q}_{BA}$ at end-exercise during H2 ($p < 0.05$). Note 1) no differences among end-exercise $\dot{Q}_{BA}$ values at (estimated) and above CF suggesting a maximal response in the severe-intensity domain and 2) the disproportionately lower $\dot{Q}_{BA}$ above CF compared to values predicted from tests below CF.

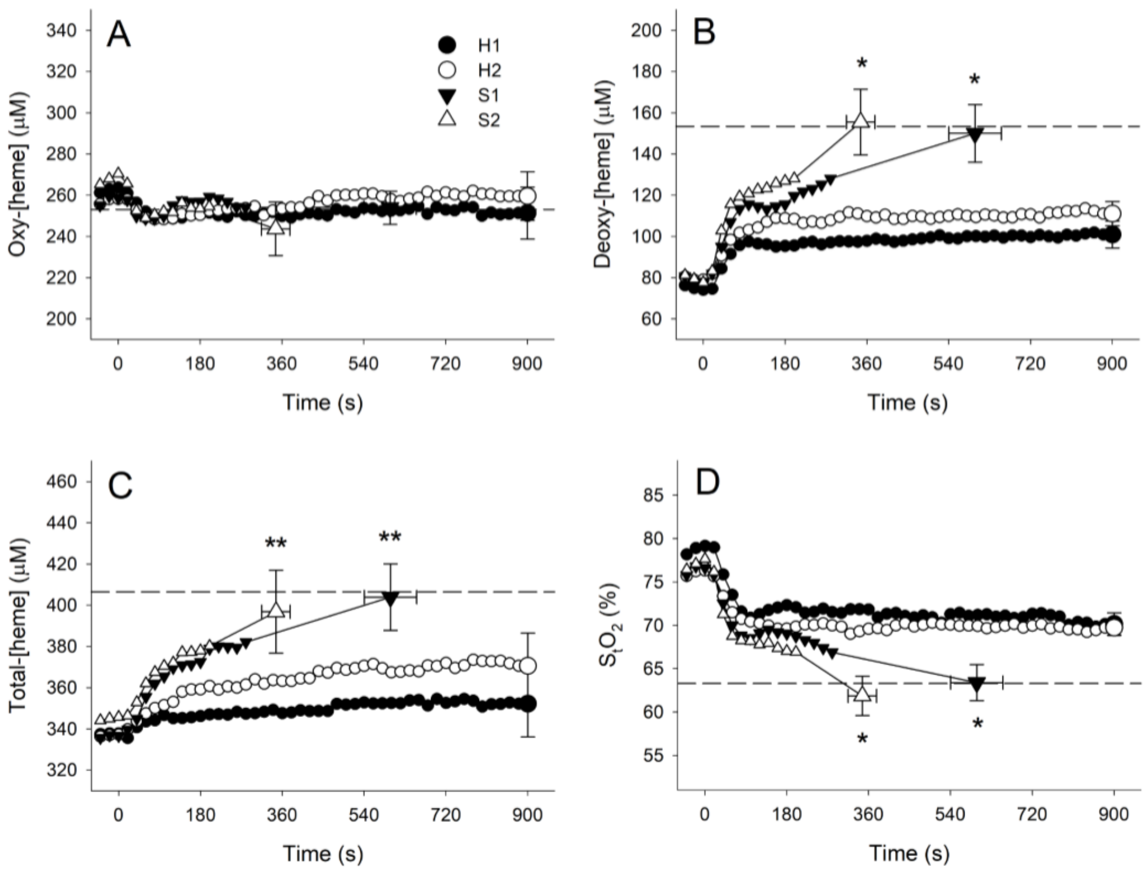

Figure 2.5 Frequency-domain near-infrared spectroscopy (FD-NIRS) measurements of muscle oxygenation during the constant target-force tests.

Shown are temporal responses of oxygenated- (oxy-[heme]; A), deoxygenated- (deoxy-[heme]; B), and total- (total-[heme]; C) heme concentrations with percent tissue saturation (S_tO_2; D) during exercise below (● H1 and ○ H2) and above (▼ S1 and Δ S2) critical force (CF). Dashed lines indicate average end-exercise values of respective FD-NIRS signals during the maximal-effort test (MET). * Significantly different from end-exercise during H1 and H2 ($p < 0.05$). ** Significantly greater than total-[heme] at end-exercise during H2 ($p < 0.05$)

Chapter 3 - Influence of muscular contraction on vascular conductance during exercise above vs. below critical power

Summary

Critical power (CP) is an important physiological threshold that differentiates between steady-state and progressive metabolic and neuromuscular responses to exercise. Limb blood flow (LBF) and microvascular oxygen delivery appeared to reach task-specific physiological maximums above CP. Increases in muscular contraction intensity are concomitant with a more-negative influence of muscular contractions on LBF. While these observations have wide-reaching implications for muscular performance and fatigue development, they remain to be contextualized within the CP framework of exercise tolerance. The aim of this study was to determine if CP represents a threshold for muscular contraction-induced impedance of LBF during dynamic locomotor-muscle exercise. We hypothesized that limb vascular conductance (LVC) would increase during the immediate recovery phase of dynamic exercise above, but not below, CP indicating a threshold for muscular contraction-induced impedance of LBF. CP (115 ± 26 W) was determined in seven men and seven women who subsequently performed ~5-min of near-supine cycling exercise both below and above CP. LVC was calculated as the quotient of LBF and mean arterial pressure (MAP) both of which were measured at end-exercise and during immediate recovery. LVC increased immediately during recovery and remained elevated following both the below- and above-CP exercise tests (all $p < 0.001$). However, LVC demonstrated a greater increase during immediate recovery and remained significantly higher following exercise above CP compared to below CP (all $p < 0.001$). Power-output was significantly associated with the immediate increases in LVC following exercise above, but not below, CP ($p < 0.001$; $r = 0.85$). Additionally, variance in percent

LBF impedance was significantly lower above (CV: 10.7%), compared to below (CV: 53.2%), CP ($p < 0.01$). CP appears to represent a threshold above which the characteristics of LBF impedance by muscular contraction become intensity-dependent. Further, this evidence suggests a critical level of LBF impedance relative to contraction intensity exists and, once attained, may promote the progressive metabolic and neuromuscular responses known to occur above CP.

Introduction

Skeletal muscle contractions are accompanied by increases in intramuscular pressure and therefore mechanical compression of blood vessels and increased vascular resistance (Barcroft & Dornhorst, 1949; Sadamoto *et al.*, 1983; Sjogaard *et al.*, 1986; Gaffney *et al.*, 1990; Radegran & Saltin, 1998). During rhythmic exercise, blood flow is highest during the relaxation phase of the contraction-relaxation cycle when intramuscular pressure is low (Barcroft & Dornhorst, 1949; Walloe & Wesche, 1988; Robergs *et al.*, 1997; Radegran & Saltin, 1998; Lutjemeier *et al.*, 2005). Thus, altering relaxation time between contractions (i.e., duty-cycle or contraction-frequency) has a profound effect on muscle blood flow (Hoelting *et al.*, 2001; Broxterman *et al.*, 2014; Bentley *et al.*, 2017; Caldwell *et al.*, 2018). Indeed, Broxterman et al. demonstrated that an increase in duty cycle (i.e., reduced relaxation time) attenuated the blood flow response to exhaustive rhythmic handgrip exercise (Broxterman *et al.*, 2014). Additionally, the time to task failure (T_{lim}), and therefore the asymptote of the hyperbolic power-duration relationship (i.e., critical power; CP), was significantly reduced (Broxterman *et al.*, 2014). While the oxygen delivery dependency of CP is well documented (Moritani *et al.*, 1981; Vanhatalo *et al.*, 2010; Dekerle *et al.*, 2012), the influence of muscular contraction on limb vascular conductance (LVC) during exercise above versus below CP remains unknown.

CP is an important physiological threshold (Poole *et al.*, 2016) that differentiates between steady-state and progressive metabolic (Poole *et al.*, 1988; Jones *et al.*, 2008) and neuromuscular (Burnley *et al.*, 2012) responses to exercise. Recently, our lab has demonstrated that limb blood flow (LBF) and microvascular oxygen extraction responses to isometric handgrip exercise above critical force (CF; the isometric analog of CP) are distinct from those below CF. Specifically, while steady-state responses were demonstrated below CF, LBF and microvascular oxygen delivery appeared to reach task-specific physiological maximums above CF suggesting intensity-dependent limitations (Chapter 2). Additionally, threshold-like (i.e., biphasic) responses in microvascular oxygen delivery have been observed during incremental exercise with apparent limitations (i.e., submaximal plateaus) existing at higher intensities (Boushel *et al.*, 2002; Habazettl *et al.*, 2010; Chin *et al.*, 2011; Koga *et al.*, 2014; Hammer *et al.*, 2018). These findings are consistent with those of Lutjemeier et al. who experimentally described the effect of muscular contraction on LBF as being positive and neutral at low and moderate work rates, respectively, but negative (i.e., blood flow impedance) at higher intensities (Lutjemeier *et al.*, 2005). These observations have wide-reaching implications for muscular performance and fatigue development yet remain to be contextualized within the CP framework of exercise tolerance.

The aim of this study was to determine if CP represents a threshold for muscular contraction-induced impedance of LBF during dynamic locomotor-muscle exercise. Specifically, we compared LVC during steady-state 10-degree head-up tilt cycling to changes in LVC immediately following exercise termination. Assuming the vasodilatory state of the vasculature remains unchanged during the immediate recovery phase, changes in LVC subsequent to the near-instantaneous cessation of muscular contractions have been previously used to inversely reflect the influence of contraction on LBF during exercise (Barcroft & Dornhorst, 1949; Tschakovsky *et al.*, 2004; Lutjemeier *et al.*, 2005; Broxterman *et al.*, 2014). We hypothesized that LVC would increase during the immediate recovery phase of dynamic exercise above, but not below, CP. If confirmed, we would interpret these findings to indicate that CP represents a threshold for muscular contraction-induced impedance of LBF during dynamic locomotor-muscle exercise.

Methods

Ethical approval

All experimental procedures were approved by the Institutional Review Board for Research Involving Human Subjects at Kansas State University (#9954) and conformed to the standards set forth by the Declaration of Helsinki with the exception of database registration. Subjects were informed of all testing procedures and potential risks of participation before providing written, informed consent.

Subjects

Seven men and seven women (mean ± SD; 23 ± 3 yr, 172 ± 8 cm, 70.7 ± 16.3 kg) volunteered to participate in this study. It has been demonstrated that muscle blood flow during exercise is not modulated by phases of the menstrual cycle (Limberg *et al.*, 2010; Smith *et al.*, 2017), therefore no attempt was made to control for menstrual cycle phase in the women. Each subject completed a medical health history evaluation to confirm the absence of any known cardiovascular, pulmonary, or metabolic disease. Subjects were instructed to abstain from vigorous activity 12 hrs. prior and caffeine and food consumption 2 hrs. prior to the scheduled testing times. A minimum of 24 hrs. was mandated between each test.

Experimental design

Subjects were familiarized with all testing procedures and equipment prior to any experimental testing. All exercise tests were performed on a modified near-supine (10-degree head-up tilt) cycle ergometer (Lode, Groningen, The Netherlands). A relatively slow pedal cadence (45 rpm) and short crank-arm length (16 cm) were utilized during all cycling tests to reduce the frequency and magnitude of hip-angle fluctuations, respectively, and facilitate high-quality Doppler ultrasound signals of the femoral artery. Pedal position was adjusted for each subject to achieve a slight knee bend at bottom dead center and utilized on all subsequent test days to minimize day-to-day biomechanical variability. Additionally, shoulder supports were installed to minimize extraneous muscular work related to body stabilization. T_{lim} was defined as an inability to maintain a pedal cadence above 40 rpm for > 5 s despite strong verbal encouragement for each exercise test performed until exhaustion.

Subjects first performed a 10 Watt·min^{-1} incremental ramp cycling test until exhaustion to determine peak power-output (P_{peak}). P_{peak} was determined as the greatest power-output achieved during the incremental ramp test. Subjects next performed a minimum of three constant power-output cycling tests on separate days. P_{peak} was utilized to determine power-outputs for the constant-power cycling tests that would elicit exhaustion between ~2-15 min. The T_{lim} of each test was recorded and linear regression of the $1/T_{lim}$ vs. power-output relationship for each subject was used to determine CP (the power-output intercept). Goodness-of-fit criteria were established a priori to ensure accurate determination of CP. If standard error of the power-output intercept (i.e., CP) was greater than 10% of CP, a fourth constant power-output test was performed in an attempt to improve the intercept confidence interval. Finally, subjects performed ~5-min constant power-output tests at 10% below and 10% above CP in random order. 10% was chosen to ensure the respective power-outputs were confidently below and above CP according to the goodness-of-fit criteria. A 20-Watt warm-up was performed for 1 min immediately preceding the transition to the below and above CP power-outputs to allow a trained sonographer to identify the movement patterns of the femoral artery. Following confirmation of high-quality Doppler signal from the trained sonographer, a countdown was commenced in synchrony with the subject's pedal cadence such that at exercise cessation the right leg would be straight and relaxed. Exercise was terminated between 4.5 and 5.5 min for all below- and above-CP tests.

Measurements

Oxygen consumption ($\dot{V}O_2$). Breath-by-breath $\dot{V}O_2$ was measured continuously during the incremental ramp cycling test (Ultima CardiO$_2$; Medical Graphics Corp., MN, USA) to characterize the aerobic capacity of each subject. The metabolic system was calibrated prior to each use according to the manufacturer's instructions. Breath-by-breath $\dot{V}O_2$ were converted into 10s time-binned mean values and peak $\dot{V}O_2$ ($\dot{V}O_{2peak}$) was determined as the highest 10 s time-binned mean $\dot{V}O_2$ achieved during the incremental ramp test.

Limb blood flow (LBF). A Doppler ultrasound system (LOGIQ S8; GE Medical Systems, Milwaukee, WI) equipped with a multi-frequency linear array transducer operating at 10 MHz was utilized to simultaneously measure common-femoral artery diameter and peak blood velocity (V_{peak}). Doppler ultrasound measurements were made during the below- and above-CP tests at baseline, during the final min of exercise, and the first min of early recovery. All measurements were made ~ 3 cm proximal to the bifurcation of the deep- and superficial-femoral arteries to minimize the influence of bifurcation-induced turbulent flow. Doppler sample volume was set to the full width of the vessel and all Doppler velocity measurements were performed at a Doppler frequency of 4.0 MHz with an insonation angle < 60 degrees. V_{peak} was defined as the time-averaged peak velocity across each complete cardiac-cycle at baseline and during early recovery. During exercise, V_{peak} was defined as the time-averaged peak velocity during an 8 s (6 complete pedal revolutions) time-window immediately preceding the termination of the test. V_{peak} was intentionally utilized over the time-averaged mean velocities (V_{mean}) as the parabolic-like profiles of arterial blood flow place V_{peak} near the center of the vessel lumen and require less confidence in maintaining wall-to-wall sample volume (Ade *et al.*, 2012). Subsequently, V_{mean} was calculated as $V_{peak}/2$ which has previously been reported to be a reliable estimate (Ade *et al.*, 2012). Common-femoral artery vessel diameter was analyzed at a perpendicular angle along the central axis of the vessel. Cross-sectional area (CSA) of the vessel was then calculated as CSA = πr^2. LBF was calculated as the product of CSA and V_{mean} at baseline, during the final 8s of exercise, and for 9 cardiac-cycles (3 cardiac-cycle bins: CC_{1-3}, CC_{4-6}, and CC_{7-9}) in early recovery.

Hemodynamic responses. Heart rate (HR) and beat-by-beat systolic, mean, and diastolic blood pressures (SBP, MAP, and DBP, respectively) were measured continuously during the below- and above-CP tests via calibrated finger photoplethysmography (Finometer Pro; Finapress Medical Systems, Amsterdam, The Netherlands). Blood pressure measurements were made on the third middle phalanx of the left hand which was placed on a height-adjustable platform to ensure stability during the cycling protocols. All blood pressure and hemodynamic measurements were averaged over the same time-windows as Doppler ultrasound measurements. The rate pressure product (RPP) was calculated as (SBP×HR)/100 and used as an index of myocardial work (Kitamura *et al.*, 1972; Gobel *et al.*, 1978). Cardiac output ($\dot{Q}$) was calculated as the product of HR and stroke volume (SV), with SV calculated using the ModelFlow method (Finometer Pro; Finapress Medical Systems) after correction for age, sex, body mass, and stature (Bogert & van Lieshout, 2005). Blood pressure and LBF data were time-aligned and LVC was calculated as the quotient of LBF and MAP. Lastly, assuming that LVC at CC_{1-3} reflects the LVC during exercise without the influence of muscular contractions, the percent-impedance of LBF ($\%IMP_{LBF}$) at end-exercise was calculated as:

$$\%IMP_{LBF} = \left[\frac{LVC_{CC_{1-3}} - LVC_{End}}{LVC_{CC_{1-3}}}\right] \times 100$$

Statistical analysis

Data are expressed as means ± standard deviation unless otherwise noted. All statistical analyses were performed using SigmaStat (Systat Software; Point Richmond, CA). Linear regression was used to determine CP from the three constant power-output cycling tests. Two-way repeated-measures ANOVAs were used to compare LBF, blood pressure, and hemodynamic measurements at baseline and end-exericse between below- and above-CP tests (time× intensity). Two-way repeated-measures ANOVAs were used to test for changes in LBF, MAP, and LVC throughout the early recovery phase following the below- and above-CP exercise tests (time × intensity). When a significant overall effect was detected, a Tukey's post hoc analysis was performed to determine where significant differences existed. Paired t-tests were used to test for differences in both $\%IMP_{LBF}$ at end-exercise and %-change in LVC during immediate recovery between below- and above-CP exercise tests. Linear regression was used to detect significant relationships between test power-output and $\%IMP_{LBF}$ and changes in LVC. Finally, a Levene's test was used to test for differences in variance of LVC and $\%IMP_{LBF}$ responses between below- and above-CP tests. Results were considered statistically significant when $p < 0.05$.

Results

Incremental ramp data and determination of CP. P_{peak} and $\dot{V}O_{2peak}$ were 146 ± 30 W and 33.1 ± 7.2 mL/kg/min, respectively. CP was 115 ± 26 W (79.0 ± 8.4 %P_{peak}). Standard error of the power-output intercept used to determine CP ranged from 0.39 – 6.27 %CP. Power-outputs below and above CP were 71.1 ± 7.6 and 86.9 ± 9.2 %P_{peak}, respectively.

Hemodynamic responses to exercise. Hemodynamic values at baseline and end-exercise during the below- and above-CP tests are presented in Table 1. No significant differences were detected in any hemodynamic measurements at baseline between tests. HR increased significantly from baseline to end-exercise during both tests (both $p < 0.001$) but was significantly greater at end-exercise above CP compared to below CP ($p < 0.001$). SV increased significantly from baseline to end-exercise only below CP ($p < 0.01$) and no significant differences were detected in end-exercise SV between tests. $\dot{Q}$ increased significantly from baseline to end-exercise during both tests (both $p < 0.001$) but was significantly greater at end-exercise above CP compared to below CP ($p < 0.01$). SBP, DBP, and RPP increased significantly from baseline to end-exercise during both tests (all $p < 0.001$) but were each significantly greater at end-exercise above CP compared to below CP (all $p < 0.05$).

LBF, MAP, and LVC responses during exercise and early recovery. LBF was not different at baseline between below- and above-CP tests and increased significantly from baseline to end-exercise during both tests (both $p < 0.001$; Fig. 1A)). LBF was not different at end-exercise between tests (Fig. 1A). LBF increased immediately during recovery (end-to-CC_{1-3}) and remained elevated (CC_{4-6} and CC_{7-9}) following both the below- and above-CP exercise tests (all $p < 0.001$; Fig. 2A). However, LBF demonstrated a greater immediate increase during recovery (end-to-CC_{1-}

$_{3}$) and remained significantly higher (CC_{4-6} and CC_{7-9}) following exercise above CP compared to below CP (all $p < 0.001$; Fig. 2A).

MAP was not different at baseline between below- and above-CP tests and increased significantly from baseline to end-exercise during both tests (both $p < 0.001$; Fig. 1B). MAP was significantly greater at end-exercise above CP compared to below CP ($p < 0.01$; Fig. 1B). Following exercise below CP, MAP remained unchanged during immediate recovery (end-to-CC_{1-3}) but was significantly lower during CC_{4-6} and CC_{7-9} compared to end-exercise (both $p < 0.001$; Fig. 2B). Following exercise above CP, MAP decreased significantly during immediate recovery (end-to-CC_{1-3}) and remained lower during CC_{4-6} and CC_{7-9} compared to end exercise (all $p < 0.001$; Fig. 2B). MAP was significantly lower during all stages of early recovery above CP compared to below CP ($p < 0.001$; Fig. 2B).

LVC was not different at baseline between tests and increased significantly from baseline to end-exercise during both tests (both $p < 0.001$; Fig. 1C). LVC was significantly lower at end-exercise above CP compared to below CP ($p < 0.05$; Fig. 1C). LVC increased immediately during recovery (end-to-CC_{1-3}) and remained elevated (CC_{4-6} and CC_{7-9}) following both the below- and above-CP exercise tests (all $p < 0.001$; Fig. 2C). However, LVC demonstrated a greater increase during immediate recovery (end-to-CC_{1-3}) and remained significantly higher (CC_{4-6} and CC_{7-9}) following exercise above CP compared to below CP (all $p < 0.001$; Fig. 2C).

Immediate changes in LVC, $\%IMP_{LBF}$, and power-output. $\%IMP_{LBF}$ at end-exercise (Fig. 3A) and $\%\Delta LVC$ during immediate recovery (Fig. 3B) were significantly greater above, compared to below, CP (both $p < 0.001$). Neither $\%IMP_{LBF}$ at end-exercise (Fig. 3A) nor $\%\Delta LVC$ during immediate recovery (Fig. 3B) were significantly associated with power-output below or above CP. Variance in $\%\Delta LVC$ during immediate recovery was not different between below- and above-CP tests, however variance in $\%IMP_{LBF}$ was significantly lower above (CV: 10.7%), compared to below (CV: 53.2%), CP ($p < 0.01$). Cycling power-output was not associated with the absolute increases in LVC immediately following exercise (end-to-CC_{1-3}) below CP (Fig. 4). However, power-output was significantly associated with the absolute increases in LVC immediately following exercise (end-to-CC_{1-3}) above CP ($p < 0.001$; $r = 0.85$; Fig. 4). No relationships were detected between individual subject CPs and the percent-difference between immediate changes in LVC (end-to-CC_{1-3}) during the below- or above-CP tests (Fig. 5).

Discussion

Major Findings

This study determined that CP represents a threshold for intensity-dependent characteristics of muscular contraction-induced impedance of LBF during dynamic locomotor-muscle exercise. Consistent with our hypothesis, LVC increased significantly during the immediate recovery phase of dynamic exercise above CP (Fig. 2C) suggesting impedance of LBF by muscular contractions. However, in contrast to our hypothesis, LVC also increased significantly, albeit less, during the immediate recovery phase of dynamic exercise below CP (Fig. 2C). These findings do not support the presence of a hardline threshold for LBF impedance at CP. However, the degree of LBF impedance during exercise was significantly greater above, compared to below, CP (Fig. 3). Further, intensity-dependent changes in LVC during immediate recovery existed exclusively above CP (Fig. 4). Importantly, these intensity-dependent characteristics were not a result of differences in CP among subjects (Fig. 5). Together, these findings suggest that CP represents a threshold above which muscular contraction intensity becomes a significant determinant of LBF impedance during exercise.

LBF impedance is not exclusive to exercise above CP. During early recovery, LVC increased below CP suggesting some degree of LBF impedance by muscular contractions (Fig. 2C). This is in direct contrast with our hypothesis that LBF impedance would become manifest exclusively above CP. Lutjemeier et al. demonstrated a net impedance effect of muscular contractions on LBF during knee-extension exercise at ~60-75% of P_{peak} (Lutjemeier *et al.*, 2005). This study determined CP to be 79.0% of P_{peak} and the power-output 10% below CP to be 71.1% of P_{peak} on average. Given this, our data suggesting the presence of LBF impedance below CP, although in contrast to our hypothesis, is consistent with the previous findings of Lutjemeier et al.

(Lutjemeier *et al.*, 2005). While increases in LVC during immediate recovery (Fig. 2C and 3B) and %IMP_{LBF} at end-exercise (Fig. 3A) were significantly greater above CP, data from this study cannot support the existence of a hardline threshold at CP. However, the determinants of absolute LBF impedance during exercise above CP appear to be distinct from those below CP (Fig. 4).

The absolute magnitude of LBF impedance during exercise (indicated by the absolute change in LVC during immediate recovery) appears to be determined by exercise power-output exclusively above CP (Fig. 4; solid triangles). Specifically, despite a relatively wide range of test power-outputs (73–151W) across subjects, the absolute magnitude of LBF impedance during exercise was not associated with contraction intensity below CP (Fig. 4; open triangles). In contrast, subjects with higher CPs, and thus higher above-CP contraction intensities, were characterized with higher levels of absolute LBF impedance above CP (Fig. 4; solid triangles). Per our study design, individuals with higher CPs were asked to perform exercise across a wider absolute range of power-outputs (±10% of CP). Therefore, it is important to note that the difference in the percent-increase in LVC during immediate recovery from below-to-above CP was not associated with individual subject CPs (Fig. 5). Thus, absolute changes in power-outputs within subjects from below-to-above CP were unlikely the root cause of this association. Considering that contraction-induced retrograde arterial flow reaches a maximum at very light contraction intensities (Hoelting *et al.*, 2001), any power-output associations are likely dependent on the magnitude of inter-contraction hyperemia (i.e., during the relaxation phase). Together, these data suggest that absolute LBF impedance is dependent, at least in part, on muscular contraction intensity above, but not below, CP. Further, the capacity to rapidly perfuse skeletal muscle during the relaxation phase may play a significant role in determining CP (Broxterman *et al.*, 2014).

Implications for skeletal muscle fatigue and exercise tolerance. Although the intrinsic coupling of CP to oxygen delivery is well known (Moritani *et al.*, 1981; Jones *et al.*, 2010; Vanhatalo *et al.*, 2010; Dekerle *et al.*, 2012; Broxterman *et al.*, 2015; Poole *et al.*, 2016), this is the first study to evaluate the magnitude of LBF impedance above versus below this exercise threshold. The greater limitations imposed on oxygen delivery above CP during this study (Fig. 2 and 3) would suggest a diminished relative contribution of aerobic metabolism to energy production and thus greater reliance on finite anaerobic energy sources. Exercise tolerance above CP has been associated with the rate of anaerobic energy store utilization (Smith *et al.*, 1998; Miura *et al.*, 1999; Miura *et al.*, 2000), concomitant accumulation of metabolic byproducts (Jones *et al.*, 2008; Burnley *et al.*, 2010; Vanhatalo *et al.*, 2010), and progressive loss of skeletal muscle efficiency (Vanhatalo *et al.*, 2011). Indeed, intensity-independent critical levels of metabolite accumulation (e.g., inorganic phosphate and hydrogen ions) (Burnley *et al.*, 2010; Vanhatalo *et al.*, 2010) and peripheral skeletal muscle fatigue (Burnley *et al.*, 2012) appear to exist above CP and, once attained, limit exercise tolerance. These findings, combined with those of this study, suggest that LBF impedance by skeletal muscle contraction contributes toward the development of metabolite-induced skeletal muscle fatigue more above, compared to below, CP.

The present study offers novel insight to the contraction-dependency characteristics of CP (Hill *et al.*, 1995; McNaughton & Thomas, 1996; Hoelting *et al.*, 2001; Barker *et al.*, 2006; Broxterman *et al.*, 2014). Specifically, the observation that $\%IMP_{LBF}$ above CP demonstrated a significantly lower degree of variance across subjects (CV: 10.7%) compared to below CP (CV: 53.2%) (Fig. 3A) suggests that a specific level of LBF impedance, relative to oxygen demand, might be ‘tolerated’ before precipitating the well-documented above-CP exercise responses (i.e., progressive metabolite and fatigue accumulation) (Jones *et al.*, 2008; Burnley *et al.*, 2012). This interpretation is consistent with previous findings suggesting LBF reaches a similar end-exercise value, despite increases in contraction force, above critical force (CF; the isometric analog of CP) (Chapter 2). Combined with a greater reliance on low-oxidative muscle fibers (Copp *et al.*, 2010), limitations to the overall LBF response above CP would further complicate the matching of oxygen delivery to oxygen demand during exercise and promote the utilization of anaerobic energy stores that are associated with the development of peripheral fatigue (Jones *et al.*, 2008).

Implications for blood flow heterogeneity. It is important to highlight that this study utilized bulk LBF measurements of a major conduit artery (i.e., common femoral) to assess changes in LVC and provided no index for microvascular oxygen delivery or distribution. As such, we can only speculate as to the impact of bulk LBF impedance on the heterogeneity of microvascular oxygen delivery known to exist during exercise (Koga *et al.*, 2014; Heinonen *et al.*, 2015; Vogiatzis *et al.*, 2015). Increases in blood flow from below-to-above critical power are distributed primarily to low-oxidative muscle fibers (Copp *et al.*, 2010). Additionally, differences in blood flow among fiber-types have been attributed to variances in both local vasodilator and vasoconstrictor sensitivities and the degree of sympathetically controlled vasoconstriction (Behnke *et al.*, 2011; Laughlin *et al.*, 2012). Given that increases in exercise intensity rely on recruitment of additional unique motor-units (Chin *et al.*, 2011; Hammer *et al.*, 2018; Okushima *et al.*, 2020), fiber-type differences in vascular control may lead to heterogeneity in the physiological consequences of increased blood flow impedance.

The relatively widespread range of $\%IMP_{LBF}$ during exercise below CP suggests a lesser role for intramuscular pressures in the physiological responses to steady-state exercise (Fig. 3A). In contrast, ~40% relative impedance to LBF was experienced by all subjects above CP. The heterogeneity of this impedance among individual muscles or muscle regions remains to be elucidated. However, it is possible that fiber-type specific mechanisms of flow regulation are differentially limited above, compared to below, CP at this level of $\%IMP_{LBF}$. For example, shear-stress mediated nitric oxide (NO) production is thought to play a major role in distributing blood flow to highly-oxidative muscles below CP while neuronal NO synthase appears to preferentially augment vascular conductance in highly-glycolytic muscles above CP (Copp *et al.*, 2013). Additionally, neuronal NO synthase is thought to play a major role in duty cycle- and intensity-dependent inhibition of sympathetic vasoconstriction (i.e., sympatholysis) (Tschakovsky *et al.*, 2002; Thomas *et al.*, 2003; Caldwell *et al.*, 2018). Considering the inherent dependency on blood flow, it seems reasonable to speculate that shear-stress mediated regulation of vascular conductance would be largely impacted by LBF impedance. Thus, highly oxidative regions may be particularly susceptible to increases in intramuscular pressures, resulting in oxygen delivery and oxygen demand mismatching and perhaps the augmented metabolite accumulation (Jones *et al.*, 2008), contractile inefficiency (Vanhatalo *et al.*, 2011), and $\dot{V}O_2$ response (Poole *et al.*, 1988) observed above CP.

Experimental considerations

This study measured the impedance of LBF during dynamic locomotor-muscle exercise as opposed to simple single-joint exercises such as handgrip or knee-extension. To accomplish this, high-quality Doppler ultrasound images of the common femoral artery were required. Unlike gold-standard techniques for measuring LBF (e.g., thermodilution), movement of the target vessel relative to the Doppler transducer can influence measured blood velocity values by altering the angle of insonation (Gliemann *et al.*, 2018). To improve our ability to maintain a consistent Doppler angle and attempt to minimize these effects, near-supine exercise, a relatively slow pedal cadence, and shortened pedal rotation were intentionally utilized. The findings from this study should be interpreted while considering these known limitations of the Doppler ultrasound technique and with this specific exercise modality in mind. During supine exercise, LBF (MacDonald *et al.*, 1998) and $\dot{V}O_2$ (MacDonald *et al.*, 1998; Koga *et al.*, 1999) demonstrate slowed on-kinetic responses to exercise compared to upright exercise. To avoid the influence of posture during the on-transient phase and to ensure that changes in LBF and MAP during early recovery would reflect the influence of contractions during steady-state exercise, end-exercise measurements were made between 4.5- and 5.5-min. LBF is determined by downstream vascular resistance and driving pressure. During supine exercise, driving pressure into the legs is reduced by a decreased gravitational effect (i.e., reduced hydrostatic column). Therefore, downstream vascular resistance would have a proportionally greater influence on LBF and the influence of muscle contraction on LBF may have been exacerbated during this study.

Reductions in contraction frequency have been demonstrated to elevate the LBF response to exercise (Hoelting *et al.*, 2001) and increase CP (but not the metabolic rate at which it occurs) (Barker *et al.*, 2006) during upright exercise. While the influence of contraction frequency on LBF and CP was not investigated in the present study, it is possible that a relatively slow pedal cadence augmented the LBF response through greater relaxation time between pedal strokes and thus reduced the net influence of muscular contractions. However, a slow pedal cadence combined with reductions in mechanical advantage (i.e., decreased crank-arm length) and posture associated increases in muscle activation (Egana *et al.*, 2013) may have increased the net influence of muscular contractions on LBF during this study compared to traditional cycling exercise. Indeed, the contraction characteristics of this study (contraction frequency and range-of-motion) were more similar to those of stair-climbing (Heller *et al.*, 2001; Holsgaard-Larsen *et al.*, 2011).

Therefore, our findings are generalizable to activities of daily living, particularly in populations whose CP is at a low absolute work rate (e.g., aging, heart failure, and pulmonary disease) (Neder *et al.*, 2000a, b; van der Vaart *et al.*, 2014). However, while our findings suggest that muscular contraction-induced LBF impedance may play a substantial role in determining CP in young and healthy individuals, it is important to consider that other factors (i.e., dyspnea, central cardiac limitations, microvascular dysfunction) may become proportionally more limiting in older individuals or those with chronic disease.

Conclusions

This is the first study to our knowledge that provides LBF measurements during locomotive-like exercise below and above the CP threshold in humans. This study demonstrated that muscular contraction-induced impedance to LBF was significantly greater above, compared to below, CP. Additionally, CP appears to represent a threshold above which the characteristics of LBF impedance by muscular contraction become intensity-dependent. Remarkably, while it remains to be elucidated if greater LBF impedance occurs with further increases in exercise intensity, a comparatively consistent degree of relative LBF impedance was demonstrated above CP. This evidence suggests a critical level of LBF limitation relative to contraction intensity exists and, once attained, may promote the progressive metabolic and neuromuscular responses known to occur above CP. Finally, future studies should aim to uncover differences in the interactions between energetic demand and the concomitant mechanical consequences associated with higher-intensity muscular contractions across the CP threshold.

References

Ade CJ, Broxterman RM, Wong BJ & Barstow TJ. (2012). Anterograde and retrograde blood velocity profiles in the intact human cardiovascular system. *Experimental physiology* **97,** 849-860.

Barcroft H & Dornhorst AC. (1949). The Blood Flow through the Human Calf during Rhythmic Exercise. *J Physiol-London* **109,** 402-&.

Barker T, Poole DC, Noble ML & Barstow TJ. (2006). Human critical power-oxygen uptake relationship at different pedalling frequencies. *Exp Physiol* **91,** 621-632.

Behnke BJ, Armstrong RB & Delp MD. (2011). Adrenergic control of vascular resistance varies in muscles composed of different fiber types: influence of the vascular endothelium. *Am J Physiol-Reg I* **301,** R783-R790.

Bentley RF, Poitras VJ, Hong T & Tschakovsky ME. (2017). Characteristics and effectiveness of vasodilatory and pressor compensation for reduced relaxation time during rhythmic forearm contractions. *Experimental Physiology* **102,** 621-634.

Bogert LWJ & van Lieshout JJ. (2005). Non-invasive pulsatile arterial pressure and stroke volume changes from the human finger. *Experimental Physiology* **90,** 437-446.

Boushel R, Langberg H, Gemmer C, Olesen J, Crameri R, Scheede C, Sander M & Kjaer M. (2002). Combined inhibition of nitric oxide and prostaglandins reduces human skeletal muscle blood flow during exercise. *J Physiol* **543,** 691-698.

Broxterman RM, Ade CJ, Craig JC, Wilcox SL, Schlup SJ & Barstow TJ. (2015). Influence of blood flow occlusion on muscle oxygenation characteristics and the parameters of the power-duration relationship. *Journal of applied physiology (Bethesda, Md : 1985)* **118,** 880-889.

Broxterman RM, Ade CJ, Wilcox SL, Schlup SJ, Craig JC & Barstow TJ. (2014). Influence of duty cycle on the power-duration relationship: observations and potential mechanisms. *Respir Physiol Neurobiol* **192,** 102-111.

Burnley M, Vanhatalo A, Fulford J & Jones AM. (2010). Similar metabolic perturbations during all-out and constant force exhaustive exercise in humans: a 31P magnetic resonance spectroscopy study. *Experimental Physiology* **95,** 798-807.

Burnley M, Vanhatalo A & Jones AM. (2012). Distinct profiles of neuromuscular fatigue during muscle contractions below and above the critical torque in humans. *J Appl Physiol* **113,** 215-223.

Caldwell JT, Sutterfield SL, Post HK, Lovoy GM, Banister HR, Hammer SM & Ade CJ. (2018). Vasoconstrictor responsiveness through alterations in relaxation time and metabolic rate during rhythmic handgrip contractions. *Physiol Rep* **6,** e13933.

Chin LM, Kowalchuk JM, Barstow TJ, Kondo N, Amano T, Shiojiri T & Koga S. (2011). The relationship between muscle deoxygenation and activation in different muscles of the quadriceps during cycle ramp exercise. *Journal of applied physiology (Bethesda, Md : 1985)* **111,** 1259-1265.

Copp SW, Hirai DM, Musch TI & Poole DC. (2010). Critical speed in the rat: implications for hindlimb muscle blood flow distribution and fibre recruitment. *J Physiol-London* **588,** 5077-5087.

Copp SW, Holdsworth CT, Ferguson SK, Hirai DM, Poole DC & Musch TI. (2013). Muscle fibre-type dependence of neuronal nitric oxide synthase-mediated vascular control in the rat during high speed treadmill running. *J Physiol-London* **591,** 2885-2896.

Dekerle J, Mucci P & Carter H. (2012). Influence of moderate hypoxia on tolerance to high-intensity exercise. *Eur J Appl Physiol* **112,** 327-335.

Egana M, Columb D & O'Donnell S. (2013). Effect of low recumbent angle on cycling performance, fatigue, and V O(2) kinetics. *Med Sci Sports Exerc* **45,** 663-673.

Gaffney FA, Sjogaard G & Saltin B. (1990). Cardiovascular and Metabolic Responses to Static Contraction in Man. *Acta Physiologica Scandinavica* **138,** 249-258.

Gliemann L, Mortensen SP & Hellsten Y. (2018). Methods for the determination of skeletal muscle blood flow: development, strengths and limitations. *Eur J Appl Physiol* **118,** 1081-1094.

Gobel FL, Norstrom LA, Nelson RR, Jorgensen CR & Wang Y. (1978). The rate-pressure product as an index of myocardial oxygen consumption during exercise in patients with angina pectoris. *Circulation* **57,** 549-556.

Habazettl H, Athanasopoulos D, Kuebler WM, Wagner H, Roussos C, Wagner PD, Ungruhe J, Zakynthinos S & Vogiatzis I. (2010). Near-infrared spectroscopy and indocyanine green derived blood flow index for noninvasive measurement of muscle perfusion during exercise. *Journal of applied physiology (Bethesda, Md : 1985)* **108,** 962-967.

Hammer SM, Alexander AM, Didier KD, Smith JR, Caldwell JT, Sutterfield SL, Ade CJ & Barstow TJ. (2018). The noninvasive simultaneous measurement of tissue oxygenation and microvascular hemodynamics during incremental handgrip exercise. *J Appl Physiol* **124,** 604-614.

Heinonen I, Koga S, Kalliokoski KK, Musch TI & Poole DC. (2015). Heterogeneity of Muscle Blood Flow and Metabolism: Influence of Exercise, Aging, and Disease States. *Exerc Sport Sci Rev* **43,** 117-124.

Heller MO, Bergmann G, Deuretzbacher G, Durselen L, Pohl M, Claes L, Haas NP & Duda GN. (2001). Musculo-skeletal loading conditions at the hip during walking and stair climbing. *J Biomech* **34,** 883-893.

Hill DW, Smith JC, Leuschel JL, Chasteen SD & Miller SA. (1995). Effect of Pedal Cadence on Parameters of the Hyperbolic Power - Time Relationship. *Int J Sports Med* **16,** 82-87.

Hoelting BD, Scheuermann BW & Barstow TJ. (2001). Effect of contraction frequency on leg blood flow during knee extension exercise in humans. *J Appl Physiol (1985)* **91,** 671-679.

Holsgaard-Larsen A, Caserotti P, Puggaard L & Aagaard P. (2011). Stair-ascent performance in elderly women: effect of explosive strength training. *J Aging Phys Act* **19,** 117-136.

Jones AM, Vanhatalo A, Burnley M, Morton RH & Poole DC. (2010). Critical power: implications for determination of V O2max and exercise tolerance. *Med Sci Sports Exerc* **42,** 1876-1890.

Jones AM, Wilkerson DP, DiMenna F, Fulford J & Poole DC. (2008). Muscle metabolic responses to exercise above and below the "critical power" assessed using 31P-MRS. *American journal of physiology Regulatory, integrative and comparative physiology* **294,** R585-593.

Kitamura K, Jorgensen CR, Gobel FL, Taylor HL & Wang Y. (1972). Hemodynamic correlates of myocardial oxygen consumption during upright exercise. *J Appl Physiol* **32,** 516-522.

Koga S, Rossiter HB, Heinonen I, Musch TI & Poole DC. (2014). Dynamic heterogeneity of exercising muscle blood flow and O2 utilization. *Medicine and science in sports and exercise* **46,** 860-876.

Koga S, Shiojiri T, Shibasaki M, Kondo N, Fukuba Y & Barstow TJ. (1999). Kinetics of oxygen uptake during supine and upright heavy exercise. *J Appl Physiol (1985)* **87,** 253-260.

Laughlin MH, Davis MJ, Secher NH, van Lieshout JJ, Arce-Esquivel AA, Simmons GH, Bender SB, Padilla J, Bache RJ, Merkus D & Duncker DJ. (2012). Peripheral Circulation. *Compr Physiol* **2,** 321-447.

Limberg JK, Eldridge MW, Proctor LT, Sebranek JJ & Schrage WG. (2010). Alpha-adrenergic control of blood flow during exercise: effect of sex and menstrual phase. *Journal of applied physiology (Bethesda, Md : 1985)* **109,** 1360-1368.

Lutjemeier BJ, Miura A, Scheuermann BW, Koga S, Townsend DK & Barstow TJ. (2005). Muscle contraction-blood flow interactions during upright knee extension exercise in humans. *Journal of applied physiology (Bethesda, Md : 1985)* **98,** 1575-1583.

MacDonald MJ, Shoemaker JK, Tschakovsky ME & Hughson RL. (1998). Alveolar oxygen uptake and femoral artery blood flow dynamics in upright and supine leg exercise in humans. *J Appl Physiol (1985)* **85,** 1622-1628.

McNaughton L & Thomas D. (1996). Effects of differing pedalling speeds on the power-duration relationship of high intensity cycle ergometry. *Int J Sports Med* **17,** 287-292.

Miura A, Kino F, Kajitani S, Sato H & Fukuba Y. (1999). The effect of oral creatine supplementation on the curvature constant parameter of the power-duration curve for cycle ergometry in humans. *Jpn J Physiol* **49,** 169-174.

Miura A, Sato H, Sato H, Whipp BJ & Fukuba Y. (2000). The effect of glycogen depletion on the curvature constant parameter of the power-duration curve for cycle ergometry. *Ergonomics* **43,** 133-141.

Moritani T, Nagata A, Devries HA & Muro M. (1981). Critical Power as a Measure of Physical Work Capacity and Anaerobic Threshold. *Ergonomics* **24,** 339-350.

Neder JA, Jones PW, Nery LE & Whipp BJ. (2000a). Determinants of the exercise endurance capacity in patients with chronic obstructive pulmonary disease. The power-duration relationship. *Am J Respir Crit Care Med* **162,** 497-504.

Neder JA, Jones PW, Nery LE & Whipp BJ. (2000b). The effect of age on the power/duration relationship and the intensity-domain limits in sedentary men. *Eur J Appl Physiol* **82,** 326-332.

Okushima D, Poole DC, Barstow TJ, Kondo N, Chin LMK & Koga S. (2020). Effect of differential muscle activation patterns on muscle deoxygenation and microvascular haemoglobin regulation. *Experimental Physiology* **105,** 531-541.

Poole DC, Burnley M, Vanhatalo A, Rossiter HB & Jones AM. (2016). Critical Power: An Important Fatigue Threshold in Exercise Physiology. *Med Sci Sports Exerc* **48,** 2320-2334.

Poole DC, Ward SA, Gardner GW & Whipp BJ. (1988). Metabolic and respiratory profile of the upper limit for prolonged exercise in man. *Ergonomics* **31,** 1265-1279.

Radegran G & Saltin B. (1998). Muscle blood flow at onset of dynamic exercise in humans. *Am J Physiol-Heart C* **274,** H314-H322.

Robergs RA, Icenogle MV, Hudson TL & Greene ER. (1997). Temporal inhomogeneity in brachial artery blood flow during forearm exercise. *Med Sci Sport Exer* **29,** 1021-1027.

Sadamoto T, Bondepetersen F & Suzuki Y. (1983). Skeletal-Muscle Tension, Flow, Pressure, and Emg during Sustained Isometric Contractions in Humans. *Eur J Appl Physiol O* **51,** 395-408.

Sjogaard G, Kiens B, Jorgensen K & Saltin B. (1986). Intramuscular Pressure, Emg and Blood-Flow during Low-Level Prolonged Static Contraction in Man. *Acta Physiologica Scandinavica* **128,** 475-484.

Smith JC, Stephens DP, Hall EL, Jackson AW & Earnest CP. (1998). Effect of oral creatine ingestion on parameters of the work rate-time relationship and time to exhaustion in high-intensity cycling. *Eur J Appl Physiol Occup Physiol* **77,** 360-365.

Smith JR, Hageman KS, Harms CA, Poole DC & Musch TI. (2017). Respiratory muscle blood flow during exercise: Effects of sex and ovarian cycle. *Journal of applied physiology (Bethesda, Md : 1985)* **122,** 918-924.

Thomas GD, Shaul PW, Yuhanna IS, Froehner SC & Adams ME. (2003). Vasomodulation by skeletal muscle-derived nitric oxide requires alpha-syntrophin-mediated sarcolemmal localization of neuronal Nitric oxide synthase. *Circ Res* **92,** 554-560.

Tschakovsky ME, Rogers AM, Pyke KE, Saunders NR, Glenn N, Lee SJ, Weissgerber T & Dwyer EM. (2004). Immediate exercise hyperemia in humans is contraction intensity dependent: evidence for rapid vasodilation. *J Appl Physiol* **96,** 639-644.

Tschakovsky ME, Sujirattanawimol K, Ruble SB, Valic Z & Joyner MJ. (2002). Is sympathetic neural vasoconstriction blunted in the vascular bed of exercising human muscle? *J Physiol-London* **541,** 623-635.

van der Vaart H, Murgatroyd SR, Rossiter HB, Chen C, Casaburi R & Porszasz J. (2014). Selecting constant work rates for endurance testing in COPD: the role of the power-duration relationship. *COPD* **11,** 267-276.

Vanhatalo A, Fulford J, DiMenna FJ & Jones AM. (2010). Influence of hyperoxia on muscle metabolic responses and the power-duration relationship during severe-intensity exercise in humans: a 31P magnetic resonance spectroscopy study. *Experimental Physiology* **95,** 528-540.

Vanhatalo A, Poole DC, DiMenna FJ, Bailey SJ & Jones AM. (2011). Muscle fiber recruitment and the slow component of O-2 uptake: constant work rate vs. all-out sprint exercise. *Am J Physiol-Reg I* **300,** R700-R707.

Vogiatzis I, Habazettl H, Louvaris Z, Andrianopoulos V, Wagner H, Zakynthinos S & Wagner PD. (2015). A method for assessing heterogeneity of blood flow and metabolism in exercising normal human muscle by near-infrared spectroscopy. *Journal of applied physiology (Bethesda, Md : 1985)* **118,** 783-793.

Walloe L & Wesche J. (1988). Time Course and Magnitude of Blood-Flow Changes in the Human Quadriceps Muscles during and Following Rhythmic Exercise. *J Physiol-London* **405,** 257-273.

Table 3.1 Hemodynamic responses to exercise below and above critical power (CP)

	Baseline		End-exercise	
	Below CP	Above CP	Below CP	Above CP
HR (bpm)	68 ± 10	69 ± 11	131 ± 13 *	151 ± 15 *†
SV (mL)	86.8 ± 9.0	90.0 ± 9.7	101 ± 15 *	96.7 ± 15.7
$\dot{Q}$ (L·min-1)	5.8 ± 0.9	6.10 ± 1.2	13 ± 2.3 *	15 ± 3.1 *†
SBP (mmHg)	130 ± 6	130 ± 7	175 ± 18 *	186 ± 14 *†
DBP (mmHg)	77 ± 6.1	75 ± 6.2	94 ± 9.2 *	101 ± 12 *†
RPP (bpm·mmHg·10^{-2})	87 ± 14	89 ± 14	227 ± 28 *	279 ± 33 *†

Values are means ± SD. HR, heart rate; SV, stroke volume; $\dot{Q}$, cardiac output; SBP and DBP, systolic and diastolic blood pressures, respectively; RPP, rate pressure product. * Significantly greater than baseline ($p < 0.01$). † Significantly greater than below CP ($p < 0.05$).

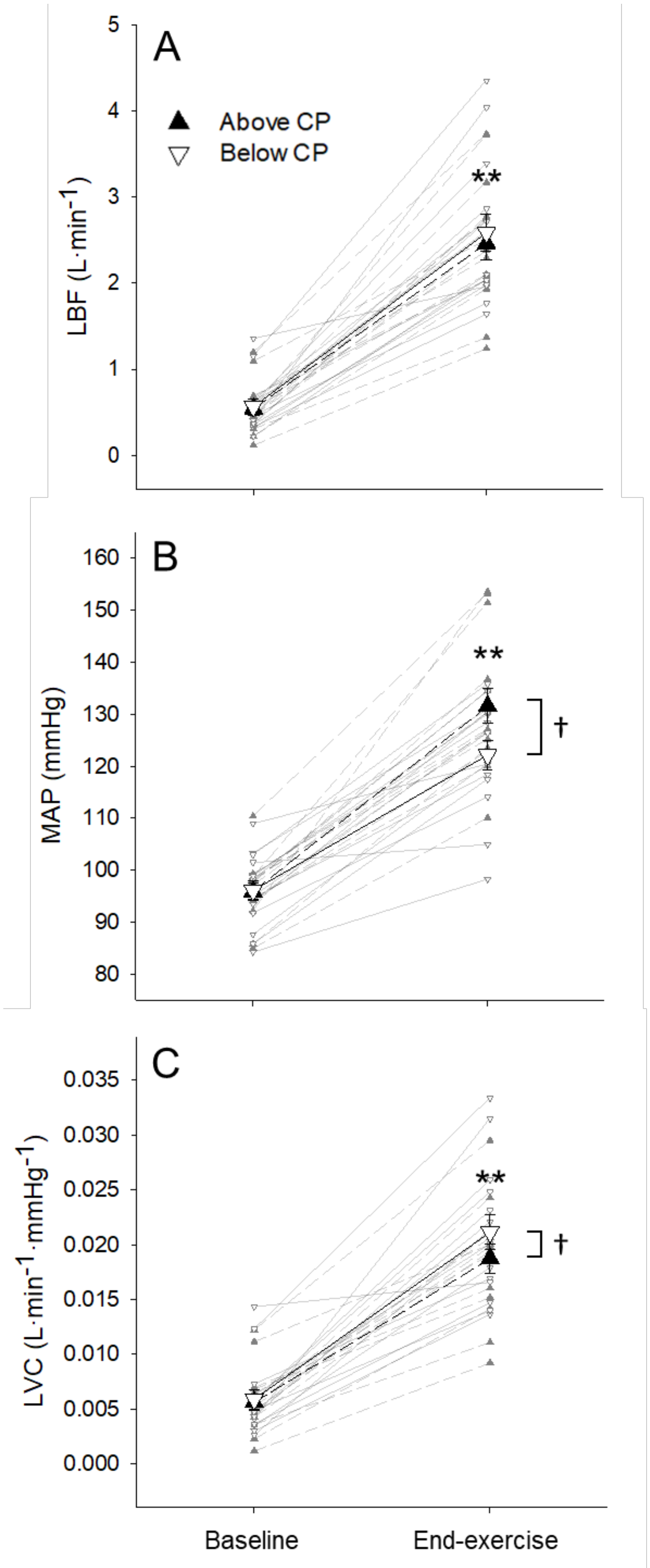

Figure 3.1 Cardiovascular responses to exercise.

The mean absolute values of limb blood flow (LBF; **A**), mean arterial pressure (MAP; **B**), and limb vascular conductance (LVC; **C**) at baseline and end-exercise below (▽) and above (▲) CP. Individual responses are presented in the background. * Significantly greater than baseline ($p < 0.001$). † Significant difference between below- and above-CP tests ($p < 0.05$).

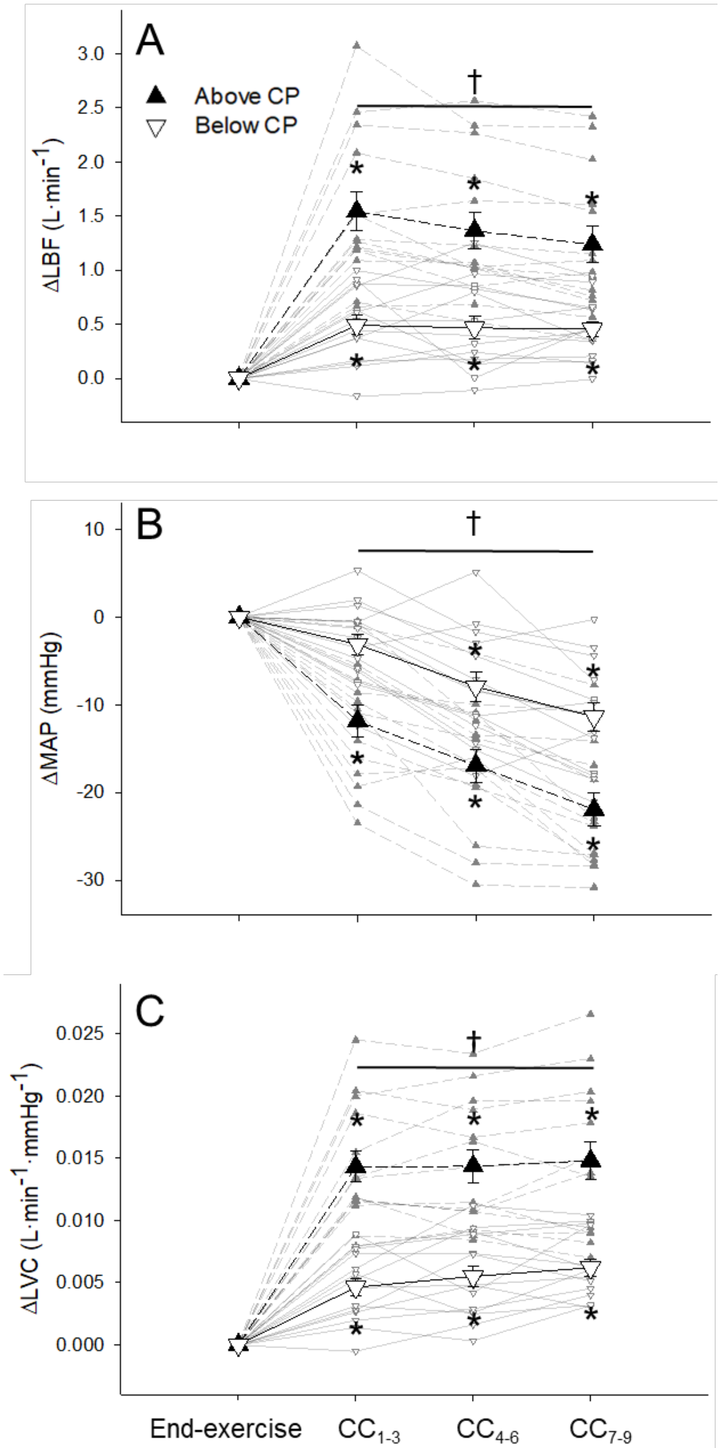

Figure 3.2 Cardiovascular responses during early recovery from exercise.

The mean absolute change in limb blood flow (LBF; **A**), mean arterial pressure (MAP; **B**), and limb vascular conductance (LVC; **C**) from end-exercise to early recovery (cardiac cycles 1-3, 4-6, and 7-9; $CC_{1\text{-}3}$, $CC_{4\text{-}6}$, and $CC_{7\text{-}9}$, respectively) following exercise below (▽) and above (▲) CP. Individual responses are presented in the background. * Significantly different from end-exercise ($p < 0.001$). † Significant difference between below- and above-CP tests ($p < 0.001$).

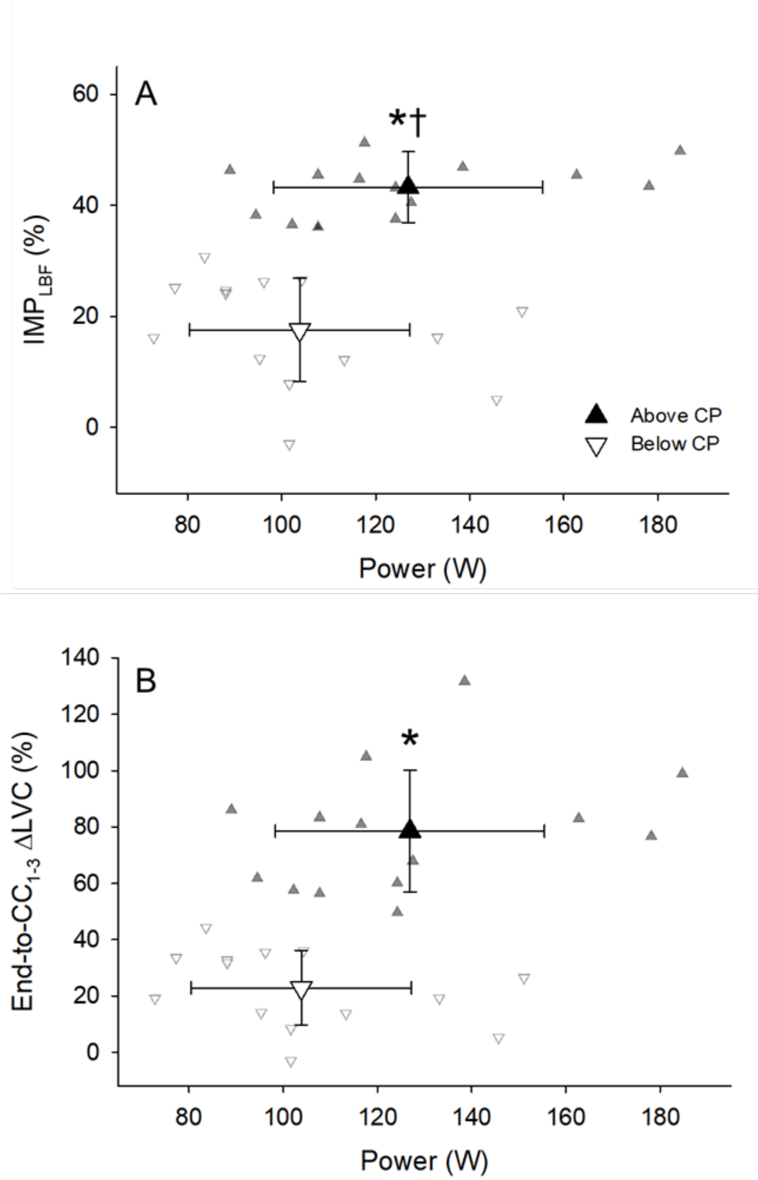

Figure 3.3 Percent impedance of limb blood flow and percent change in limb vascular conductance during immediate recovery as a function of power-output.

The mean percent impedance of limb blood flow (%IMP_{LBF}; **A**) and percent change in limb vascular conductance (ΔLVC; **B**) from end-exercise to immediate recovery (cardiac cycles 1-3; CC_{1-3},) following exercise below (▽) and above (▲) CP. Individual responses are presented in the background. * Significantly greater than below CP ($p < 0.001$). † Significant difference in variance between below- and above-CP tests ($p < 0.01$).

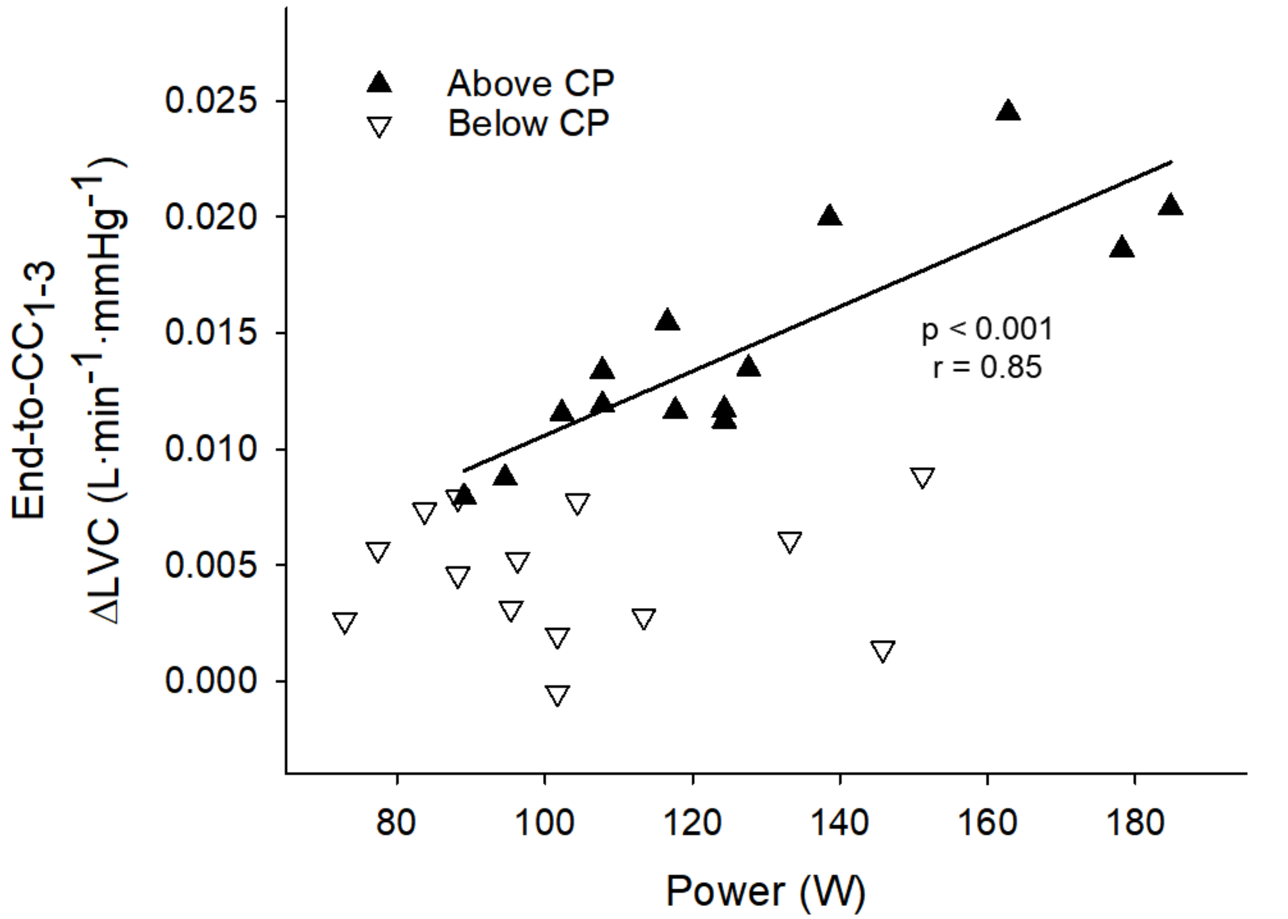

Figure 3.4 Changes in limb vascular conductance during immediate recovery as a function of power-output.

The absolute change in limb vascular conductance (ΔLVC) during immediate recovery (cardiac cycles 1-3; $CC_{1\text{-}3}$) from exercise below (▽) and above (▲) CP as a function of test power-output for each subject. Note the significant relationship between ΔLVC and power-output above, but not below, CP (solid line; $p < 0.001$; $r = 0.85$).

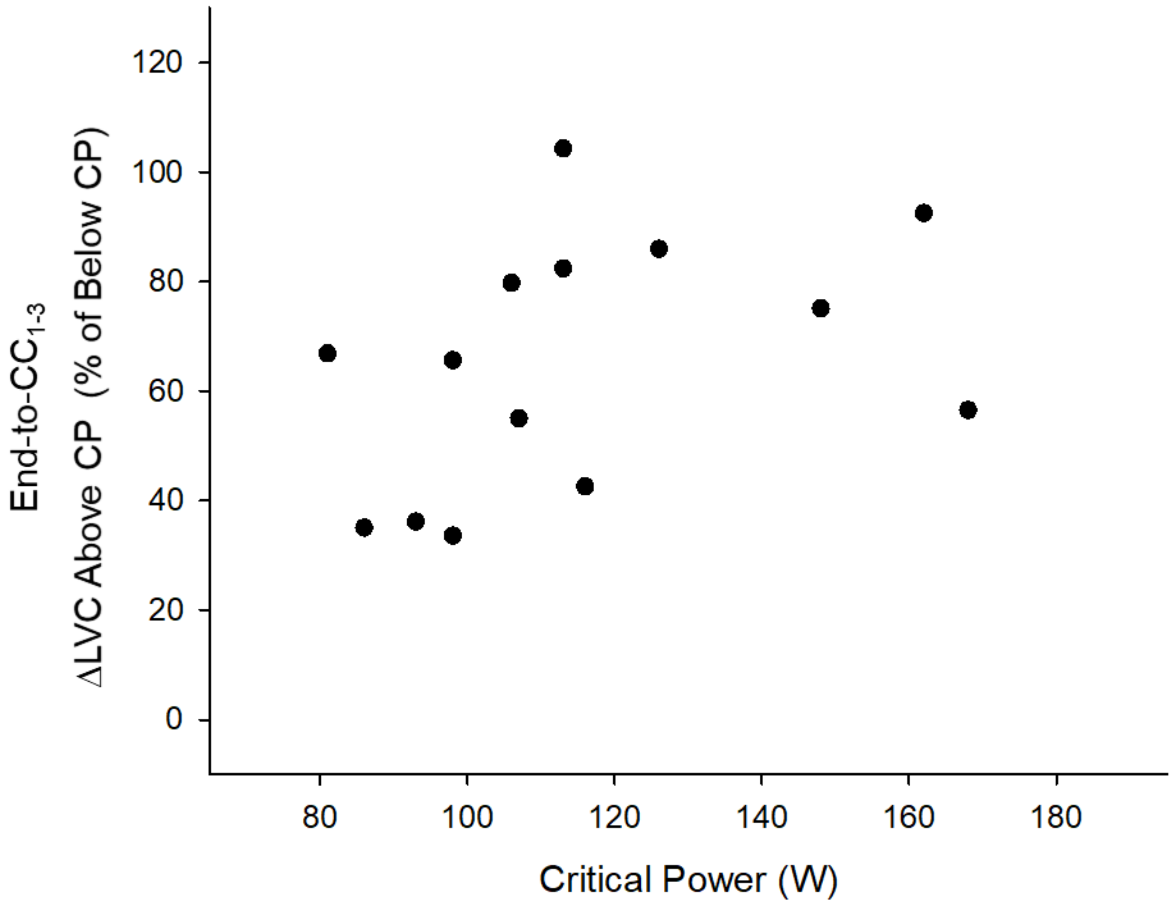

Figure 3.5 Relationship between critical power and below-versus-above critical power differences in limb vascular conductance changes during immediate recovery.

Individual critical powers (CPs) and changes in limb vascular conductance (ΔLVC) during immediate recovery ($CC_{1\text{-}3}$) above CP as a percent of the below-CP response. Note no significant relationship suggesting individual differences in CP (and therefore below-to-above CP power-output differences) do not explain the relationship between absolute ΔLVC and power-output above-CP in Fig. 3.4.

Chapter 4 - Influence of blood flow occlusion on muscular recruitment and fatigue during maximal-effort small muscle mass exercise

Summary

High-levels of skeletal muscle sensory feedback are thought to restrict motor-unit activation and limit exercise tolerance. The roles of muscle fatigue development and motor-unit activation in determining the heavy-to-severe intensity threshold (critical force; CF) remain unclear. This study utilized blood flow occlusion (OCC) to determine the relationships between skeletal muscle fatigue development and motor-unit recruitment patterns during the determination of CF. We hypothesized that (1) OCC would exacerbate peripheral fatigue development and increase the rate of motor-unit deactivation and (2) blood flow reperfusion (REP) would result in muscle recovery and re-recruitment of motor-units despite continuous maximal effort (3) resulting in an end-exercise force not different from CF. Seven young, healthy subjects performed maximal-effort rhythmic handgrip exercise for 5-min under control conditions (CON) and during OCC and REP. Peripheral fatigue development and motor-unit activation levels were measured during each test. OCC resulted in significantly greater peripheral fatigue development than CON ($p<0.001$). Motor-unit deactivation was only observed during OCC ($p<0.001$). REP resulted in significant peripheral recovery ($p<0.001$) and the re-recruitment of motor-units ($p<0.001$) to levels not different from CON. While OCC resulted in a significantly greater reduction in force production compared to CON ($p<0.001$), REP resulted in the restoration of maximal-effort force production (266±19 N; $p<0.001$) to levels not different from CF (276±55 N). These data suggest that CF

reflects an oxygen-delivery dependent balance between motor-unit activation and peripheral fatigue development. Furthermore, this study established that mechanisms which determine the total force-producing capacity of exercising skeletal muscle are significantly altered during OCC.

Introduction

Numerous studies have demonstrated the importance of skeletal muscle sensory feedback in reflexive control of cardiovascular (Amann *et al.*, 2010; Hureau *et al.*, 2018b), ventilatory (Amann *et al.*, 2010), and neuromuscular (Amann *et al.*, 2009; Amann & Dempsey, 2016; Blain *et al.*, 2016; Broxterman *et al.*, 2018; Sidhu *et al.*, 2018) function during exercise. Additionally, a critical level of metabolite-induced fatigue development appears to define severe-intensity exercise tolerance (Amann *et al.*, 2006; Amann & Dempsey, 2008; Hureau *et al.*, 2014; Hureau *et al.*, 2016). Accordingly, it has been postulated that ensemble sensory input from skeletal muscle group III/IV afferents contributes toward volitional termination of exhaustive exercise (Gandevia, 2001; Hureau *et al.*, 2018a). Specifically, the "sensory tolerance limit" (STL) hypothesis suggests a centrally-originating critical tolerance level to feedback associated with skeletal muscle metabolic perturbation that, once attained, reduces skeletal muscle activation through the restriction of central motor drive (CMD) (i.e., central fatigue). Indeed, it has been demonstrated that pharmacological blockade of sensory feedback during exercise, effectively omitting the perception of metabolite accumulation by skeletal muscle afferent nerve endings, results in greater levels of CMD (Amann *et al.*, 2009; Blain *et al.*, 2016). However, greater levels of peripheral fatigue (i.e., at or distal to the neuromuscular junction) and metabolic perturbation are also incurred (Amann *et al.*, 2009; Blain *et al.*, 2016; Broxterman *et al.*, 2018). These findings suggest that restrictions to CMD, despite the negative effect on exercise performance, are physiologically necessary to prevent detrimental levels of metabolic perturbation within skeletal muscle.

Task failure during severe-intensity exercise at a constant work rate (CWR) is characterized by similar levels of skeletal muscle oxygen delivery (Broxterman *et al.*, 2015a; Hammer *et al.*, 2020). Additionally, end-exercise levels of muscular metabolic perturbation

(Burnley *et al.*, 2010; Vanhatalo *et al.*, 2010) and peripheral fatigue development (Amann *et al.*, 2006; Burnley *et al.*, 2012) during severe-intensity CWR exercise appear independent of task duration. Interestingly, both oxygen delivery (Hammer *et al.*, 2020) and peripheral fatigue development (Burnley, 2009) at task failure during CWR exercise are nearly identical to levels reached, and sustained, during continuous maximal-effort exercise. While severe-intensity CWR exercise is performed with submaximal exertion (i.e., effort only reaches maximal levels near task failure) and motor-unit recruitment progressively increases, sustained maximal-effort exercise has resulted in progressive deactivation of motor-units during both whole-body (Vanhatalo *et al.*, 2011) and single-joint exercise (Burnley, 2009). Moreover, time to task failure (T_{lim}) is not defined by the inability to meet force- or power-output requirements and exercise continues until a nadir in maximal-effort force- (critical force; CF) or power-output (critical power; CP) is reached (Vanhatalo *et al.*, 2007; Burnley, 2009). CP/CF demarcates the boundary between the heavy- and severe-intensity exercise domains and has been established as an important threshold for skeletal muscle metabolism (Poole *et al.*, 1988; Jones *et al.*, 2008), oxygen delivery (Poole *et al.*, 1988; Copp *et al.*, 2010; Hammer *et al.*, 2020), neuromuscular fatigue (Burnley *et al.*, 2012), and therefore exercise tolerance (Poole *et al.*, 2016).

Attenuation of sensory input has clearly demonstrated that skeletal muscle group III/IV afferents are central in regulating skeletal muscle contractile efficiency (Broxterman *et al.*, 2017b; Broxterman *et al.*, 2018) and whole-body exercise responses (Amann *et al.*, 2010; Amann *et al.*, 2011b). However, Broxterman et al. observed no effect of group III/IV afferent attenuation on CF determination during maximal-effort knee-extension exercise (Broxterman *et al.*, 2018). While, pharmacological blockade allows the role of group III/IV afferents to be elucidated without compromising skeletal muscle oxygen delivery (Hureau *et al.*, 2019), these interventions also obfuscate the observation of sensory input-induced restrictions to CMD (i.e., reduced motor-unit activation). Restricting oxygen delivery via limb blood flow occlusion has been shown to exacerbate the magnitudes of both central and peripheral fatigue development during CWR small muscle-mass exercise (Russ & Kent-Braun, 2003; Broxterman *et al.*, 2015c). However, given the progressive recruitment of motor-units (Vanhatalo *et al.*, 2011; Burnley *et al.*, 2012) and force-dependent definition of T_{lim}, CWR exercise is not conducive for elucidating relationships that may exist between the constraint of motor-unit activation and determination of CF.

Considering the effects of limb blood flow occlusion on metabolite accumulation and group III/IV sensory afferent nerve firing rates (Rowell & O'Leary, 1990; Adreani & Kaufman, 1998), manipulations in blood flow may elucidate if any relationship exists between STL-mediated restriction to motor-unit activation and CF determination during maximal-effort exercise. Therefore, the primary aim of this study was to determine the influence of complete limb blood flow occlusion on skeletal muscle fatigue development and motor-unit recruitment patterns during maximal-effort isometric handgrip exercise. We hypothesized that (1) blood flow occlusion would exacerbate the development of muscle fatigue and significantly increase the rate of motor-unit deactivation. Further, we hypothesized that (2) restoration of blood flow would result in skeletal muscle recovery and significant re-recruitment of motor-units despite continuous maximal effort (3) resulting in an end-exercise force not different from CF. Lastly, we hypothesized that (4) motor-unit activation levels would be associated with the magnitude of peripheral muscular fatigue development independent of blood flow.

Methods

Seven young, healthy subjects (mean ± SD; 22 ± 4 yr; 174 ± 7 cm; 77.3 ± 10.4 kg; 2 women) volunteered to participate in this study. All experimental procedures were approved by the Institutional Review Board for Research Involving Human Subjects at Kansas State University and conformed to the standards set forth by the Declaration of Helsinki with the exception of database registration. Subjects were informed of all testing procedures and potential risks of participation before providing written, informed consent. Each subject completed a medical health history evaluation to confirm the absence of any known cardiovascular, pulmonary, or metabolic disease. Subjects were instructed to abstain from vigorous activity 12 hrs. prior and caffeine and food consumption 2 hrs. prior to each testing session. Although differences exist in skeletal muscle fatigue development during exercise (Hunter, 2014), these differences either do not appear to be modulated by phases of the menstrual cycle (Janse de Jonge *et al.*, 2001) or are greater in effect size than differences across menstrual cycle phases (Hunter, 2016). Therefore, no attempt was made to control for menstrual cycle phase in the women subjects.

Experimental Design

All subjects were familiarized with the testing protocols prior to data collection. Subsequent to a familiarization visit, subjects reported to the laboratory on two separate occasions separated by at least 48 hrs. In randomized order, subjects performed a rhythmic single-arm isometric-handgrip maximal-effort test (MET) under control conditions (CON) or during limb blood flow occlusion (OCC) and reperfusion (REP). All exercise tests were performed on a custom-built single-arm isometric handgrip system. A handle was fixed 5.5 cm from a palmar support rail via a cable system instrumented with an in-line tension load cell. Force-output from the load cell was digitized and displayed on a nearby monitor. The system was calibrated prior to the study. All tests were performed in the supine position with the right arm outstretched 90 degrees at heart level. Handgrip exercise was performed at 20 contractions per min with a 50% duty-cycle (i.e., 1.5 s contraction and 1.5 s relaxation). Contraction and relaxation cues were provided to each subject via a prerecorded audio file. During OCC trials, blood flow occlusion of the brachial artery was accomplished via rapid inflation of a vascular cuff (E20 Rapid Cuff Inflator, Hokanson, Bellevue, WA) positioned around the brachial region of the exercising limb. The vascular cuff was inflated to suprasystolic pressure (> 250 mmHg) and blood flow occlusion was verified by the absence of a radial pulse.

Maximal-effort tests. The rhythmic isometric MET used in this study has been used previously by our laboratory to determine CF during handgrip exercise (Hammer *et al.*, 2020) and has been previously validated in the forearm (Kellawan & Tschakovsky, 2014) and during knee extension exercise (Burnley, 2009) against conventional methods of CF determination (i.e., multiple CWR exercise tests to failure). The MET consisted of subjects performing an isometric maximal voluntary contraction (MVC) for 1.5 s followed by 1.5 s of relaxation before performing another MVC. This cycle was repeated for the duration of the test (5-min). During the MET, a finite force-generating capacity is gradually utilized during the early phase of the test when force production (or power output during cycling) regressively falls until plateauing at CF (Vanhatalo *et al.*, 2007, 2008). Previous data from our laboratory has demonstrated that a 5-min MET protocol under control conditions was sufficient to elicit a ~60 s plateau in maximal force production at the same contraction frequency and duty-cycle used in this study (20 contractions per min; 50% duty-cycle) (Hammer *et al.*, 2020). During each experimental trial, subjects were blinded to force production during the MET to avoid voluntary force targeting and instill confidence in the end-test force plateaus. Additionally, subjects remained unaware of the time or number of contractions remaining in the test. Subjects were strongly encouraged to produce maximal voluntary force during each contraction and to relax fully between contractions.

Unlike CON trials, during which substantial force production (i.e., ≥ CF) was possible for the entire duration of the MET (5-min), OCC trials were performed until contraction force was < 15% of F_{peak} (150 ± 12 s). After falling below this force threshold, a ~15 s period of rest was executed to accommodate neuromuscular fatigue measurements prior to rapid deflation of the vascular cuff. Following cuff release (REP), subjects were instructed to immediately continue MVCs in concert with the prerecorded audio cues. This REP portion of the MET was continued until a total test time of 5-min was reached.

Measurements

Force production. Force was sampled continuously at 1000 Hz during each MET and during pre- and post-MET neuromuscular function testing. Average force production was calculated from 0.25 s to 1.25 s of each 1.5 s contraction to minimize the effect of delayed force commencement or premature relaxation. Peak force production (F_{peak}) during each of the METs was defined as the highest average force of any single contraction. CF of each subject was determined as the average force production during the final 10 contractions (30 s) of the CON MET. Force at the start of CON and OCC METs was determined as the average force production during the first 3 contractions of each test. Force at the end of the CON MET and at the end of OCC and REP stages was determined as the average force production during the final 3 contractions of each respective stage. The force impulse (J) was calculated as the area under the force-time curve for each condition. J was calculated above CF (J_{CON}) and above OCC_{end} force (J_{OCC}).

Surface electromyography (EMG). Surface EMG measurements were made continuously during each test using a commercially available system (Trigno EMG; Delsys Inc.; Boston, MA, USA). The EMG sensor consisted of four electrodes (5 × 1 mm) arranged in a 2 × 2 configuration to make single differential measurements. The flexor digitorum superficialis (FDS) of the right forearm was identified via palpation and EMG placement was confirmed by strong EMG activity during finger-flexion and lack of signal during ulnar- and radial-deviation. Adhesive tape was used to secure the EMG sensor along the belly of the muscle and indelible ink was used to ensure placement reproducibility. The EMG data were collected at a sampling rate of 1000 Hz and band-pass filtered (13–400 Hz) using a fifth-order Butterworth filter. The EMG signal corresponding to each muscle contraction was detected using software previously developed in our laboratory (MATLAB R2011a; The Mathworks; Natick, MA). The amplitude characteristics were described using the root mean square (RMS) to provide an index of muscle activation and motor-neuron firing rate for each muscular contraction during both METs. The frequency characteristics were described using the median power frequency (MedPF) to provide an index of the muscle action potential conduction velocity for each muscular contraction during both METs. RMS and MedPF at the start of each test were determined as the average RMS and MedPF values, respectively, during the first 3 contractions. End-stage RMS and MedPF were determined as the average RMS and MEdPF values, respectively, during the final 3 contractions of each respective stage.

Neuromuscular function. Neuromuscular function testing was performed on the exercising arm prior-to and immediately after each MET. An additional measurement was made immediately following (within 1.5 s) OCC_{end} during which blood flow remained occluded. Neuromuscular function was assessed using the same single-arm isometric handgrip system used for the METs to facilitate near-immediate recovery measurements (i.e., subjects were not required to move prior to post-test neuromuscular assessment). Stimulation electrodes (1.25 in diameter) were adhered to the antebrachial region of the right arm to electrically induce finger-flexion. The anode was positioned distal to the olecranon process and the cathode was positioned over the median nerve on the posterior and anterior antebrachial regions of the forearm, respectively. The cathode placement that elicited the greatest finger-flexion force production was determined via repeated electrical stimulations and marked with indelible ink. The medial nerve was stimulated using a high-voltage constant-current electrical stimulator (DS7AH, Digitimer; Welwyn Garden City, UK). Paired stimuli (doublets) were delivered at 400 V with 100 μs square-wave pulse durations and a 10 ms pulse interval. Maximal stimulation current was determined prior to each MET. Stimulation intensity was initiated at 50 mA and was increased by 25 mA until the measured force and compound muscle action potential (M-wave) demonstrated a plateau. The stimulator current was then increased an additional 30% to ensure supramaximal stimulation. Prior to each MET, subjects performed a series of six, 3 s MVCs, beginning every 30 sec. Doublet muscle stimulations were delivered 5 s prior to each MVC, 1.5 s into the MVC, and 5 s after each MVC to obtain measurements of unpotentiated, superimposed (Q_{sup}), and potentiated doublet (Q_{pot}) forces, respectively. MVC during neuromuscular function testing was determined as the greatest force attained prior to Q_{sup}. Voluntary activation (VA) was calculated using doublet interpolation (Behm *et al.*, 1996) corrected for when Q_{sup} stimulation did not occur at MVC plateau force:

$$\%VA = \left[1 - \left(\frac{force\ prior\ to\ Q_{sup}}{MVC\ plateau\ force}\right) \times \left(\frac{Q_{sup}}{Q_{pot}}\right)\right]$$

Changes in MVC, Q_{pot}, and %VA have been used extensively to quantify global, peripheral, and central fatigue, respectively (Bigland-Ritchie *et al.*, 1986; Burnley *et al.*, 2012;

Broxterman *et al.*, 2015c; Alexander *et al.*, 2019). Previous data suggests the degree of potentiation is decreased after two MVCs (Kufel *et al.*, 2002). Therefore, the last four MVCs were used for data analysis during baseline (BL) neuromuscular function assessment. Alexander et al. suggested that significant neuromuscular recovery may occur within 30 s of end-exercise (Alexander *et al.*, 2019). To minimize any effects of recovery and reflect the end-stage neuromuscular condition as accurately as possible, end-stage neuromuscular function assessment was determined using the MVC immediately following the final contraction of each stage.

Statistical Analysis

Statistical analyses were performed using SigmaStat (Systat Software Inc.; Point Richmond, CA, USA). Data are expressed as mean ± SD, unless otherwise noted. The final 10 contractions of each MET were compared across condition using a two-way ANOVA with repeated measures (condition × contraction). Student's paired t-tests were used to compare both F_{peak} and J across conditions. Force and EMG measurements were compared across each test stage using two-way ANOVAs with repeated measures (condition × stage). Neuromuscular function measurements were compared at BL and immediately following each test stage using a two-way ANOVA with repeated measures (condition × stage). If significant main effects were determined, a Tukey's post hoc analysis was performed to determine where significant differences existed. Linear regression was used to determine changes in force over time during the final 10 contractions of each MET. Linear regression was used to identify any significant relationships among J, EMG, and neuromuscular function measurements within each experimental condition. Differences and relationships were considered significant when $p < 0.05$.

Results

Force. The mean force profiles during each MET are presented in Fig. 4.1. F_{peak} was not different between CON and OCC. Force decreased significantly during CON ($p < 0.001$). During the final 10 contraction (30 s) of CON, linear regression revealed a force/time slope (-0.57 ± 1.09 N/s) that was not significantly different from zero suggesting a plateau in end-test force production at 276 ± 55 N (44.8 ± 8.6 % F_{peak}) which was defined as CF. Force decreased significantly during OCC ($p < 0.001$). OCC_{end} force was significantly lower (73.5%) than CON_{end} ($p < 0.001$). Following cuff release, force increased significantly ($p < 0.001$) during REP resulting in a REP_{end} force that was not different from CON_{end}. During the final 10 contraction (30 s) of REP, linear regression revealed a force/time slope (-0.01 ± 0.67 N/s) that was not significantly different from zero suggesting a plateau in end-test force production. Additionally, force of the final 10 contractions of REP and CON (i.e., CF) were not different (see inset of Fig. 4.1). Lastly, J_{OCC} (2339 ± 659 N·s) was significantly greater than J_{CON} (1118 ± 630 N·s; $p < 0.001$) (Fig. 4.2B).

EMG. The mean RMS profiles during each MET, normalized to RMS at F_{peak} for each condition, are presented in Fig. 4.3A. RMS at the start of each MET was not different between CON and OCC. RMS remained unchanged during CON suggesting continuous maximal recruitment. However, RMS decreased significantly during OCC ($p < 0.001$) resulting in a RMS at OCC_{end} that was significantly lower than at CON_{end} ($p < 0.001$) suggesting progressive deactivation of motor-units during OCC but not CON. Following cuff release, RMS increased significantly during REP ($p < 0.001$) resulting in a RMS level at REP_{end} that was not different from CON_{end} suggesting a similar level of activation to that of exercise at CF.

The mean profiles of force production (% F_{peak}) per RMS level (% RMS at F_{peak}) during each MET are presented in Fig. 4.3B. Force/RMS decreased significantly during both CON and

OCC (both $p < 0.001$). Interestingly, the force/RMS from 70-80s during the METs was significantly greater during OCC compared to CON ($p < 0.001$) suggesting a biphasic response. However, force/RMS at OCC_{end} was significantly lower than at CON_{end} ($p < 0.001$) suggesting a functional impairment in the excitation-to-contraction processes. Following cuff release, force/RMS increased significantly during REP ($p < 0.001$) resulting in a force/RMS at REP_{end} that was not different from CON_{end}.

The mean MedPF profiles during each MET, normalized to MedPF at F_{peak} for each condition, are presented in Fig. 4.3C. MedPF at the start of each MET was not different between CON and OCC. MedPF decreased significantly during both CON and OCC (both $p < 0.001$). However, MedPF at OCC_{end} was significantly lower than at CON_{end} ($p < 0.001$) suggesting slower action potential conduction velocity. Following cuff release, MedPF remained unchanged during REP resulting in a MedPF value at REP_{end} that was significantly lower than CON_{end} suggesting no recovery in action potential conduction velocity characteristics.

Neuromuscular function. Mean values for MVC at BL and following each stage of the CON and OCC METs are presented in Fig. 4.4A. BL MVC was not different between CON and OCC. MVC decreased significantly during CON and OCC (both $p < 0.001$). However, MVC was significantly lower at OCC_{end} compared to CON_{end} ($p < 0.001$) suggesting greater global fatigue development during OCC compared to CON. Additionally, REP_{end} MVC was significantly greater compared to OCC_{end} ($p < 0.001$) but was not different from CON_{end} suggesting recovery during REP to a similar level of global fatigue at the end of each MET.

Mean values for Q_{pot} at BL and following each stage of the CON and OCC METs are presented in Fig. 4.4B. BL Q_{pot} was not different between CON and OCC. Q_{pot} decreased significantly during CON and OCC (both $p < 0.001$); however, Q_{pot} at OCC_{end} was significantly lower than at CON_{end} ($p < 0.001$) suggesting a greater degree of peripheral fatigue accumulation during OCC compared to CON. Q_{pot} increased significantly during REP ($p < 0.001$). However, Q_{pot} at REP_{end} was not different from CON_{end} suggesting recovery of peripheral (i.e., intramuscular) mechanisms of force production during REP and a similar level of peripheral fatigue at the end of each MET.

Mean values for %VA at BL and following each stage of the CON and OCC METs are presented in Fig. 4.4C. BL %VA was not different between CON and OCC. %VA decreased significantly during CON and OCC (both $p < 0.001$) such that end-stage %VA was not different. Unlike other neuromuscular function measurements, %VA was further reduced during REP ($p < 0.001$) consequent to a significantly greater Q_{sup} at REP_{end} (6.85 ± 2.06 N) compared to CON_{end} (3.91 ± 1.91 N; $p < 0.05$). Therefore, %VA was significantly lower at REP_{end} compared to CON_{end} ($p < 0.001$) suggesting a reservation in muscular force producing capabilities in addition to those being voluntarily activated.

Neuromuscular function, J, and RMS. J_{CON} was significant associated with the percent decline in Q_{pot} ($r = 0.76$; $p < 0.05$; Fig. 4.5B) but not %VA ($p = 0.83$; Fig. 4.5C) or MVC ($p = 0.11$; Fig. 4.5A). J_{OCC} was not associated with the percent decline in Q_{pot} ($p = 0.25$; Fig. 4.5B) but was significantly associated with percent decline in both %VA ($r = 0.83$; $p < 0.05$; Fig. 4.5C) and MVC ($r = 0.93$; $p < 0.01$; Fig. 4.5A). Additionally, neither J_{CON} nor J_{OCC} were associated with RMS (%F_{peak}) ($p = 0.09$ & 0.79, respectively). Percent decline in Q_{pot} was significantly associated with RMS (%F_{peak}) during CON ($r = 0.86$; $p = 0.01$), but not OCC ($p = 0.12$) or REP ($p = 0.63$) (Fig 4.6). Neither percent change in %VA nor MVC were significantly related to changes in RMS (%F_{peak}) during CON ($p = 0.13$ and 0.22, respectively), OCC ($p = 0.38$ and 0.94, respectively), or REP ($p = 0.88$ and 0.97, respectively).

Discussion

Major Findings

This study determined the influence of blood flow occlusion on fatigue development and recruitment patterns in skeletal muscle during maximal-effort isometric handgrip exercise. Consistent with our first hypothesis, blood flow occlusion led to greater peripheral fatigue development (Fig. 4.4B) and reduced motor-unit activation (Fig. 4.3A) during continuous maximal-effort exercise. Further, supporting our second hypothesis, restoration of blood flow resulted in rapid recovery of maximal-effort force production (Fig. 4.1) and re-recruitment of previously deactivated FDS motor-units (Fig. 4.3A). Remarkably, confirming our third hypothesis, maximal-effort force production following reperfusion was not different from CF (Fig. 4.1) and levels of motor-unit activation and peripheral fatigue were not different from those at CF under free-flowing conditions (Fig. 4.3A & 4.4B, respectively). Following the partial recovery of peripheral fatigue during vascular reperfusion (Fig. 4.4B), motor-unit activation of the FDS returned to near maximal levels (Fig. 4.3A). Combined, these data suggest that CF represents, not only a specific metabolic rate (Barker *et al.*, 2006; Poole *et al.*, 2016), but also the highest maximal-effort force production at which a dynamic balance between muscle activation level and peripheral fatigue development exists.

Maximal-effort vs. CWR exercise. This study utilized continuous maximal-effort exercise and omitted any force-determined definitions of task failure from the experimental design. This strategy was intentional and superior to CWR exercise for detecting CMD restriction because it allowed 1) constant maximal voluntary engagement of CMD and 2) muscle activation levels to decline without test termination. Broxterman et al. determined that blood flow occlusion during dynamic CWR handgrip exercise exacerbated the development of both peripheral and central fatigue (Broxterman *et al.*, 2015c). These findings were evinced by significantly greater pre- to post-exercise reductions in Q_{pot} and %VA, respectively. In the present study, blood flow occlusion led to a ~30% greater reduction in Q_{pot} (Fig. 4.4B) but had no effect on %VA (Fig. 4.4C). Considering the STL hypothesis, reductions in CMD (i.e., motor-unit activation) would be expected to accompany greater levels of peripheral fatigue (reflecting greater intramuscular metabolic perturbation) (Amann *et al.*, 2009; Blain *et al.*, 2016). While no differences in muscle recruitment responses (i.e., EMG) between freely perfused and occluded conditions were demonstrated during CWR exercise (Broxterman *et al.*, 2015a; Broxterman *et al.*, 2015c), utilizing continuous maximal-effort exercise, the present study clearly demonstrates reduced FDS motor-unit activation during OCC (Fig. 4.3A). These differences among studies may result from dissimilarities in muscle recruitment patterns between CWR and maximal-effort exercise.

As motor-units fatigue, CWR exercise is acutely sustained through the recruitment of additional motor-units (Burnley, 2009; Vanhatalo *et al.*, 2011). Once the subject is no longer able to maintain the required force- or power-output, despite maximal recruitment levels (Burnley *et al.*, 2012), the test is terminated. Therefore, any STL induced restriction to motor-unit recruitment would occur immediately preceding task failure and may not manifest itself within muscle activation measurements. In contrast, maximal-effort exercise permits the progressive decline in force production (Broxterman *et al.*, 2017a; Hammer *et al.*, 2020) that may result from CMD restriction (Fig. 4.3A). Similar rationale was offered during repeated cycling sprints (i.e., 10s of maximal-effort) to demonstrate that plateaus in power output, muscle activation, and %VA are initiated at similar levels of peripheral fatigue development (Hureau *et al.*, 2014; Hureau *et al.*, 2016). These findings support the hypothesis that CMD restriction is likely a means to prevent excess peripheral fatigue development within active skeletal muscle.

Fatigue development during maximal-effort exercise. It is well established that levels of both intramuscular metabolite concentrations (Jones *et al.*, 2008; Vanhatalo *et al.*, 2010) and peripheral fatigue development (Burnley, 2009; Burnley *et al.*, 2012) reach similar endpoints during CWR exhaustive exercise. Remarkably, Burnley et al. demonstrated that the level of peripheral fatigue development at task failure from constant target-torque knee-extension tests was identical to the level developed during a 5-min maximal-effort test (Burnley, 2009; Burnley *et al.*, 2010). Additionally, levels of fractional oxygen extraction (Hammer *et al.*, 2020), oxidative ATP production (Broxterman *et al.*, 2017a), and intramuscular metabolic perturbation (Broxterman *et al.*, 2017a) plateau early-on during maximal-effort tests while force production continues to decline until reaching CF. Together, these findings suggest that CF represents the greatest intermittent force production at which metabolic ATP-demand and resulting fatigue-inducing metabolite accumulation remain dynamically balanced.

Prior induction of muscle fatigue is associated with dose-dependent decreases in CMD (Amann & Dempsey, 2008; Amann *et al.*, 2013). Further, blockade of skeletal muscle sensory feedback via fentanyl results in greater levels of CMD and exacerbation of peripheral fatigue development (Amann *et al.*, 2009; Amann *et al.*, 2011a). These data clearly indicate inhibition of muscle activation via skeletal muscle sensory feedback and strongly suggest peripheral fatigue development (i.e., metabolic perturbation (Blain *et al.*, 2016)) is the principle regulator of CMD restriction during exercise. The RMS (Fig. 4.3A) and Q_{pot} (Fig. 4.4B) responses from METs in this study are consistent within this paradigm.

Muscle recruitment during maximal-effort exercise. Interestingly, the activation patterns of the FDS during the CON MET (Fig. 4.3A) are unlike those reported previously of the vastus lateralis (VL) during both cycling (Vanhatalo *et al.*, 2011) and knee-extension exercise (Burnley, 2009). Vanhatalo et al. demonstrated a progressive decline in muscle activation during a 3-min maximal-effort cycling test and described progressive fatigue in predominantly type II fibers during the early portions of the test as a potential mechanism for this response (Vanhatalo *et al.*, 2011). Force/RMS remained relatively high during the initial ~90s of OCC and was significantly greater, compared to CON, between 70 and 80s of the MET (Fig. 4.3B). These data are consistent with fatigue in a more-glycolytic pool of muscle fibers (Vanhatalo *et al.*, 2011) and ATP-production from primarily non-oxidative energy sources (Broxterman *et al.*, 2017a; Broxterman *et al.*, 2018) during early stages of maximal-effort exercise.

The muscular force requirements during cycling exercise are far lower than the maximal force producing capabilities of the quadriceps (< 50% MVC) (Lollgen *et al.*, 1980). Thus, preferential recruitment strategies are possible (e.g., a relative shift from type II to type I fibers) and muscular fatigue can be distributed among motor-units and muscles throughout the duration of the test (Vanhatalo *et al.*, 2011). The EMG data from this study are better suited for comparisons to muscular recruitment patterns during exercise modalities that elicit MVC-like activation at exercise onset. Burnley et al. observed an average ~30% decline in VL activation during a 5-min maximal-effort isometric knee-extension test (Burnley, 2009). While a high degree of intersubjective variability exists (Fig. 4.6), the mean RMS response during CON in the present study does not support a progressive deactivation of motor-units in the FDS during a MET under control conditions (Fig. 4.3A).

However, partially confirming our first hypothesis, reduced oxygen delivery (via blood flow occlusion) precipitated clear deactivation of FDS motor-units (Fig. 4.3A). These data, combined with the alternative findings of Burnley et al. (Burnley, 2009), might suggest unique composition (e.g., fiber-type) and functional recruitment strategies between muscle groups and/or portions of the VL (i.e., superficial) experience greater oxygen delivery limitations during isometric maximal-effort exercise. Indeed, differences and variability in fiber-type composition between the superficial VL (Johnson *et al.*, 1973; Carter *et al.*, 2004) and FDS (Dahmane *et al.*, 2005; Hwang *et al.*, 2013) may result in differences in EMG-sampled fiber-type and explain discrepancies between the muscle activation patterns of the thigh (Burnley, 2009) and the forearm (this study). Lastly, although this study did not characterize fiber-type, variability among subjects in recruitment patterns and the significant association between changes in RMS and Q_{pot} (Fig. 4.6) during CON may result from fiber-type variance within forearm flexor muscles (Johnson *et al.*, 1973; Dahmane *et al.*, 2005; Hwang *et al.*, 2013).

Influence of blood flow occlusion. Broxterman et al. demonstrated severely diminished exercise tolerance, significantly greater fractional oxygen extraction, and a prominent reduction in muscle tissue saturation during ischemic CWR handgrip exercise (Broxterman *et al.*, 2015a). Additionally, blood flow occlusion strongly influences the development of both central and peripheral fatigue during small muscle mass exercise (Russ & Kent-Braun, 2003; Broxterman *et al.*, 2015c). Peripheral impairment of muscle performance during ischemia appears to result primarily from its detrimental effects on oxygen delivery, and concomitant metabolite production, and not reduced metabolite removal per se (Hogan *et al.*, 1994; Hepple, 2002). Thus, greater peripheral fatigue development during blood flow occlusion ((Broxterman *et al.*, 2015c); Fig.

4.4B) is likely a consequence of diminished oxygen delivery and resulting exacerbation of anaerobic metabolism.

While progressive motor-unit deactivation was hypothesized under both experimental conditions, significant reductions in FDS motor-unit activation were only demonstrated during OCC (Fig. 4.3A). However, motor-unit activation level during CON was associated with the level of peripheral fatigue development (Fig. 4.6) suggesting that peripherally originating factors are involved in regulating the level of CMD. Whereas afferent blockade masks the rise in metabolite accumulation and peripheral fatigue development, thus allowing CMD to remain uninhibited (Amann *et al.*, 2009; Amann *et al.*, 2011a), profound reductions in motor-unit activation (Fig. 4.3A) and greater peripheral fatigue development (Fig. 4.4B) were observed during OCC. Peripheral sensory feedback appears to limit anaerobic glycolysis and thus limit the degree of metabolic perturbation. Indeed, an anaerobic metabolic reserve appears to exist under control conditions during maximal-effort small muscle-mass exercise (Broxterman *et al.*, 2018). The extreme oxygen delivery limitation imposed by complete limb occlusion almost certainly obligated utilization of any anaerobic reserve, presumably leading to greater metabolite accumulation and peripheral fatigue development, and ultimately resulting in the inhibition of CMD.

Attenuation of group III/IV afferents enhances motor-unit activation levels (Amann *et al.*, 2009; Amann *et al.*, 2011a) and improves maximal-force output during intermittent isometric exercise (Broxterman *et al.*, 2018). However, sensory feedback also appears to play a significant role in preserving muscular contractile efficiency during exercise. Indeed, attenuation of group III/IV afferent feedback resulted in greater ATP cost associated with muscular contraction and rise in fatigue-inducing metabolite production (e.g., P_i) (Broxterman *et al.*, 2017a; Broxterman *et al.*, 2018). Further, it has been recognized that these impairments in muscular performance are likely a consequence of diminished oxygen delivery (Hureau *et al.*, 2019). Therefore, the detrimental influence of blood flow occlusion on muscle recruitment and force production demonstrated in this study may be directly related to attainment of a STL which is effectively raised, and perhaps not reached, in studies employing group III/IV afferent blockades. Importantly, attainment of a STL is thought to reflect the ensemble sensory input from all possible origins (Deschamps *et al.*, 2014; Hureau *et al.*, 2018a). Thus, the combined influences of occlusion (e.g., pain) must be considered and not only those directly related to oxygen delivery.

Neuromuscular determinants of J and CF. We have previously demonstrated that fractional oxygen extraction during maximal-effort isometric handgrip exercise plateaus much earlier than force production (Hammer *et al.*, 2020). Additionally, the ceiling in fractional oxygen extraction during a MET was similar to levels at task failure during exercise above CF (Hammer *et al.*, 2020). These findings suggest that a task-specific upper-limit in fractional oxygen extraction exists such that energy production can only sustain force generation at CF under free-flow conditions (i.e., CON). The oxygen delivery limitation posed by blood flow occlusion results in greater reliance on the finite reserve of non-oxidative energy stores (i.e., phosphocreatine and muscle glycogen). Utilization of these intramuscular energy stores and concomitant accumulation of fatigue-inducing metabolites (e.g., P_i and H^+) are described by the mathematical curvature constant (W') of the intensity-duration relationship that exists above CP (Monod & Scherrer, 1965; Broxterman *et al.*, 2015a; Broxterman *et al.*, 2015b; Poole *et al.*, 2016). For clarity, W' represents the finite amount of work that can be accomplished above CP during CWR exercise. Although W' is the culmination of many integrated physiological mechanisms related to the development of neuromuscular fatigue (Broxterman *et al.*, 2015c; Zarzissi *et al.*, 2019), it appears certain that oxygen availability (Dekerle *et al.*, 2012; Broxterman *et al.*, 2015a; Simpson *et al.*, 2015) and skeletal muscle oxidative efficiency (Murgatroyd *et al.*, 2011; Vanhatalo *et al.*, 2011), together, play a significant role in determining its rate of utilization during exercise.

Although important differences exist (Burnley, 2009), J is the MET-analog to W' as it reflects the summation of force generation performed above CF. Condition-dependent relationships between J and neuromuscular fatigue measurements were identified in this study (Fig 4.5). These findings suggest unique determinants of skeletal muscle performance between CON and OCC. However, it is possible that with a larger sample size, additional relationships may have been established between J and indices of neuromuscular fatigue (e.g., between J_{CON} and %-change in MVC; Fig 4.5A). Further, it is important to consider that J_{OCC} was calculated as the area under the force-time curve above OCC_{END} force and not above a force plateau. Therefore, J_{OCC} does not reflect the total severe-intensity force-impulse capacity but only that which was utilized during each OCC trial. This method for calculating J_{OCC} allows for comparisons between the total force-impulse performed and the development of muscle fatigue during each exercise task. The predictability of peripheral fatigue development by J_{CON} is consistent with previous findings (Broxterman *et al.*, 2015c; Zarzissi *et al.*, 2019) and the notion that severe-intensity exercise tolerance is determined primarily by peripheral factors (Fig. 4.5B) (Jones *et al.*, 2008; Burnley *et al.*, 2012). Interestingly, J_{OCC} was not associated with the decline in Q_{pot} (Fig. 4.5B), but rather was a significant predictor of decline in %VA (Fig. 4.5C). Q_{pot} reached near minimal values at OCC_{end} (Fig. 4.5B), likely a consequence of study design i.e., the continuance of exercise until force was <15% of F_{peak} (Fig 4.1). Considering the STL paradigm, the persistent maximal-effort during OCC, despite significantly greater levels of peripheral fatigue development (Fig 4.4B), might predict the observed restriction of CMD (indicated by decreased RMS; Fig. 4.3A). It is noteworthy that, while %VA was not different between CON and OCC, %VA continued to fall during REP (Fig. 4.4C).

This might suggest different time-courses in recovery between peripherally- and centrally-originating mechanisms of fatigue (Jones, 1996). Similarly, MedPF demonstrated no recovery during REP (Fig. 4.3C) suggesting that, in contrast to motor-unit recruitment, action potential conduction velocity characteristics remained significantly impaired. The supra-physiological inflation of peripheral fatigue during OCC likely explains the significantly greater J_{OCC} compared to J_{CON} (Fig. 4.2B). However, the dissociation between peripheral and central recovery-times following OCC, and potential relationships with J_{OCC}, require further investigation.

While heterogeneity of muscle composition (i.e., fiber-type; (Dahmane *et al.*, 2005; Hwang *et al.*, 2013)) and recruitment patterns (Hammer *et al.*, 2018) might explain the variability in RMS data during CON (Fig. 4.6) and lack of evidence for CMD restriction (discussed above; Fig. 4.3A), a clear plateau in end-test force production among all subjects established that CF was, in fact, reached (Fig 4.1). Interestingly, pharmacological blockage of skeletal muscle sensory feedback does not alter CF (Broxterman *et al.*, 2018). To the contrary, it has been established that vascular occlusion reduces the heavy-to-severe intensity threshold below resting metabolic levels (i.e., < 0 Watts) (Broxterman *et al.*, 2015a). Therefore, vascular occlusion in this study effectively removed the possibility to reach an acutely sustainable level of force production during OCC. Nonetheless, CMD restriction was observed through reductions in RMS until exercise termination at markedly low force values (Fig. 4.3A and Fig. 4.1, respectively). By itself, the reduction in force during OCC to below CF is unremarkable. However, the rapid recovery of force production during REP to CF-like values within ~20-25 s is particularly noteworthy (Fig 4.1). Interestingly, while brachial artery blood flow has been demonstrated to peak within ~10 s after cuff-release during a vascular occlusion test (Joannides *et al.*, 1995; Bopp *et al.*, 2014; Didier *et al.*, 2020), the time courses for post-occlusive microvascular hyperemia (Didier *et al.*, 2020) and tissue oxygenation (Bopp *et al.*,

2011) of the forearm appear similar to the rise in force production from the present study. Together, these data suggest that microvascular oxygen availability may be a primary determinant of muscle force-generating capacity. Additionally, recovery of peripheral fatigue (Fig. 4.4B), but not central-fatigue (Fig. 4.4C), and re-activation of muscle motor units (Fig. 4.3A) during REP, combined with CF-like maximal force-output, suggest that CF reflects an oxygen delivery dependent balance between motor-unit activation and peripheral fatigue development.

Experimental considerations

Conclusions from this study are based upon data collected during isometric small muscle-mass exercise. Although it can neither be confirmed nor refuted based on the findings of this study alone, the oxygen-dependency of the STL appears to be exercise modality (whole-body vs. small muscle-mass) and intervention (manipulation of arterial oxygen content vs. blood flow) specific (Amann *et al.*, 2006; Broxterman *et al.*, 2015c). While whole-body exercise is certainly more generalizable to real-world scenarios, small muscle-mass exercise is advantageous for establishing relationships between neuromuscular fatigue and muscle activation. Specifically, well-controlled muscle electrical stimulation protocols used for neuromuscular function testing can elicit only simple, single-joint movements (e.g., handgrip and knee-extension). Therefore, indices of fatigue development (e.g., decline in Q_{pot}) can only reflect changes in a relatively small group of muscles. Additionally, EMG measurements aim to capture muscle activation levels of individual muscles. Thus, relationships between EMG and neuromuscular fatigue measurements via electrical stimulation are better suited for single-joint exercise. Further, isometric protocols facilitate rapid neuromuscular function measurements compared to dynamic protocols which require a time delay for electrical stimulation setup. Therefore, this study utilized an isometric exercise protocol to better characterize the end-exercise condition of the muscle.

Conclusions

This study provides additional evidence that the determination of CF is orchestrated by oxygen-delivery dependent mechanisms related to fatigue-induced restriction of CMD. Specifically, parallel changes in force production, peripheral fatigue development, and motor-unit activation during complete blood flow occlusion and vascular reperfusion suggest that CF reflects an oxygen-delivery dependent balance between motor-unit activation and peripheral fatigue development. Additionally, the relationships elucidated by this study suggest that motor-unit activation is significantly related to peripheral fatigue development only under normal physiological conditions and that vascular occlusion results in maximal levels of peripheral fatigue development independent of muscular activation level. Further, this study established that mechanisms which determine the total force-producing capacity of exercising skeletal muscle are significantly altered during blood flow occlusion. These findings may have wide-spread implications for exercise tolerance in patient populations who experience partial vascular occlusion or altered neuromuscular reflexes.

References

Adreani CM & Kaufman MP. (1998). Effect of arterial occlusion on responses of group III and IV afferents to dynamic exercise. *J Appl Physiol (1985)* **84,** 1827-1833.

Alexander AM, Didier KD, Hammer SM, Dzewaltowski AC, Kriss KN, Lovoy GM, Hammer JL, Smith JR, Ade CJ, Broxterman RM & Barstow TJ. (2019). Exercise tolerance through severe and extreme intensity domains. *Physiological reports* **7,** e14014.

Amann M, Blain GM, Proctor LT, Sebranek JJ, Pegelow DF & Dempsey JA. (2010). Group III and IV muscle afferents contribute to ventilatory and cardiovascular response to rhythmic exercise in humans. *J Appl Physiol (1985)* **109,** 966-976.

Amann M, Blain GM, Proctor LT, Sebranek JJ, Pegelow DF & Dempsey JA. (2011a). Implications of group III and IV muscle afferents for high-intensity endurance exercise performance in humans. *J Physiol* **589,** 5299-5309.

Amann M & Dempsey JA. (2008). Locomotor muscle fatigue modifies central motor drive in healthy humans and imposes a limitation to exercise performance. *J Physiol* **586,** 161-173.

Amann M & Dempsey JA. (2016). Ensemble Input of Group III/IV Muscle Afferents to CNS: A Limiting Factor of Central Motor Drive During Endurance Exercise from Normoxia to Moderate Hypoxia. *Adv Exp Med Biol* **903,** 325-342.

Amann M, Eldridge MW, Lovering AT, Stickland MK, Pegelow DF & Dempsey JA. (2006). Arterial oxygenation influences central motor output and exercise performance via effects on peripheral locomotor muscle fatigue in humans. *J Physiol* **575,** 937-952.

Amann M, Proctor LT, Sebranek JJ, Pegelow DF & Dempsey JA. (2009). Opioid-mediated muscle afferents inhibit central motor drive and limit peripheral muscle fatigue development in humans. *J Physiol* **587,** 271-283.

Amann M, Runnels S, Morgan DE, Trinity JD, Fjeldstad AS, Wray DW, Reese VR & Richardson RS. (2011b). On the contribution of group III and IV muscle afferents to the circulatory response to rhythmic exercise in humans. *J Physiol* **589,** 3855-3866.

Amann M, Venturelli M, Ives SJ, McDaniel J, Layec G, Rossman MJ & Richardson RS. (2013). Peripheral fatigue limits endurance exercise via a sensory feedback-mediated reduction in spinal motoneuronal output. *J Appl Physiol (1985)* **115,** 355-364.

Barker T, Poole DC, Noble ML & Barstow TJ. (2006). Human critical power-oxygen uptake relationship at different pedalling frequencies. *Exp Physiol* **91,** 621-632.

Behm DG, St-Pierre DM & Perez D. (1996). Muscle inactivation: assessment of interpolated twitch technique. *J Appl Physiol (1985)* **81,** 2267-2273.

Bigland-Ritchie B, Furbush F & Woods JJ. (1986). Fatigue of intermittent submaximal voluntary contractions: central and peripheral factors. *J Appl Physiol (1985)* **61,** 421-429.

Blain GM, Mangum TS, Sidhu SK, Weavil JC, Hureau TJ, Jessop JE, Bledsoe AD, Richardson RS & Amann M. (2016). Group III/IV muscle afferents limit the intramuscular metabolic perturbation during whole body exercise in humans. *J Physiol* **594,** 5303-5315.

Bopp CM, Townsend DK & Barstow TJ. (2011). Characterizing near-infrared spectroscopy responses to forearm post-occlusive reactive hyperemia in healthy subjects. *Eur J Appl Physiol* **111,** 2753-2761.

Bopp CM, Townsend DK, Warren S & Barstow TJ. (2014). Relationship between brachial artery blood flow and total [hemoglobin+myoglobin] during post-occlusive reactive hyperemia. *Microvasc Res* **91,** 37-43.

Broxterman RM, Ade CJ, Craig JC, Wilcox SL, Schlup SJ & Barstow TJ. (2015a). Influence of blood flow occlusion on muscle oxygenation characteristics and the parameters of the power-duration relationship. *J Appl Physiol (1985)* **118,** 880-889.

Broxterman RM, Craig JC, Ade CJ, Wilcox SL & Barstow TJ. (2015b). The effect of resting blood flow occlusion on exercise tolerance and W'. *American journal of physiology Regulatory, integrative and comparative physiology* **309,** R684-691.

Broxterman RM, Craig JC, Smith JR, Wilcox SL, Jia C, Warren S & Barstow TJ. (2015c). Influence of blood flow occlusion on the development of peripheral and central fatigue during small muscle mass handgrip exercise. *J Physiol* **593,** 4043-4054.

Broxterman RM, Hureau TJ, Layec G, Morgan DE, Bledsoe AD, Jessop JE, Amann M & Richardson RS. (2018). Influence of group III/IV muscle afferents on small muscle mass exercise performance: a bioenergetics perspective. *J Physiol-London* **596,** 2301-2314.

Broxterman RM, Layec G, Hureau TJ, Amann M & Richardson RS. (2017a). Skeletal muscle bioenergetics during all-out exercise: mechanistic insight into the oxygen uptake slow component and neuromuscular fatigue. *J Appl Physiol* **122,** 1208-1217.

Broxterman RM, Layec G, Hureau TJ, Morgan DE, Bledsoe AD, Jessop JE, Amann M & Richardson RS. (2017b). Bioenergetics and ATP Synthesis during Exercise: Role of Group III/IV Muscle Afferents. *Med Sci Sport Exer* **49,** 2404-2413.

Burnley M. (2009). Estimation of critical torque using intermittent isometric maximal voluntary contractions of the quadriceps in humans. *J Appl Physiol* **106,** 975-983.

Burnley M, Vanhatalo A, Fulford J & Jones AM. (2010). Similar metabolic perturbations during all-out and constant force exhaustive exercise in humans: a 31P magnetic resonance spectroscopy study. *Experimental Physiology* **95,** 798-807.

Burnley M, Vanhatalo A & Jones AM. (2012). Distinct profiles of neuromuscular fatigue during muscle contractions below and above the critical torque in humans. *J Appl Physiol* **113,** 215-223.

Carter H, Pringle JS, Boobis L, Jones AM & Doust JH. (2004). Muscle glycogen depletion alters oxygen uptake kinetics during heavy exercise. *Med Sci Sports Exerc* **36,** 965-972.

Copp SW, Hirai DM, Musch TI & Poole DC. (2010). Critical speed in the rat: implications for hindlimb muscle blood flow distribution and fibre recruitment. *J Physiol-London* **588,** 5077-5087.

Dahmane R, Djordjevic S, Simunic B & Valencic V. (2005). Spatial fiber type distribution in normal human muscle Histochemical and tensiomyographical evaluation. *J Biomech* **38,** 2451-2459.

Dekerle J, Mucci P & Carter H. (2012). Influence of moderate hypoxia on tolerance to high-intensity exercise. *Eur J Appl Physiol* **112,** 327-335.

Deschamps T, Hug F, Hodges PW & Tucker K. (2014). Influence of experimental pain on the perception of action capabilities and performance of a maximal single-leg hop. *J Pain* **15,** 271 e271-277.

Didier KD, Hammer SM, Alexander AM, Caldwell JT, Sutterfield SL, Smith JR, Ade CJ & Barstow TJ. (2020). Microvascular blood flow during vascular occlusion tests assessed by diffuse correlation spectroscopy. *Exp Physiol* **105,** 201-210.

Gandevia SC. (2001). Spinal and supraspinal factors in human muscle fatigue. *Physiol Rev* **81,** 1725-1789.

Hammer SM, Alexander AM, Didier KD, Huckaby LM & Barstow TJ. (2020). Limb blood flow and muscle oxygenation responses during handgrip exercise above vs. below critical force. *Microvascular Research*.

Hammer SM, Alexander AM, Didier KD, Smith JR, Caldwell JT, Sutterfield SL, Ade CJ & Barstow TJ. (2018). The noninvasive simultaneous measurement of tissue oxygenation and microvascular hemodynamics during incremental handgrip exercise. *J Appl Physiol* **124,** 604-614.

Hepple RT. (2002). The role of O2 supply in muscle fatigue. *Can J Appl Physiol* **27,** 56-69.

Hogan MC, Richardson RS & Kurdak SS. (1994). Initial fall in skeletal muscle force development during ischemia is related to oxygen availability. *J Appl Physiol (1985)* **77,** 2380-2384.

Hunter SK. (2014). Sex differences in human fatigability: mechanisms and insight to physiological responses. *Acta Physiol (Oxf)* **210,** 768-789.

Hunter SK. (2016). Sex differences in fatigability of dynamic contractions. *Experimental physiology* **101,** 250-255.

Hureau TJ, Ducrocq GP & Blain GM. (2016). Peripheral and Central Fatigue Development during All-Out Repeated Cycling Sprints. *Med Sci Sports Exerc* **48,** 391-401.

Hureau TJ, Olivier N, Millet GY, Meste O & Blain GM. (2014). Exercise performance is regulated during repeated sprints to limit the development of peripheral fatigue beyond a critical threshold. *Exp Physiol* **99,** 951-963.

Hureau TJ, Romer LM & Amann M. (2018a). The 'sensory tolerance limit': A hypothetical construct determining exercise performance? *Eur J Sport Sci* **18,** 13-24.

Hureau TJ, Weavil JC, Thurston TS, Broxterman RM, Nelson AD, Bledsoe AD, Jessop JE, Richardson RS, Wray DW & Amann M. (2018b). Identifying the role of group III/IV muscle afferents in the carotid baroreflex control of mean arterial pressure and heart rate during exercise. *J Physiol* **596,** 1373-1384.

Hureau TJ, Weavil JC, Thurston TS, Wan HY, Gifford JR, Jessop JE, Buys MJ, Richardson RS & Amann M. (2019). Pharmacological attenuation of group III/IV muscle afferents improves endurance performance when oxygen delivery to locomotor muscles is preserved. *J Appl Physiol (1985)*.

Hwang K, Huan F & Kim DJ. (2013). Muscle fibre types of the lumbrical, interossei, flexor, and extensor muscles moving the index finger. *J Plast Surg Hand Surg* **47,** 268-272.

Janse de Jonge XA, Boot CR, Thom JM, Ruell PA & Thompson MW. (2001). The influence of menstrual cycle phase on skeletal muscle contractile characteristics in humans. *J Physiol* **530,** 161-166.

Joannides R, Haefeli WE, Linder L, Richard V, Bakkali EH, Thuillez C & Luscher TF. (1995). Nitric oxide is responsible for flow-dependent dilatation of human peripheral conduit arteries in vivo. *Circulation* **91,** 1314-1319.

Johnson MA, Polgar J, Weightman D & Appleton D. (1973). Data on the distribution of fibre types in thirty-six human muscles. An autopsy study. *J Neurol Sci* **18,** 111-129.

Jones AM, Wilkerson DP, DiMenna F, Fulford J & Poole DC. (2008). Muscle metabolic responses to exercise above and below the "critical power" assessed using 31P-MRS. *American journal of physiology Regulatory, integrative and comparative physiology* **294,** R585-593.

Jones DA. (1996). High-and low-frequency fatigue revisited. *Acta Physiol Scand* **156,** 265-270.

Kellawan JM & Tschakovsky ME. (2014). The single-bout forearm critical force test: a new method to establish forearm aerobic metabolic exercise intensity and capacity. *PLoS One* **9,** e93481.

Kufel TJ, Pineda LA & Mador MJ. (2002). Comparison of potentiated and unpotentiated twitches as an index of muscle fatigue. *Muscle Nerve* **25,** 438-444.

Lollgen H, Graham T & Sjogaard G. (1980). Muscle metabolites, force, and perceived exertion bicycling at varying pedal rates. *Med Sci Sports Exerc* **12,** 345-351.

Monod H & Scherrer J. (1965). The Work Capacity of a Synergic Muscular Group. *Ergonomics* **8,** 329-338.

Murgatroyd SR, Ferguson C, Ward SA, Whipp BJ & Rossiter HB. (2011). Pulmonary O2 uptake kinetics as a determinant of high-intensity exercise tolerance in humans. *J Appl Physiol (1985)* **110,** 1598-1606.

Poole DC, Burnley M, Vanhatalo A, Rossiter HB & Jones AM. (2016). Critical Power: An Important Fatigue Threshold in Exercise Physiology. *Med Sci Sports Exerc* **48,** 2320-2334.

Poole DC, Ward SA, Gardner GW & Whipp BJ. (1988). Metabolic and respiratory profile of the upper limit for prolonged exercise in man. *Ergonomics* **31,** 1265-1279.

Rowell LB & O'Leary DS. (1990). Reflex control of the circulation during exercise: chemoreflexes and mechanoreflexes. *J Appl Physiol (1985)* **69,** 407-418.

Russ DW & Kent-Braun JA. (2003). Sex differences in human skeletal muscle fatigue are eliminated under ischemic conditions. *J Appl Physiol (1985)* **94,** 2414-2422.

Sidhu SK, Weavil JC, Thurston TS, Rosenberger D, Jessop JE, Wang E, Richardson RS, McNeil CJ & Amann M. (2018). Fatigue-related group III/IV muscle afferent feedback facilitates intracortical inhibition during locomotor exercise. *J Physiol* **596,** 4789-4801.

Simpson LP, Jones AM, Skiba PF, Vanhatalo A & Wilkerson D. (2015). Influence of hypoxia on the power-duration relationship during high-intensity exercise. *Int J Sports Med* **36,** 113-119.

Vanhatalo A, Doust JH & Burnley M. (2007). Determination of critical power using a 3-min all-out cycling test. *Med Sci Sport Exer* **39,** 548-555.

Vanhatalo A, Doust JH & Burnley M. (2008). A 3-min all-out cycling test is sensitive to a change in critical power. *Med Sci Sport Exer* **40,** 1693-1699.

Vanhatalo A, Fulford J, DiMenna FJ & Jones AM. (2010). Influence of hyperoxia on muscle metabolic responses and the power-duration relationship during severe-intensity exercise in humans: a 31P magnetic resonance spectroscopy study. *Experimental Physiology* **95,** 528-540.

Vanhatalo A, Poole DC, DiMenna FJ, Bailey SJ & Jones AM. (2011). Muscle fiber recruitment and the slow component of O-2 uptake: constant work rate vs. all-out sprint exercise. *Am J Physiol-Reg I* **300,** R700-R707.

Zarzissi S, Zghal F, Bouzid MA, Hureau TJ, Sahli S, Ben Hassen H & Rebai H. (2019). Centrally-mediated regulation of peripheral fatigue during knee extensor exercise and consequences on the force-duration relationship in older men. *Eur J Sport Sci*, 1-9.

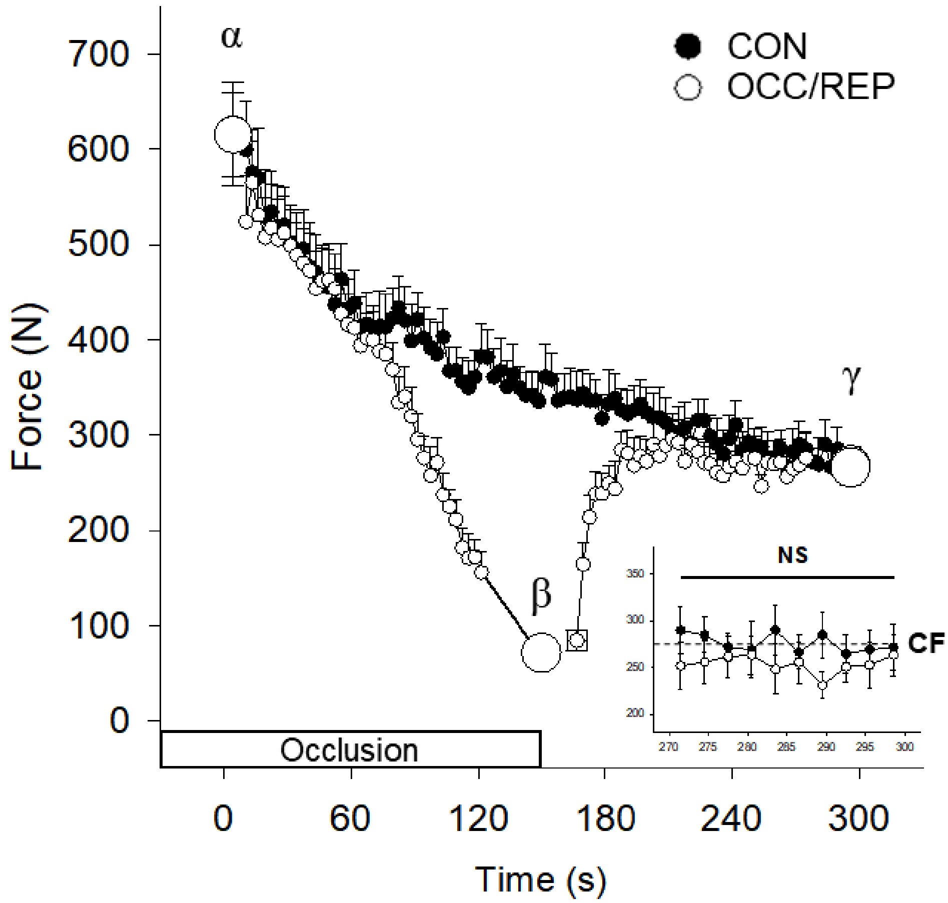

Figure 4.1 Mean force profile for each maximal-effort test (MET).

Critical force (CF) was determined as the average force production during the final 10 contractions (30 s) of the control (CON) MET (see inset). Values are means ± SE. Different symbols (α, β, γ) reflect significant differences among time-points ($p < 0.001$). Force was significantly reduced during occlusion (OCC) compared to CON. Note no significant difference in force production during the final 10 contractions (30 s) between CON and reperfusion (REP) (see inset).

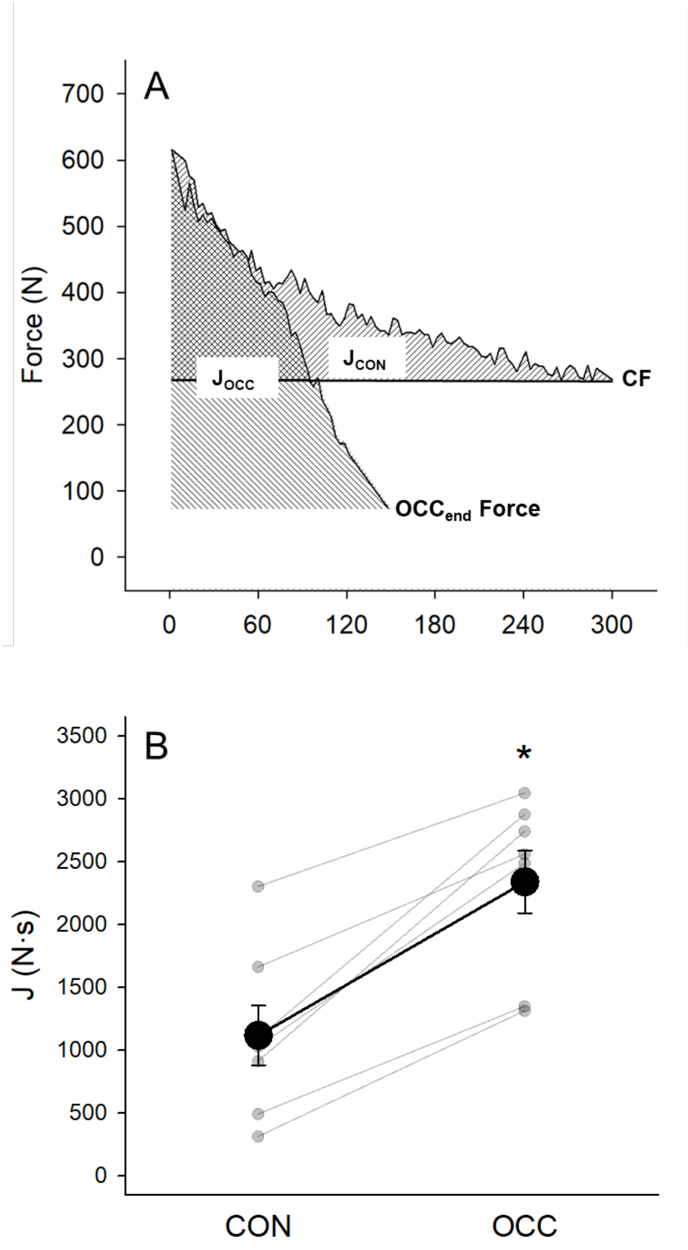

Figure 4.2 Total force impulse (J) for each maximal-effort test (MET).

J was calculated above critical force (CF) during control (J_{CON}) and above end-occlusion (OCC_{end}) force during occlusion (J_{OCC}) (**Panel A**). Individual (●) and mean (●) J during control (CON) and occlusion (OCC) METs (**Panel B**). Values are means ± SE. * Significantly greater than CON ($p < 0.001$).

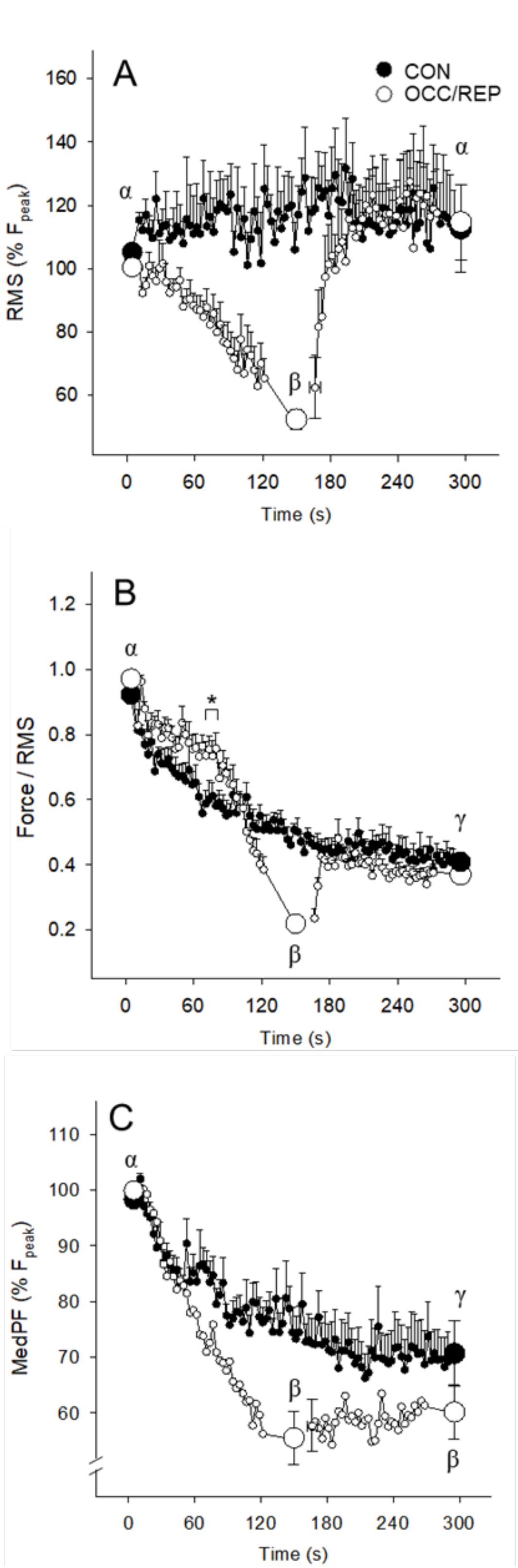

Figure 4.3 Electromyography (EMG) data for each maximal-effort test (MET).

Root mean square (RMS; **Panel A**), force/RMS (**Panel B**), and median power frequency (MedPF; **Panel C**) during control (CON) and occlusion and reperfusion (OCC/REP) METs. All values are means ± SE. Different symbols (α, β, γ) reflect significant differences among time-points ($p < 0.001$). * Significantly greater than CON ($p < 0.001$).

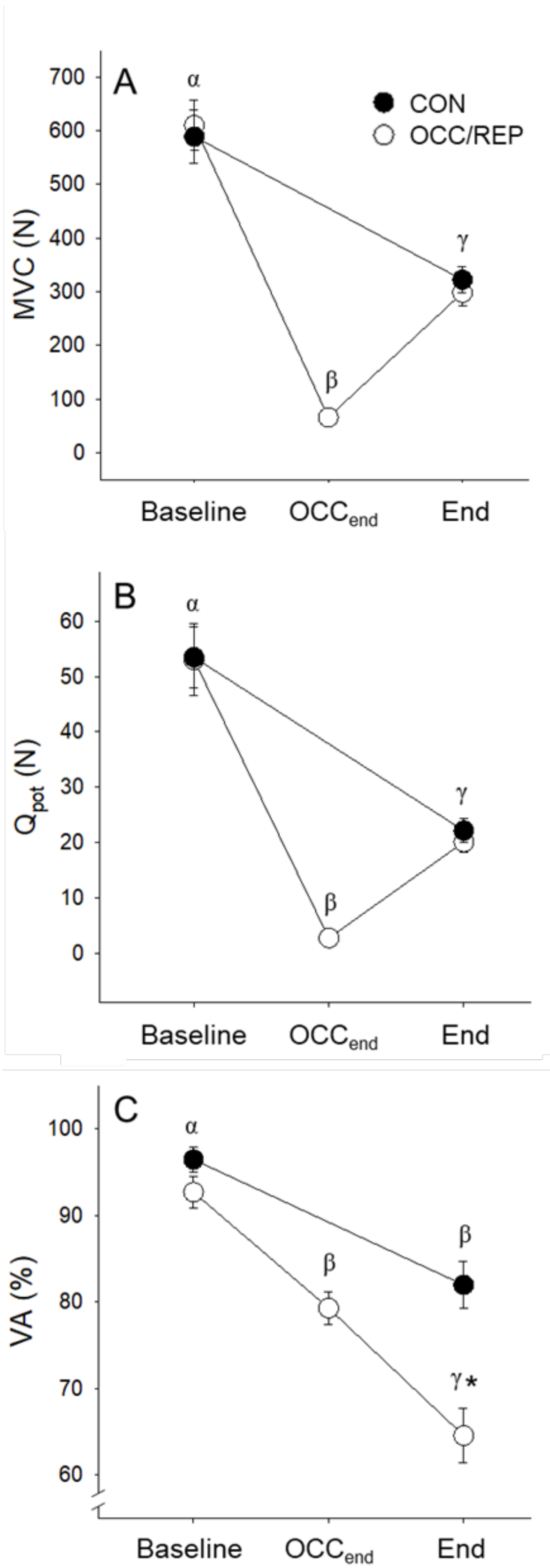

Figure 4.4 Neuromuscular function data for each maximal-effort test (MET).

Maximal voluntary contraction (MVC; **Panel A**), potentiated twitch force (Q_{pot}; **Panel B**), and percent voluntary activation (VA; **Panel C**) during control (CON) and occlusion and reperfusion (OCC/REP) METs. All values are means ± SE. Different symbols (α, β, γ) reflect significant differences among time-points ($p < 0.001$). * Significantly less than CON ($p < 0.001$).

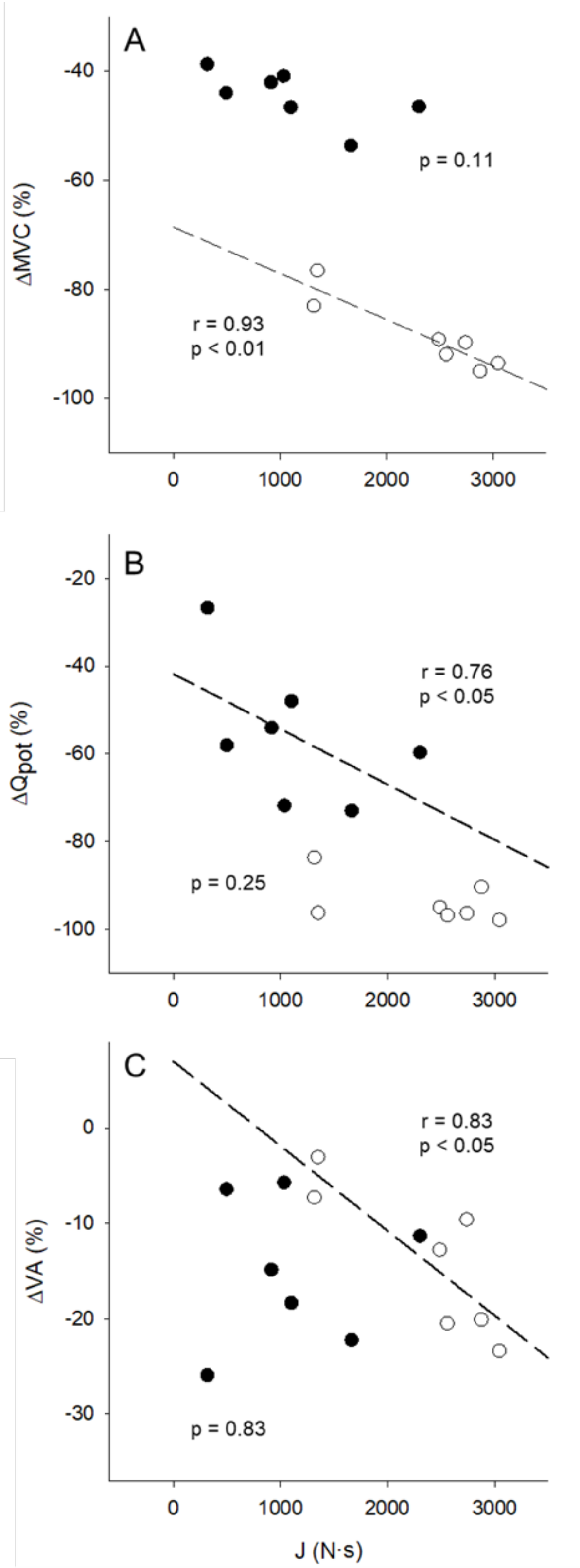

Figure 4.5 Relationships between J neuromuscular function.

Changes in maximal voluntary contraction (ΔMVC; **Panel A**), potentiated twitch force (ΔQ_{pot}; **Panel B**), and percent voluntary activation (ΔVA; **Panel C**) during control (● CON) and occlusion (○ OCC) as a function of J. Dashed lines represent significant relationships ($p < 0.05$) within experimental conditions.

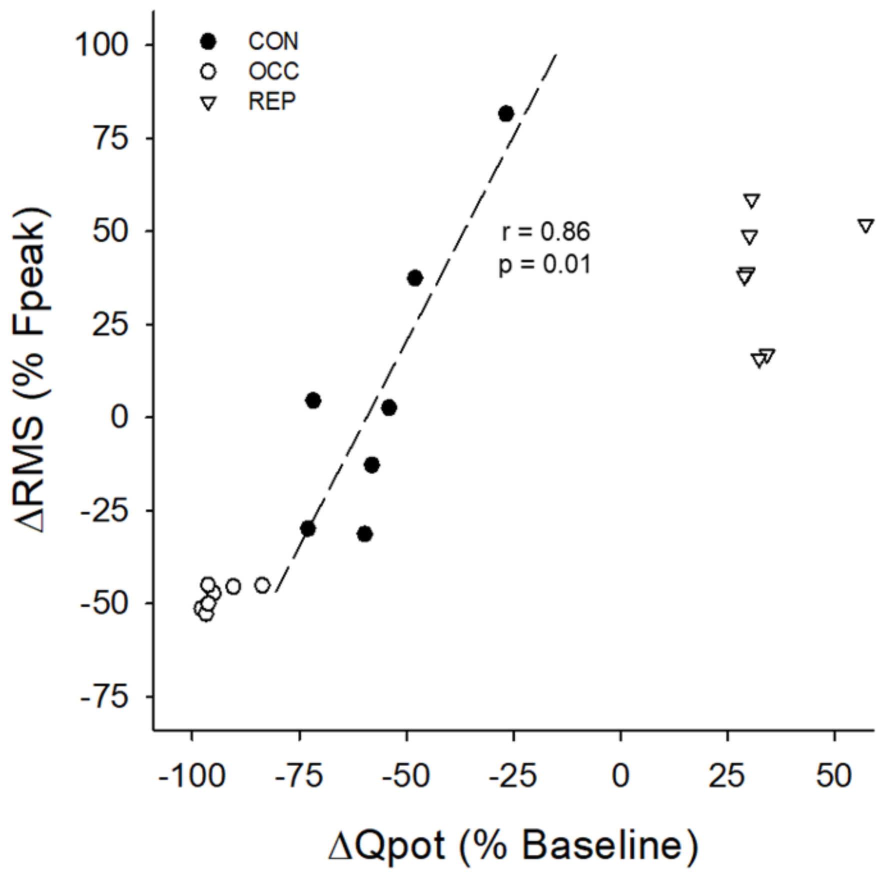

Figure 4.6 Relationship between peripheral fatigue development and change in motor-unit activation level.

Change in root mean square (ΔRMS) during control (CON), occlusion (OCC), and reperfusion (REP) as a function of change in potentiated twitch force (Q_{pot}). Dashed line represents a significant relationship within CON ($p < 0.05$).

Chapter 5 - Conclusions

The overall aim of the dissertation was to determine potential contraction-intensity dependent alterations in limb blood flow (LBF) and microvascular oxygen delivery and investigate the effect of oxygen delivery limitations on neuromuscular function at the heavy-to-severe intensity exercise threshold (i.e., critical power/force; CP/CF). It was demonstrated that that LBF and microvascular oxygen delivery responses during isometric handgrip exercise reach a physiological ceiling above, but not below, CF. Additionally, CF was the highest contraction-intensity at which this level of microvascular oxygen delivery could acutely sustain maximal-effort exercise. Further, we provide evidence limb vascular conductance is limited above, but not below, CP during dynamic locomotor-like exercise and demonstrate that these limitations to LBF during severe-intensity exercise may result from muscular contraction-induced vascular impedance. Finally, we identified fatigue-induced restriction to central motor drive during maximal-effort handgrip exercise under the condition of complete LBF occlusion and established that CF represents an oxygen delivery-dependent balance between motor-unit activation and peripheral fatigue development.

Collectively, contraction-intensity dependent limitations in oxygen delivery appear to exist during severe-intensity exercise such that progressive metabolite accumulation and the concomitant development of peripheral fatigue may result in restrictions to motor-unit activation. Importantly, CP/CF is an integrative physiological threshold with multifactorial determinants. Thus, while this dissertation provides evidence that muscular contraction-induced limitations to oxygen delivery may play a role in determining CP/CF, these conclusions must be considered in the context of other important metabolic and neuromuscular mechanisms of exercise tolerance, particularly in diseased or aging populations. The novel findings presented in this dissertation significantly contribute to our overall understanding of the integrative physiological determinants of oxygen delivery and fatigue development during severe-intensity exercise. Finally, the implications of our data for exercise tolerance and may be particularly relevant in patient populations that experience pathological limitations to oxygen delivery during exercise (e.g., heart failure and peripheral artery disease).

Appendix A - Curriculum Vitae

SHANE M. HAMMER, M.S.

CURRICULUM VITAE

KANSAS STATE UNIVERSITY

8 Natatorium, 920 Denison Ave., Manhattan, KS 66506 | 620-205-7487 | shammer@k-state.edu

EDUCATION

Kansas State University
Ph.D. in Kinesiology — **Expected Graduation Date: 2020**
Emphasis: Integrative Physiology

Kansas State University
M.S. in Kinesiology — **2017**
Thesis: "Perfusive and diffuse oxygen transport in skeletal muscle during incremental handgrip exercise"
Emphasis: Integrative Physiology

Kansas State University
B.S. in Kinesiology (with Honors) — **2015**
Emphasis: Exercise Physiology

HONORS & AWARDS

Kinesiology Department Outstanding Doctoral Student Award	2020
College of Human Ecology Outstanding Research Award	2019
American Kinesiology Association Graduate Writing Award	2019
Graduate Student Teaching Excellence Award (Nominee)	2019
Kobe Design University Research Fellowship	2018
Graduate Student Council Research Travel Award	2018
College of Human Ecology Research Travel Award	2018
Timothy R. Donoghue Graduate Scholarship	2018
Graduate Student Teaching Excellence Award (Nominee)	2018
American Kinesiology Association Masters Scholar Award	2017
College of Human Ecology Research Travel Award	2017
Graduate Student Council Research Travel Award	2017
Timothy R. Donoghue Graduate Scholarship	2017
Graduate Student Teaching Excellence Award (Nominee)	2016
Graduate Student Council Research Travel Award	2016
Ruth Hoeflin Home Economics Scholarship	2016

GRANT APPLICATIONS

College of Human Ecology Dissertation Research Award (***Funded**: $996*)	2019
2019 Arts, Humanities & Social Sciences Small Research Grant (***Funded: $1,000***)	2019
ACSM Foundation Doctoral Student Research Grant (Not Funded)	2019
Kansas State University Global Campus Development Grant (***Funded: $9,901***)	2019
Kansas State University Global Campus Development Grant (Not Funded)	2018

PUBLICATIONS

ORIGINAL RESEARCH

1. **Shane M. Hammer**, Andrew M Alexander, Kaylin D. Didier, Lillie M. Huckaby, Thomas J. Barstow. "Limb blood flow and muscle oxygenation responses during handgrip exercise above vs. below critical force" *Microvascular Research, 2020*

2. **Shane M. Hammer**, Lillie M. Huckaby, Andrew M. Alexander, Kaylin D. Didier, Dennis Huebner, Dana K. Townsend, Thomas J. Barstow. "Effects of assuming constant tissue scattering on muscle oxygenation measurements during ischemia and vascular reperfusion" *Journal of Applied Physiology, 2019*

3. Kaylin D. Didier, **Shane M. Hammer**, Andrew M. Alexander, Jacob T. Caldwell, Shelbi L. Sutterfield, Joshua R. Smith, Carl J. Ade, Thomas J. Barstow. "Microvascular blood flow during post-occlusive reactive hyperemia assessed by diffuse correlation spectroscopy" *Experimental Physiology, 2019*

4. Andrew M. Alexander, Shelbi L. Sutterfield, Karly N. Kriss, Kaylin D. Didier, **Shane M. Hammer**, Jacob T. Caldwell, Alex C. Dzewaltowski, Carl J. Ade, Thomas J. Barstow. "Prediction of emergency capsule egress performance" *Journal of Aeronautics & Space Exploration, 2019*

5. Shelbi L. Sutterfield, Andrew M. Alexander, **Shane M. Hammer**, Kaylin D. Didier, Jacob T. Caldwell, Thomas J. Barstow, Carl J. Ade. "Prediction of planetary critical mission task performance: Implications for long-duration spaceflight aerobic fitness levels" *In review: Medicine & Science in Sports & Exercise, 2019*

6. Andrew M. Alexander, Kaylin D. Didier, **Shane M. Hammer**, Alex C. Dzewaltowski, Karly N. Kriss, Garrett M. Lovoy, Joseph L. Hammer, Joshua R. Smith, Carl J. Ade, Ryan M. Broxterman, Thomas J. Barstow. "Exercise tolerance through severe and extreme intensity domains" *Physiological Reports, 2019*

7. **Shane M. Hammer**, Andrew M. Alexander, Kaylin D. Didier, Joshua R. Smith, Jacob T. Caldwell, Shelbi L. Sutterfield, Carl J. Ade, Thomas J. Barstow. "The noninvasive simultaneous measurement of tissue oxygenation and microvascular hemodynamics during incremental handgrip exercise" *Journal of Applied Physiology, 2018*

8. Jacob T. Caldwell, Shelbi L. Sutterfield, Hunter K. Post, Garrett M. Lovoy, Heather R. Banister, **Shane M. Hammer**, Carl J. Ade. "Vasoconstrictor responsiveness through alterations in relaxation time and metabolic rate during rhythmic handgrip contractions" *Physiological Reports, 2018*

9. Joshua R. Smith, Shelbi L. Sutterfield, Dryden R. Baumfalk, Kaylin D. Didier, **Shane M. Hammer**, Jacob T. Caldwell, and Carl J. Ade "Left Ventricular Strain Rate is Reduced during Voluntary Apnea in Healthy Humans" *Journal of Applied Physiology, 2017*

10. Joshua R. Smith, Kaylin D. Didier, **Shane M. Hammer**, Andrew M. Alexander, Stephanie P. Kurti, Steven W. Copp, Thomas J. Barstow, Craig A. Harms. "Effect of cyclooxygenase inhibition on the inspiratory muscle metaboreflex-induced cardiovascular consequences" *Journal of Applied Physiology, 2017*

11. Joshua R. Smith, Ryan M. Broxterman, **Shane M. Hammer**, Andrew M. Alexander, Kaylin D. Didier, Thomas J. Barstow, Stephanie P. Kurti, and Craig A. Harms. "Cardiovascular consequences of the inspiratory muscle metaboreflex: effects of age and sex" *American Journal of Physiology Heart & Circulatory Physiology, 2017*

12. Joshua R. Smith, Ryan M. Broxterman, **Shane M. Hammer**, Andrew M. Alexander, Kaylin D. Didier, Stephanie P. Kurti, Thomas J. Barstow, and Craig A. Harms. "Sex differences in the cardiovascular consequences of the inspiratory muscle metaboreflex" *American Journal of Physiology-Regulatory, Integrative and Comparative Physiology, 2016*

13. Joshua R. Smith, Ryan M. Broxterman, Carl J. Ade, Kara K. Evans, Stephanie P. Kurti, **Shane M. Hammer**, Thomas J. Barstow, and Craig A. Harms. "Acute supplementation of N-acetylcysteine does not affect muscle blood flow and oxygenation characteristics during handgrip exercise" *Physiological reports, 2016*

MANUSCRIPTS IN REVIEW

1. **Shane M. Hammer**, Kaylin D. Didier, Andrew M Alexander, Thomas J. Barstow. "Influence of blood flow occlusion on muscular recruitment and fatigue during maximal-effort small muscle mass exercise" *In Review (Journal of Physiology)*

MANUSCRIPTS IN PREPARATION

1. **Shane M. Hammer,** Stephen T. Hammond, Shannon K. Parr, Andrew M. Alexander, Vanessa-Rose G. Turpin, Zachary J. White, Kaylin D. Didier, Thomas J. Barstow, Carl J. Ade. "Influence of muscular contraction on vascular conductance during exercise above versus below critical power" *In preparation*

PRESENTED RESEARCH ABSTRACTS

1. **Shane M. Hammer**, Andrew M. Alexander, Kaylin D. Didier, Thomas J. Barstow. "Limb blood flow and muscle oxygenation responses to rhythmic exercise below and above critical force" *April 2020*

2. Andrew M. Alexander, **Shane M. Hammer**, Kaylin D. Didier, Thomas J. Barstow. "Effect of Extreme Intensity Exercise on Muscle Force Between Men and Women" *April 2020*

3. Kaylin D. Didier, Andrew M. Alexander, **Shane M. Hammer**, Thomas J. Barstow. "The Effect of Acute Passive Heating on Microvascular Oxygen Delivery, Exercise Tolerance and Recovery" *April 2020*

4. **Shane M. Hammer**, Andrew M. Alexander, Kaylin D. Didier, Lillie M. Huckaby, Camryn N. Webster, Thomas J. Barstow. "Effect of acute hyperglycemia on microvascular hemodynamics and tissue oxygenation during handgrip exercise" ***Oral Presentation****: American College of Sports Medicine. Orlando, FL. May 2019*

5. Andrew M. Alexander, **Shane M. Hammer**, Kaylin D. Didier, Lillie M. Huckaby, Camryn N. Webster, Thomas J. Barstow. "Sex differences in recovery from extreme and severe intensity exercise" *Presented: American College of Sports Medicine. Orlando, FL. May 2019*

6. Camryn N. Webster, **Shane M. Hammer**, Andrew M. Alexander, Kaylin D. Didier, Lillie M. Huckaby, Thomas J. Barstow. "Oxygen utilization during the contraction-relaxation of isometric knee extension exercise" *Presented: American College of Sports Medicine. Orlando, FL. May 2019*

7. Lillie M. Huckaby, Andrew M. Alexander, Kaylin D. Didier, **Shane M. Hammer**, Camryn N. Webster, Thomas J. Barstow. "The effect of passive stretch on vascular control during exercise" *Presented: American College of Sports Medicine. Orlando, FL. May 2019*

8. Kaylin D. Didier, Lillie M. Huckaby, Andrew M. Alexander, **Shane M. Hammer**, Camryn N. Webster, Thomas J. Barstow. "Effects of passive heating on perfusive and diffuse microvascular oxygen delivery" *Presented: American College of Sports Medicine. Orlando, FL. May 2019*

9. **Shane M. Hammer**, Kaylin D. Didier, Andrew M. Alexander, Lillie M. Huckaby, Thomas J. Barstow. "Tissue oxygenation and microvascular hemodynamics in recovery from incremental handgrip exercise" *Presented: Integrative Physiology of Exercise. San Diego, CA. September 2018*

10. Andrew M. Alexander, **Shane M. Hammer**, Kaylin D. Didier, Lillie M. Huckaby, Thomas J. Barstow. "Recovery from extreme and severe intensity exercise" *Presented: Integrative Physiology of Exercise. San Diego, CA. September 2018*

11. Kaylin D. Didier, Andrew M. Alexander, **Shane M. Hammer**, Lillie M. Huckaby, Thomas J. Barstow. "Impact of passive heating on critical torque" *Presented: Integrative Physiology of Exercise. San Diego, CA. September 2018*

12. Lillie M. Huckaby**, Shane M. Hammer**, Andrew M. Alexander, Kaylin D. Didier, Dana K. Townsend, Dennis M. Huebner, Thomas J. Barstow. "Effects of constant scattering on muscle oxygenation measurements during ischemia and vascular reperfusion" *Presented: Integrative Physiology of Exercise. San Diego, CA. September 2018*

13. **Shane M. Hammer**, Jacob T. Caldwell, Kaylin D. Didier, Andrew M. Alexander, Carl J. Ade, Thomas J. Barstow. "Perfusive and diffusive microvascular oxygen delivery during simulated hypovolemia and dynamic forearm exercise" ***Oral Presentation****: American College of Sports Medicine. Minneapolis, MN. June 2018*

14. Kaylin D. Didier, **Shane M. Hammer**, Kelsey J. Phelps, John M. Gonzalez, Thomas J. Barstow. "Near-infrared spectroscopy derived total heme vs. assay derived total heme" *Presented: American College of Sports Medicine. Minneapolis, MN. June 2018*

15. Lillie M. Huckaby**, Shane M. Hammer**, Dana K. Townsend, Thomas J. Barstow. "Changes in scattering, absorption, and resulting differential pathlength factor during arterial occlusion and reperfusion" *Presented: American College of Sports Medicine. Minneapolis, MN. June 2018*

16. Andrew M. Alexander, Kaylin D. Didier, **Shane M. Hammer**, Thomas J. Barstow. "Oxygenation characteristics during knee extension exercise in severe and extreme domain" *Presented: American College of Sports Medicine. Minneapolis, MN. June 2018*

17. Jacob T. Caldwell, **Shane M. Hammer**, Hunter K. Post, Andrew M. Alexander, Kaylin K. Didier, Garrett M. Lovoy, Carl J. Ade. "Duty cycle impairs functional sympatholysis during moderate intensity hand-grip exercise" *Presented: Experimental Biology. San Diego, CA. April 2018*

18. **Shane M. Hammer**, Andrew M. Alexander, Kaylin D. Didier, Joshua R. Smith, Jacob T. Caldwell, Shelbi L. Sutterfield, Carl J. Ade, Thomas J. Barstow. "Simultaneous measurement of perfusive and diffusive oxygen transport during incremental forearm exercise" *Presented: American College of Sports Medicine. Denver, CO. June 2017*

19. Joshua R. Smith, Ryan M. Broxterman, **Shane M. Hammer**, Andrew M. Alexander, Kaylin D. Didier, Thomas J. Barstow, Stephanie P. Kurti, and Craig A. Harms. "Cardiovascular consequences of the inspiratory muscle metaboreflex: effects of age and sex" *Presented: American College of Sports Medicine. Denver, CO. June 2017*

20. Andrew M. Alexander, **Shane M. Hammer**, Kaylin D. Didier, Dryden R. Baumfalk, Joshua R. Smith, Thomas J. Barstow. "Upper limits of exercise tolerance" *Presented: American College of Sports Medicine. Denver, CO. June 2017*

21. Kaylin D. Didier, **Shane M. Hammer**, Andrew M. Alexander, Jacob T. Caldwell, Shelbi L. Sutterfield, Carl J. Ade, Thomas J. Barstow. "Microvascular blood flow during post-occlusive reactive hyperemia assessed by diffuse correlation spectroscopy" *Presented: American College of Sports Medicine. Denver, CO. June 2017*

22. **Shane M. Hammer**, Andrew M. Alexander, Kaylin D. Didier, Dryden R. Baumfalk, Thomas J. Barstow. "Oxygenation characteristics of the vastus lateralis during cycling exercise performed above critical power" *Presented: Experimental Biology. Chicago, IL. April 2017*

23. Andrew M. Alexander, **Shane M. Hammer**, Kaylin D. Didier, Dryden R. Baumfalk, Thomas J. Barstow. "Muscle recruitment patterns above critical power" *Presented: Experimental Biology. Chicago, IL. April 2017*

24. Kaylin D. Didier, Carl J. Ade, **Shane M. Hammer**, Thomas J. Barstow. "Peak total-[hemoglobin + myoglobin] during incremental dynamic handgrip exercise and post-occlusive hyperemia" *Presented: Experimental Biology. Chicago, IL. April 2017*

25. Joshua R. Smith, Kaylin D. Didier, **Shane M. Hammer**, Andrew M. Alexander, Stephanie P. Kurti, Thomas J. Barstow, Craig A. Harms. "Contribution of prostaglandins to the inspiratory muscle metaboreflex-induced cardiovascular consequences" *Presented: Experimental Biology. Chicago, IL. April 2017*

26. **Shane M. Hammer**, Jesse C. Craig, Ryan M. Broxterman, and Thomas J. Barstow. "Oxygen utilization during the contraction-relaxation cycle of intermittent forearm exercise" *Presented: American College of Sports Medicine. Boston, MA. June 2016*

27. Kaylin D. Didier, Samuel L. Wilcox, Ryan M. Broxterman, **Shane M. Hammer**, Andrew M. Alexander, and Thomas J. Barstow. "Relationship between muscle activation and VO_2 during incremental ramp exercise" *Presented: American College of Sports Medicine. Boston, MA. June 2016*

28. Joshua R. Smith, Ryan M. Broxterman, **Shane M. Hammer**, Andrew M. Alexander, Kaylin D. Didier, Thomas J. Barstow, Stephanie P. Kurti, and Craig A. Harms. "Sex differences in the inspiratory muscle metaboreflex" *Presented: American College of Sports Medicine. Boston, MA. June 2016*

TEACHING EXPERIENCE

Kansas State University, Manhattan, KS, USA
Graduate Teaching Assistant **2015 – Present**

Kansas State University, Manhattan, KS, USA
Exercise Physiology (KIN 336) Laboratory Coordinator **2017 – Present**

Kobe University, Kobe, Hyogo Prefecture, Japan
Guest Lecturer **May, 2018**

COURSES INSTRUCTED

KIN 336 – Exercise Physiology Laboratory
The objective of this course is to explore the physiological bases of exercise. Students perform laboratory experiments, collect, analyze and interpret data.

KIN 360 – Anatomy and Physiology
This laboratory offers a rigorous, comprehensive study of human anatomy and physiology at the cellular, tissue, and systems level with an emphasis on the structure/function relationships of the different systems.

PROFESSIONAL MEMBERSHIPS & SERVICE

PROFESSIONAL MEMBERSHIPS

American College of Sports Medicine Member **2015 - Present**
American Physiological Society Member **2015 – Present**

PEER REVIEW

American Journal of Physiology
Journal of Applied Physiology

PROFESSIONAL SERVICE

College of Human Ecology Graduate Student Advisory Board **2017 - Present**
Health Day on Campus Department of Kinesiology Co-coordinator **2017 – Present**
Undergraduate Office of Research and Creative Inquiry Forum Judge **2018**